Characterisations of Europe's integrated water ~~vapor~~vapour and assessments of atmospheric reanalyses using more than two decades of ground-based GPS

Peng Yuan[1], Roeland Van Malderen[2], Xungang Yin[3], Hannes Vogelmann[4], Weiping Jiang[5], Joseph ~~Awange[5]~~Awange[6], Bernhard Heck[1], Hansjörg Kutterer[1]

[1]Geodetic Institute, Karlsruhe Institute of Technology, Karlsruhe, 76131, Germany
[2]KMI-IRM, Royal Meteorological Institute of Belgium, Brussels, B-1180, Belgium
[3]NOAA National Centers for Environmental Information~~Riverside Technology Inc~~, Asheville, NC 28801, USA
[4]Karlsruhe Institute of Technology, IMK-IFU, Garmisch-Partenkirchen, 82467, Germany
[5]Wuhan University, GNSS Research Center, Wuhan, 430079, China

[~~5~~6]Curtin University, School of Earth and Planetary Sciences, Perth, WA 6845, Australia

Correspondence to: Peng Yuan (peng.yuan@kit.edu)

Abstract. Ground-based Global Positioning System (GPS) has been extensively used to retrieve Integrated Water ~~Vapor~~Vapour (IWV) and has been adopted as a unique tool for the assessments of atmospheric reanalyses. In this study, we investigated the multi-temporal-scale variabilities and trends of IWV over Europe by using IWV time series from 108 GPS stations for more than two decades (1994-2018). We then adopted the GPS IWV as a reference to assess six ~~commonly used~~commonly used atmospheric reanalyses, namely CFSR, ERA5, ERA-Interim, JRA55, MERRA2, and NCEP2. The GPS results show that the peaks of the diurnal harmonics are within 15−21 hour in local solar time at 90% of the stations. The diurnal amplitudes are 0−1.2 kg m^{-2} ~~cycles peak within 16:00-24:00 local time with peak-to-peak amplitudes~~ (accounting for 0%-8% ~~2%-18%~~ of the daily mean IWV), and they are found to be related to seasons and locations with different mechanisms, such as solar heating, land-sea breeze, and orographic circulation. However, mismatches in the diurnal cycle of ERA5 IWV between 09 and 10 UTC as well as between 21 and 22 UTC were found and evaluated for the first time and they can be attributed to the edge effect in each ERA5 assimilation cycle. The average ERA5 IWV shifts are -0.08 and 0.19 kg m^{-2} at the two epochs and they were found to be more significant in summer and in the Alps, and in Eastern and Central Europe in some cases. Nevertheless, ERA5 outperforms the other reanalyses in reproducing diurnal IWV anomalies at all the 1-, 3-, and 6-hour temporal resolutions. ERA5 is also superior to the others in modelling the annual cycle and linear trend of IWV. For instance, the IWV trend differences between ERA5 and GPS are quite small, with a mean value and a standard deviation of 0.01% decade^{-1} and 0.97% decade^{-1}, respectively. However, due to significant discrepancies with respect to GPS, CFSR and NCEP2 are not recommend for the analysis of IWV trends over Southern Europe and the whole Europe, respectively.

~~The diurnal 1-hourly anomalies can be much more intensive with a range of −100% to 200%. The annual cycles peak in July and August with maximum values of 17-32 kg m^{-2}. The interannual variations of IWV over Europe are found to be mainly linked to the North Atlantic Oscillation (NAO) and the East Atlantic (EA) patterns. The IWV continues to increase over Europe during the last two decades at 0-0.4 kg m^{-2} decade^{-1} in the north and 0.4-1 kg m^{-2} decade^{-1} in the south. Regarding the assessments of the reanalyses, the intercomparisons with respect to GPS reveal a general superiority of the newly-released ERA5 IWV product. For instance, ERA5 only has a slight wet bias with a median value of 1%, whereas the median bias for MERRA2 is 4%. ERA5, MERRA2, and NCEP2 are the best, second best, and worst performers respectively in modelling~~

1 Introduction

Water ~~vapor~~vapour is the most important component of the Earth's atmosphere regarding the transport of energy by latent heat and radiative forcing.~~serves as an important medium of moisture and latent heat transfer in the Earth's atmosphere on the one hand, while on the other hand, it~~ It is the most important gaseous source of infrared opacity in the atmosphere, and thus, the largest contributor to the natural greenhouse effect (Kiehl and Trenberth, 1997; Harries, 1997). It plays a key role in water and energy cycle (e.g, Trenberth and Fasullo, 2013), climate change (e.g, Schneider et al., 2010), and various weather and climate processes (e.g, Haar et al., 2012), and is crucial for the understanding of many extreme ~~events~~meteorological phenomena, such as atmospheric rivers (e.g, Zhu and Newell, 1994), hurricanes (e.g, Ejigu et al., 2021), floods (e.g., Turato et al., 2004), and droughts and monsoons (e.g., Jiang et al., 2017; Fadnavis et al., 2021). However, due to its large spatiotemporal variability, its high-accuracy quantification remains a challenge.

Characterizing the multiple spatiotemporal scale variabilities and long-term trends of water ~~vapor~~vapour is of great importance for Europe, which is like a peninsula of the Eurasian landmass surrounded mainly by the Arctic Ocean, Atlantic Ocean, and Mediterranean Sea, to the north, west, and south, respectively. Owing to the moisture from the oceans carried by the prevailing westerlies, most of Western Europe has an oceanic climate with mild, wet, and turbulent weather in winter. In contrast, Southern Europe is characterised by a well-known dry-summer Mediterranean climate. Europe is generally vulnerable to the extreme events associated with abnormal water ~~vapor~~vapour transport and very sensitive to climate change (Field and Barros, 2014; Lavers et al., 2016), and has been the fastest warming up continent in recent decades (e.g., Copernicus, 2019). Since 1 K rise in temperature leads ~~could contribute~~ to a 7% increase of the water ~~vapor~~vapour holding capacity of the atmosphere as implied by the Clausius–Clapeyron equation (Trenberth et al. 2003), Europe's water ~~vapor~~vapour amount is noticeably increasing (Yuan et al., 2021). The increasing water ~~vapor~~vapour content fortifies the radiative forcing~~has a stronger greenhouse effect~~, leading to a higher temperature, which becomes most powerful if additional water vapour enters the upper troposphere and lower stratosphere ~~and thus forms a positive feedback loop~~ (Solomon et al.~~Held and Soden~~, 2010~~00~~). The warmer and moister climate impacts all weather events and aggravates the risks of extreme events (Trenberth, 2012).

Atmospheric water ~~vapor~~vapour content can be expressed by using Integrated Water ~~Vapor~~Vapour (IWV), which is defined as the total amount of water ~~vapor~~vapour present in a vertical atmospheric column from the Earth's surface to the top of the atmosphere in unit of kg m⁻² (Jones et al., 2020). The IWV is also known as the Total Column Water ~~Vapor~~Vapour (TCWV) or Precipitable Water ~~Vapor~~Vapour (PWV). At present, numerous techniques have been developed to measure

water ~~vapor~~vapour, such as balloon-borne radiosondes (e.g., Durre et al., ~~2009~~2018; Kunz et al., 2013; Müller et al., 2016), aircraft measurements (e.g., Tilmes et al., 2010; Kunz et al., 2014; Krämer et al., 2020), satellite observations (e.g., Grossi et al., 2015; Beirle et al., 2018), and ground-based methods (e.g., Kämpfer 2012; Vogelmann et al., ~~2015~~2008). Global Navigation Satellite System (GNSS), represented by the USA's NAVSTAR Global Positioning System (GPS), has been exploited for water ~~vapor~~vapour retrieval by using its ground-based measurements (e.g., Bevis et al., 1992) or space-based radio occultation (e.g., Kursinski et al., 1995) since the 1990s. ~~Al~~Though accurate vertical distribution of water ~~vapor~~vapour in the upper troposphere can be obtained by the GPS radio occultation (e.g., Randel and Wu, 2005; Randel et al., 2007), its accuracy is limited in the lower troposphere (e.g., Ao et al., 2003; Awange 2018) where the water ~~vapor~~vapour is most abundant. On the contrary, the ground-based GPS has proven to be an effective technique for IWV retrieval with advantages of high accuracy, high temporal resolution, and all-weather condition availability (Jones et al., 2020). The ground-based GPS has been utilized for IWV measurement in numerous global (e.g., Wang and Zhang, 2009; Vey et al., 2010; Chen and Liu, 2016) as well as regional (e.g., Bernet et al., 2020; Ejigu et al., 2021; Huang et al., 2021) studies. In addition, there have been nearly three decades of continuous GPS measurements with increasingly densified networks in Europe, such as the European Reference Frame (EUREF) Permanent Global Navigation Satellite System (GNSS) Network (EPN; Bruyninx et al., 2012). Given these benefits, ground-based GPS offers a unique tool to investigate the multiple spatiotemporal scale variabilities of IWV over Europe. The homogeneously reprocessed long-term time series of GPS IWV is also quite beneficial to climate change studies (e.g., Van Malderen et al., 2020). GPS has increasingly been adopted to investigate various temporal features of Europe's IWV in many studies, such as diurnal cycle (e.g., Wang et al., 2009; Diedrich et al., 2016; Steinke et al., 2019), ~~seasonal variations~~annual cycle (eg, Parracho et al., 2018; Van Malderen et al., 2022), ~~interannual variations (eg, Khutorova et al., 2018),~~ and trends (eg, Nilsson and Elgered 2008, Ning et al., 2016, Wang et al., 2016). However, the multi-temporal-scale variabilities and trends of Europe's IWV have rarely been comprehensively studied using GPS.

Atmospheric reanalyses have been extensively adopted as the data source of IWV acquisition for the last several decades, owing to the benefits of regional/global coverage, consistent spatiotemporal resolution, and the availability of many other meteorological variables. However, their products may still be subject to large uncertainty. On the one hand, this is due to the fact that the reanalyses from different providers and different versions are inconsistent in the input data, assimilation schemes, besides using different physical schemes and representations. For example, the newly released fifth generation global reanalysis from ECMWF (ERA5; Hersbach et al., 2020) has assimilated more datasets and instruments, which were not ingested in its predecessor ERA-Interim (ERAI; Dee et al., 2011). The assimilation system of ERA5 is also more advanced. On the other hand, systematic and random errors in the input data are unavoidable. For instance, the Integrated Global Radiosonde Archive (IGRA, Durre et al., 2018) provides a long record of relative humidity observations for the assimilation of reanalysis, but long-term radiosonde humidity measurements are very sensitive to changes in instrumentation and measuring practice (McCarthy et al., 2009; Dai et al., 2011). Therefore, assessments of the reanalyses' water ~~vapor~~vapour products are indispensable for the accurate understanding and interpretations of Europe's weather and climate processes. The performances of various reanalyses' IWV products in Europe have been assessed by many regional/global studies using

ground-based GPS data, as the GPS observations are not operationally assimilated by reanalyses (Hagemann et al., 2003; Bock et al., 2005; Heise et al., 2009; Vey et al., 2010; Alshawaf et al., 2018; Parracho et al., 2018; Wang et al., 2020; Yuan et al., 2021). However, it is still quite hard to draw consistent conclusions on the performances of different reanalyses from these studies, as they are different in many aspects, such as the numbers and locations of the GPS stations, period of observations, data processing strategies, and performance metrics. A consistent assessment of various reanalyses by using homogeneously reprocessed long-term time series of GPS IWV as reference in Europe is still lacking. In addition, few studies have focused on the performance of the latest ERA5 in reproducing the temporal features of Europe's IWV so far.

In this paper, we focus on characterizing the multi-temporal-scale variabilities and trends of Europe's IWV by ~using more than two decades of GPS IWV, and then we assess the performances of six reanalyses' IWV products over Europe. The paper is organized as follows: In section 2, we describe the GPS and reanalyses datasets, IWV calculation methods, and consistency evaluation metrics. Section 3 assesses the consistency in daily time series and representativeness differences, while the diurnal variations and associated diurnal cycle, annual ~~variations and interannual anomaly~~cycle, and long-term trends of Europe's IWV are investigated using GPS in sections 4, 5, and 6, respectively. The performances of the reanalyses are also assessed accordingly, and the main findings are summarised in section 7.

2 Data and methods

2.1 GPS data

To characterise the IWV over Europe and assess the reanalyses, 1-hourly GPS IWV retrievals obtained from 108 stations are used (Fig. 1). Most of GPS stations are from the EPN network (Bruyninx et al., 2001). The GPS observations are from January 1994 to December 2018 with an average time length of 21 years and an average integration rate of ~~95~~92% (Table S1). The integration rate is the ratio between the number of available daily IWV data points and the theoretical number of all possible observations in the time range. The IWV retrievals were estimated with GPS Zenith Total Delay (ZTD) provided by the Nevada Geodetic Laboratory (NGL; Blewitt et al. 2018). The GPS ZTD products from NGL were used because it covers a long time period of 25 years, so that it allows for better evaluations on the diurnal and annual climatological averages, and long-term trends. In comparison, another ZTD dataset from EPN-Repro2 (Pacione et al., 2017) only has about 19 years of data, ending in 2014.

The NGL processes the GPS data using the newly improved GipsyX v1.0 software in Precise Point Positioning (PPP) mode (Bertiger et al., 2020). Reprocessed orbits and clocks from Jet Propulsion Laboratory (JPL) Repro 3 were used together with the 2014 International GNSS Service (IGS) reference frame (IGS14; Rebischung and Schmid, 2016). The observations were weighted based on elevation (e) dependent function of sin e. The cutoff elevation~~whose cutoff~~ angle was set to 7°. The first order effect of the ionosphere was removed by employing ionosphere-free combinations of the GPS observations. The second order effect was corrected with International Geomagnetic Reference Field 12 (IGRF12; Thébault

et al., 2015) and JPL's ionosphere maps. As for the modelling of tropospheric delay, the Vienna Mapping Function 1
140   (VMF1; Boehm et al., 2006) and its associated *a priori* Zenith Hydrostatic Delay (ZHD) were adopted.

2.2 Reanalysis data

The IWV derived from six commonly used global atmospheric reanalyses, namely, the newly released fifth generation global reanalysis (ERA5) and its predecessor ERA-interim (ERAI) from ECMWF, the Japanese 55-year Reanalysis (JRA55) from Japan Meteorological Agency (JMA), the Modern-Era Retrospective Analysis for Research and Applications, version 2
145   (MERRA2) from NASA Global Modeling and Assimilation Office (GMAO), and the Climate Forecast System Reanalysis (CFSR) and NCEP-DOE AMIP-II Reanalysis (NCEP2) from National Centers for Environmental Prediction (NCEP) are analyzed. The features of the reanalyses are summarised in Table 1. It is worth noting that JRA55 only provides humidity information at 27 pressure levels from 1000 to 100 hPa, though it has 37 levels in total. These six reanalyses are selected as their IWV products cover the period of the ground-based GPS data available since 1994. Despite ERAI having been
150   decommissioned and superseded by ERA5 in August 2019, we still include it for the purpose of evaluating the progress of its successor ERA5. We therefore restricted the time range of all data records to a common period from 1994 to 2018.

2.3 Teleconnection indices

Previous studies have demonstrated that the variations of atmospheric water vapor are linked to various teleconnection patterns (e.g., Wang et al., 2018; Thomas et al., 2021). In this study, teleconnections between the extreme IWV anomalies in
155   Europe and eight indices are evaluated, including (1) North Atlantic Oscillation (NAO; Barnston and Livezey, 1987), (2) East Atlantic pattern(EA; Barnston and Livezey, 1987), (3) Arctic Oscillation (AO; Thompson and Wallace, 1998), (4) Scandinavia pattern (SCA; Comas-Bru and McDermott 2014), (5) Western Mediterranean Oscillation (WeMO; Martin-Vide and Lopez-Bustins, 2006), (6) Niño 3.4 index (Trenberth, 1997), (7) Northern Oscillation Index (NOI; Schwing et al., 2002), and (8) Quasi-Biennial Oscillation (QBO; Baldwin et al., 2001). The well-known NAO, characterized by a meridional dipole
160   in atmospheric pressure between the Azores High and Icelandic Low, is a prominent mode of winter climate variability over Europe (Hurrell 1995; Comas-Bru and McDermott., 2014). It exerts a dominant influence on air temperature, water vapor, precipitation, and wind patterns over the Atlantic/European sector, especially during the boreal winter (Trigo et al., 2002). The EA pattern is known to be the second leading mode of the climate variability over the Atlantic/European sector (Barnston and Livezey, 1987) and it can modulate the structure and climate impact of the NAO (Moore and Renfrew, 2012).
165   For information on the other indices, readers are referred to the relevant references.

2.4 3 IWV retrievals

The Zenith Total Delay (ZTD) estimates derived from GPS data processing can be converted into IWV, the total amount of water vaporvapour present in a vertical atmospheric column from the Earth's surface to the top of the atmosphere in unit kg m^{-2}, using the following equation (Bevis et al., 1992):

$$\text{IWV} = \frac{10^6}{R_V \cdot [k_2' + k_3/T_m]} \cdot (\text{ZTD} - \text{ZHD}), \tag{1}$$

where R_V denotes the gas constant for water ~~vapor~~vapour, k_2' and k_3 are atmospheric refractivity constants (Bevis et al., 1994), and T_m denotes the weighted mean temperature~~.~~:

$$T_m = \frac{\int_{H_s}^{H_{top}} \frac{e}{T} dp}{\int_{H_s}^{top} \frac{e}{T^2} dp}, \tag{2}$$

where e and T are water vapour pressure and temperature profiles from the geopotential heights of the GPS station (H_s) to the top level of reanalysis (H_{top}), respectively.

The ZHD was modelled as follows (Saastamoinen, 1972; Davis et al., 1985)~~;~~:

$$\text{ZHD} = 2.2768 \frac{\cancel{P}p_s}{1 - 2.66 \times 10^{-3} \cdot \cos(2\varphi_s) - 2.8 \times 10^{-7} H_s}, \tag{\cancel{2}3}$$

where $\cancel{P}p_s$ denotes the pressure at the GPS station with a latitude of φ_s and a height of H_s. The $\cancel{P}p_s$ and T_m are computed by using the ERA5 pressure level product (see Yuan et al., 2021 and references therein). The ERA5 is selected as it can provide a 1-hourly product without temporal interpolation.

IWV values at the GPS stations are also calculated from the six reanalyses. In this calculation, the pressure level products of the reanalyses are used rather than their surface level IWV products, though it requires a heavier workload. This is because the GPS station and its nearby reanalysis surface grids are usually related to different heights. Vertical IWV adjustment is therefore usually required for the intercomparison between the IWV estimates from GPS and reanalyses. Compared to the reanalyses' surface level products, their pressure level products allow for a better characterisation of the vertical distribution of water ~~vapor~~vapour and tends to minimize the errors of the vertical adjustment (Parracho et al., 2018).

The scheme of the calculation is illustrated in Fig. 2. Assume a GPS station with a geopotential height of H_s located between two adjacent reanalysis pressure levels ($\cancel{p}P_j$ and $\cancel{p}P_{j+1}$). We first determined its eight surrounding reanalysis grid nodes at these pressure levels ($N_i^{(j)}$ and $N_i^{(j+1)}$, i=1, 2, 3, and 4) and four auxiliary points (A_i). The auxiliary points are located at the GPS station height whereas their horizontal locations are identical to the associated reanalysis nodes. We then calculate the related meteorological variables at each auxiliary point. Exponential and linear interpolations are employed for the vertical corrections of pressure and temperature, respectively. If the auxiliary point is lower than the lowest pressure level (e.g., 1000 hPa), an extrapolation of these variables is conducted. For details of the vertical adjustment, readers are referred to Schüler (2001) and Wang et al. (2005). Next, we calculate the IWV at each auxiliary point by using a vertical integration:

$$\text{IWV}_i = \int_{H_s}^{H_{top}} \frac{q}{g} dp \cancel{\int \frac{q}{g} dP}, \tag{\cancel{3}4}$$

where q and g are specific humidity and gravitational acceleration profiles from H_s to the reanalysis top level, respectively.

It is noteworthy that geopotential height system is employed in the reanalyses. Accordingly, the geopotential heights (H_{gp}) of the GPS stations rather than their ellipsoidal (H_{el}) or orthometric heights (H_{or}) are used in the above calculations. The conversion of height systems is carried out as follows (Dirksen et al., 2014; Wang et al., 2016; World Meteorological Organization, 2018):

$$H_{or} = H_{el} - N,$$

$$H_{gp} = \frac{\gamma_s(\varphi_s)}{9.80665} \cdot \frac{R(\varphi_s) \cdot H_{or}}{R(\varphi_s) + H_{or}}, \tag{5}$$

$$\gamma_s(\varphi_s) = 9.780325 \frac{1 + 1.93185 \times 10^{-3} \cdot \sin^2(\varphi_s)}{(1 - 6.69435 \times 10^{-3} \cdot \sin^2(\varphi_s))^{0.5}}, \tag{6}$$

$$R(\varphi_s) = \frac{6.378137 \times 10^6}{1.006803 - 6.706 \times 10^{-3} \cdot \sin(\varphi_s)^2}, \tag{7}$$

where the N is the geoid heights in meter from the Earth Gravitational Model 2008 (EGM2008; Pavlis et al., 2012).

In the end, we estimate the IWV at the GPS station using a horizontal interpolation with an inverse distance weighting algorithm (Jade and Vijayan, 2008).

Representativeness differences arise in the comparison of the IWV derived by the ground-based GPS and reanalyses (Bock and Parracho, 2019). This is because local variations of IWV measured by the GPS might fail to be resolved by the reanalyses due to their coarse horizontal resolution. The representativeness differences can be evaluated statistically as proposed by Bock and Parracho (2019):

$$\delta_{\max} = ma\,x(|\text{IWV}_i - \text{IWV}_k|), \quad i, k = 1,2,3,4, \quad i \neq k, \tag{48}$$

where IWV_i and IWV_k are the IWV values of the horizontal auxiliary points A_i and A_k, respectively (Fig. 2). Bock and Parracho (2019) found that the measure $\delta_{\max}$ was correlated with the standard deviation of the IWV differences between GPS and ERAI (σ_Δ), and thus concluded that the representativeness differences between the IWV from GPS and ERAI contributed to their discrepancies. Here, we extend their work by estimating and comparing the representativeness statistics of the six reanalyses with various spatial resolutions (Table 1).

2.5 4 Pre-processing

The 1-, 3-, and 6-hourly IWV time series are screened by using a robust outlier detection method as follows (Yuan et al., 2021). For each data point, the data within a 30-day window ~~centered~~centered at this point are extracted. The 25th percentile (Q1), 75th percentile (Q3), and interquartile range (IQR) of the subsequent time series are then calculated. Finally, the data point is identified as an outlier if it is outside the range of $[\text{Q1} - 1.5 \times \text{IQR}, \text{Q3} + 1.5 \times \text{IQR}]$. The IQR threshold and the 30-day sliding window are adopted as they allow for a good robustness and a proper accommodation for the natural variability of IWV. On average, about 1% data were filtered out by the data screening.

The GPS IWV time series may have breaks due to changes in GPS data processing strategies and station-related changes like hardware changes or changes in the electromagnetic environment (Van Malderen et al., 2020 and references therein). Changes in GPS data processing strategy are avoided in this study by using the homogeneously reprocessed GPS

230 ZTD product. Moreover, the GPS IWV time series are homogenized as described in Yuan et al. (2021). The difference in time series between GPS and ERA5 IWV are then calculated, so that most of the natural IWV variabilities are removed and the small breaks are easily distinguishable. The associated GPS height time series and station log files are also inspected to find out suspicious epochs of device changes. The significances of the breaks are tested at 95% confidence level with the specific optimal noise model of each IWV difference time series. The IWV time series from reanalyses may also have breaks (e.g., Ning et al., 2016, Schröder et al, 2016), and thus we compared them with the homogenized GPS IWV time series.
235 Nevertheless, no obvious breaks were found in the reanalyses time series.

In this study, the performances of reanalyses IWV products in daily time series, 1 hourly diurnal cycle and variations, 1 monthly annual cycle and interannual variations, and long-term linear trends are evaluated. As the temporal resolutions of the datasets are different, temporal interpolation and aggregation are conducted. For the investigation of diurnal cycle and variations, the 3- and 6-hourly IWVs are linearly interpolated into 1-hourly time series. To obtain daily mean IWV values,
240 the 1-, 3-, and 6-hourly IWV time series are aggregated if they have at least 12, 4, and 2 data points in a day, respectively. The daily mean IWV time series at each station is further aggregated into monthly mean IWV series if there are at least 15 data points available in a month.

2.5 Homogenisation

The GPS IWV time series can be inhomogeneous due to changes in GPS data processing strategies and station-related
245 changes like hardware changes or changes in the electromagnetic environment (Van Malderen et al., 2020; Nguyen et al., 2021 and references therein). We employed a homogenisation approach as described in Appendix A with step-by-step details and examples at two stations (HERS and ERLA).

Here, we only provide a brief introduction on the approach. We first avoided inhomogeneities due to changes in GPS data processing strategy by using the homogeneously reprocessed GPS ZTD product. We then homogenised the GPS IWV
250 time series by using the RHtestsV4 software (Wang and Feng, 2013). This software is developed especially for the detection and adjustment of changepoints in climatic time series, and it has been used in the homogenisation of IWV time series in previous studies (Ning et al., 2016; Schröder et al., 2016; Van Malderen et al., 2020).

We took the IWV time series from all the six reanalyses as references for the GPS IWV homogenisation and used a strategy to avoid the impacts of possible changepoints in individual reanalyses. However, we did not homogenise the
255 reanalyses IWV time series because they represent the native quality of the reanalyses that we would like to assess. In addition to matching the detected changepoints with inspecting GPS metadata information (GPS station log files and IGSMAIL), we also allowed for possible undocumented changepoints in the GPS IWV time series.

2.6 Metrics for consistency evaluation

To evaluate the performances of the reanalyses in reproducing IWV, Kling-Gupta Efficiency (KGE) is employed as a metric. The KGE is a composite index introduced by Gupta et al. (2009) and modified by Kling et al. (2012). It takes bias, variability, and correlation into account in the equation below:

$$\text{KGE} = 1 - \sqrt{(\beta - 1)^2 + (\gamma - 1)^2 + (r - 1)^2}, \tag{9}$$

with

$$\beta = \frac{\mu_R}{\mu_G}, \tag{10}$$

$$\gamma = \frac{CV_R}{CV_G} = \frac{\sigma_R/\mu_R}{\sigma_G/\mu_G}, \tag{11}$$

and μ_R, σ_R, and CV_R are the mean value, standard deviation, and coefficient of variation of the reanalysis IWV time series, respectively. The μ_G, σ_G, and CV_G are the corresponding parameters for GPS. The β and γ indicate the consistencies in the mean and variability, respectively. In case of μ_R and μ_G being equal to zero, such as for the diurnal anomalies in Section 4.3, $\gamma = \frac{\sigma_R}{\sigma_G}$. The r indicates the Pearson correlation coefficient between the GPS and reanalyses time series. With perfect consistencies in mean, variability, and correlation, the values of β, γ, and r are identical to 1, respectively. From Eq. (9), it follows that a larger KGE score indicates a better consistency. Ideally, the KGE metric reaches its maximum of 1.

In addition, to be comparable to some previous studies, we also used the Root Mean Square estimation of the IWV differences between the reanalyses and GPS:

$$\text{RMS}_\Delta = \sqrt{\frac{\sum_{i=1}^{n}(\text{IWV}_R - \text{IWV}_G)^2}{n}}, \tag{12}$$

where IWV_R and IWV_G are the IWV time series at a specific station from reanalysis and GPS, respectively, and n is number of data points in the IWV time series.

3 Assessments of daily time series

3.1 Representativeness differences

Figure 3 compares the standard deviations of daily IWV difference (σ_Δ) and the representativeness statistic ($\delta_{\max}$) for the six reanalyses, respectively. The first point to note is that the σ_Δ and $\delta_{\max}$ are strongly correlated for all the reanalyses, with r values from 0.76 for NCEP2 to 0.90 for ERA5. The result is in line with Bock and Parracho (2019), who compared ERAI to a global GPS network. Figure 3 indicates that the representativeness differences contribute to the discrepancies between the reanalyses and GPS. The larger σ_Δ and $\delta_{\max}$ values are found at stations close to mountain or sea, such as BZRG (Bolzano, Italy, 11.34 °E, 46.50 °N) and TORI (Torino, Italy, 7.66 °E, 45.06 °N) at the foothills of the Alps, and ALME (Almería, Spain, 2.46 °W, 36.85 °N) near the west coast of Mediterranean Sea. On the whole, ERA5 is characterised by the lowest σ_Δ and $\delta_{\max}$, with values of 0.5−1.6 and 0.2−2.1 kg m^{-2}, respectively. In contrast, NCEP2 has the

largest σ_Δ and $\delta_{\max}$, with values of 1.21−3.0 and 1.98−5.2 kg m^{-2}, respectively. The difference could be due to the fact that the spatiotemporal resolution of ERA5 is much higher than NCEP2 as indicated in Table 1. This result indicates that ERA5, with improved spatiotemporal resolution and data assimilation, is capable of reducing the discrepancy and representativeness difference with respect to GPS.

3.2 Assessments using KGE

Figure 4 shows the geographical distributions of the ratio of mean β, the ratio of coefficient of variation γ, the correlation r, and the synthetic KGE metric for the six reanalyses by taking the daily GPS IWV time series as references. Moreover, the statistics of these scores are displayed in Fig. 5 with box-and-whisker plots. From the first column of Fig. 4 and Fig 5a we can see that β scores are slightly larger than 1 for all the reanalyses except JRA55, indicating a general wet bias with respect to the GPS IWV. For example, MERRA2 has the largest median β with a value of 1.04, indicating a general wet bias of 4%. In contrast,Only JRA55 scores a median β smaller than 1 (of 0.99, (Fig. 5a), indicating a slight dry bias of 1%. The wet and dry biases in the reanalyses have been partly reported by several previous studies. For instance, se results are in agreement with Schröder et al. (2018), who concludreported that CFSR, ERAI, and MERRA2 are too moist over Europe compared to the ensemble mean of various satellite and reanalysis IWV records, whereas JRA55 has negligible bias there. The wet bias in ERAI over Europe was also noted by Parracho et al. (2018). AnalyzingAnalysing the reasons of the biases is of potential interest; however, it would go beyond the scope of this paper.

Regarding the consistency in variability, most of the γ scores are less than 1, with the associated median values ranging between 0.96 and 0.98 (Fig. 5b). The results indicate a good reproduction of daily IWV variability by the reanalyses, albeit with a slight underestimation. The correlations are also pretty good with median values larger than 0.97 (Fig. 5c). However, the scores in variability and correlation are lower for the coastal stations, as shown in the second and third columns of Fig. 4, respectively. In particular, the γ and r of NCEP2 are less than 0.96 for some coastal stations located at Western and Southern Europe. This could be explained by the representativeness differences that impact the consistency of the IWV from reanalyses and GPS in their variabilitiesy. For a coastal GPS station with an on-site measurement of IWV, a part of its associated four reanalysis grid nodes may be located over the sea whereas others over land. As a consequence, the representativeness difference for such a coastal site is more severe than inland stations surrounded with flat terrain due to land-sea thermal contrast (Drobinski et al., 2018).

Figure 5d compares the overall consistency in daily IWV evaluated using KGE. It can be seen that ERA5 is characterised by the largest median KGE (0.97). The result reveals the superiority of ERA5 over the other reanalyses. Moreover, comparing β, γ, and r (Fig. 5a−c) shows that r tends to contribute the least to the overall inconsistency, indicating that improving the consistencies in mean values and variabilities are more important for the daily IWV time series.

4 Assessments of diurnal variations

Despite the atmospheric water ~~vapor~~vapour being quite unstable, it is characterised by a diurnal cycle ~~(Dai et al., 2002)~~. The diurnal IWV cycle can be driven by different mechanisms, such as evapotranspiration and condensation related to temperature, solar heating, and underlying surface conditions, as well as advection of air at different spatial scales (Dai et al., 2002; Diedrich et al., 2016; Koji et al., 2022).

In this section, the diurnal variations of IWV are investigated in two aspects: diurnal cycle and diurnal anomaly. The diurnal anomal~~y~~ies (IWV_{DA}) ~~is~~are calculated as follows (Diedrich et al., 2016; Steinke et al., 2019):

$$IWV_{DA} = IWV - \overline{IWV}, \quad (13)$$

~~$$IWV_{DA} = \frac{IWV - \overline{IWV}}{\overline{IWV}} \times 100\%, \quad (8)$$~~

where IWV is the 1-hourly IWV time series in one day and $\overline{IWV}$ is the associated daily mean.

Each station's diurnal cycle is computed by averaging its diurnal anomalies for each season separately and for the entire ~~year~~time span. Diurnal and semidiurnal harmonics are calculated with Least Squares Estimation (LSE) based on the seasonal and all-time averaged diurnal anomalies:

$$IWV(t) = \sum_{i=1}^{2} A_i \sin\left(\frac{2\pi}{24} \cdot i \cdot t + \varphi_i\right) \quad (14)$$

where t is Local Solar Time (LST) in hours, A_i and φ_i are the amplitudes and phases of the diurnal (D_1) and semidiurnal (D_2) cycles, respectively. The phases are then adjusted to the at the peaks of associated harmonics, with $\varphi_1 \in [0,24)$ and $\varphi_2 \in [0,12)$ LST in hours.~~We analyzed the amplitude and phases of each station's diurnal cycle. Note that, the amplitude is here defined as the difference between the maximum and minimum, i.e., the peak-to-peak amplitude. Moreover, the time of each station's diurnal variation is converted into the Local Time (LT).~~

4.1 ~~D~~Diurnal GPS IWV cycle

Starting with the all-time averaged amplitudes of the diurnal GPS IWV harmonic shown in Fig. 6e, two remarkable values can be first noted at stations NICO (Nicosia, Cyprus, 33.14 °N, 33.40 °E, 161.9 m) and ZECK (Zelenchuksky, Russia, 43.79 °N, 41.57 °E, 1143.4m) with values of 1.2 and 1.0 kg m^{-2}, respectively. Moreover, the diurnal harmonics at the Mediterranean Coast are generally stronger than the other regions in Europe (0.5−0.8 versus 0−0.5 kg m^{-2}). Obvious seasonal differences can also be seen in their diurnal harmonics, with significantly larger amplitudes in summer (June, July, and August; JJA) than the other seasons due to the stronger solar heating effect with minimal cloud coverage in Mediterranean summer (Enriquez-Alonso et al., 2016). However, the semidiurnal harmonics are much weaker, and their seasonal variations are less significant (Fig. 6f−j). The all-time averaged semidiurnal amplitudes are lower than 0.22 kg m^{-2}, except the two stations NICO and ZECK with values of 0.4 and 0.3 kg m^{-2}, respectively. The ratios between the all-time averaged semidiurnal and diurnal amplitudes are lower than 30% at 88% of the stations (95/108). As for the phases, the diurnal and

350 semidiurnal terms are generally consistent over seasons (Fig. k−t), and their all-time averaged peaks are within 15−21 LST and 01−06 LST at 90% of the stations (97/108), respectively.

In order to compare the characteristics of diurnal IWV amplitudes at different stations, we calculated each station's relative amplitude as the ratio between their respective (semi-) diurnal amplitudes and mean IWV as displayed in Fig. 7a and 7d. We classified the GPS stations into three types according to their geographical characteristics (Fig. 7a) and analysed their
355 relationships with each station's altitude and distance-to-sea (SeaDist). Firstly, we divided the stations with a limit of 20 km on their SeaDist. We further separated the stations located at Mediterranean Coast (MedCoast; SeaDist<20 km, 32 °N <Lat<46 °N, 5 °W <Lon<45 °E, 32 °N <Lat<46 °N) from the other coastal (OtherCoast) stations, because their characteristics are quite different as can be seen from Fig. 7a. Consequently, the 108 stations are classified into 62 Inland stations, 12 MedCoast stations, and 34 OtherCoast stations.
360 As can be seen from Fig. 7a−c, all the OtherCoast stations are lower than 300 m and their relative diurnal IWV amplitudes are the weakest, with a range from 0.3% to 1.9% and a median of 1.1%. Within the altitude limit of 300 m, the Inland stations are characterised with moderately larger diurnal amplitudes (1.5%−2.5%). The results indicate the effect of land-sea breeze circulation on mitigating the intensity of diurnal IWV cycle at the Atlantic coasts of Europe with respect to the Inland Europe. However, the land-sea breeze effect can be less significant for the MedCoast stations, because their
365 diurnal amplitudes are significantly larger (1.1%−4.2%) than the OtherCoast stations. The stronger diurnal IWV cycles at the MedCoast stations can be explained by the stronger solar heating effect at the Mediterranean Coast than the other European coasts, especially during summer daytime under stable and clear sky weather condition. In addition, it can be seen from Fig. 7b and 7e that the relative diurnal and semidiurnal IWV amplitudes are well correlated with altitudes, with correlation coeffieicents of 0.66 and 0.67, respectively. This relationship indicates the effect of orographic circulation, which can
370 enhance the diurnal range of temperature at higher altitudes (Diedrich et al., 2016).

In addition, we selected six stations with various altitudes, SeaDist, and climates to illustrate the diversity of diurnal IWV cycles in Europe as shown in Fig. 8. The climate zones of the GPS stations are classified according to Köppen Climate Classification (Beck et al., 2018) and the properties of the stations are listed in Table S2.

Station NICO is located on Cyprus Island with hot semi-arid climate (BSh). Despite only 21.5 km far away from
375 coastline, NICO has the largest diurnal IWV amplitude with a value of 1.2 kg m^{-2}, equivalent to a relative amplitude of 6.7%. This is mainly due to the large diurnal temperature range in Cyprus, especially in summer (Price et al., 1999).

Both the MedCoast station VALE (Valencia, Spain, 39.48 °N, 0.34 °W, 27.0 m) and the OtherCoast station NEWL (Newlyn, UK, 50.10 °N, 5.54 °W, 11.0 m) are very close to coastline, with SeaDist values of 1.2 and 0.5 km, respectively. However, their diurnal amplitudes are quite different (absolutely 0.8 versus 0.1 kg m^{-2}, relatively 3.9% versus 0.7%). As
380 explained earlier for the difference between the two station types, their weather conditions are different. VALE is located at Mediterranean Coast with cold semi-arid (BSk) climate. Its strong diurnal cycle, especially in summer with an amplitude of 1.4 kg m^{-2} (4.6%), is attributed to intense solar heating under minimal cloud coverage weather condition. In contrast, NEWL is located at the coast of the English Channel with temperate oceanic (Cfb) climate, and its smaller diurnal amplitude can be

due to the weaker solar heating effect under the unstable and cloudy weather condition, in addition to the land-sea breeze
effect on mitigating diurnal temperature range.

Station ZECK is in the Greater Caucasus with humid continental (Dfb) climate. Its diurnal amplitude is much stronger
than PENC (Penc, Hungary, 47.79 °N, 19.28 °E, 248.3 m) with the same climate (1.0 kg m^{-2} and 7.9% versus 0.2 kg m^{-2} and
1.5%). As ZECK is much higher than PENC, their difference in amplitude is consistent with the pattern for most Inland
stations, which can be explained by the effect of orographic circulation (Diedrich et al., 2016). In addition, KIR0 (Kiruna,
Sweden, 67.88 °N, 21.06 °E, 469.3 m) is typical for many stations in North Europe. Although its diurnal cycle is quite weak
with an amplitude of only 0.1 kg m^{-2} (1.7%), it is well fitted by the sinusoidal harmonic curve fitting.

4.2 Mismatches in diurnal ERA5 IWV cycle

Only the diurnal IWV cycle from the 1-hourly ERA5 time series was evaluated with respect to GPS, as the temporal
resolutions of the other reanalyses are too coarse to characterise the diurnal cycle. However, we found significant shifts in
the diurnal IWV anomalies between 09 and 10 (10-09) UTC as well as between 21 and 22 (22-21) UTC at part of the
stations, such as NEWL and PENC displayed in Fig. 8. The ERA5 developers have noticed such mismatches in the diurnal
cycles of individual meteorological variables, such as its near surface wind, temperature, and humidity products (see Known
Issues 8 and 9 in https://confluence.ecmwf.int/display/CKB/ERA5%3A+data+documentation#ERA5:datadocumentation-
Knownissues), and the problem is attributed to the edge effect in each ERA5 assimilation cycle (from 10 to 21 UTC and
from 22 to 09 UTC +1 day). However, according to our knowledge, the magnitude of the mismatch in the diurnal cycle of
ERA5 IWV and its spatiotemporal characterisations have not been investigated yet. Therefore, we will quantify and analyse
the mismatch in the ERA5 IWV over Europe in this section.

Figure 9 compares the diurnal IWV cycle from ERA5 and GPS for each season at station PENC. From this figure, we
can derive that there are no mismatches in the diurnal GPS IWV cycle, although the GPS IWV (slightly) relies on T_m (hence
humidity and temperature) from ERA5 for the ZTD to IWV conversion, as shown in Eq. (2). GPS IWV estimates are
therefore regarded as reference data to evaluate the mismatches in the diurnal cycle of ERA5 IWV. At station PENC, the
mismatches in ERA5 are seasonal dependent, which are strongest in summer (JJA) but weakest in winter (DJF).

Figure 10 compares the shifts at 10-09 UTC and 22-21 UTC from ERA5 and GPS at all the stations, respectively. The
shifts in the GPS IWV cycle are regarded as reference, representing the natural IWV changes at the two epochs. As can be
seen from Fig. 10a−e and 10k−o, the ERA5 IWV series generally drop from 09 to 10 UTC and then jump from 21 to 22
UTC. The ERA5 artificial shifts at the two epochs are most significant in summer, with average values of -0.23 and 0.35 kg
m^{-2}, respectively. In contrast, the average natural shifts in summer estimated from GPS IWV are only 0.11 and -0.08 kg m^{-2}
respectively. Moreover, the all-time averaged natural shifts in GPS IWV are only 0.05 and -0.05 kg m^{-2}, respectively.
However, the artificial shifts in ERA5 IWV are -0.08 and 0.19, respectively. As can be seen from the geographic
distributions of the shifts shown in Fig. 10e and 10o, the ERA5 shifts at 10-09 UTC are most significant at the Alps and
Eastern Europe, whereas the shifts at 22-21 UTC are more widespread in Central Europe. The reasons for their geographical

patterns are unknown and needs further investigation. Since the average diurnal amplitude of the reference GPS IWV is only 0.32 kg m^{-2}, the artificial shifts in ERA5 IWV cannot be ignored when analysing the diurnal IWV cycle in these regions.

tend to increase equatorward, with values ranging from 2% to 18%. This finding is in line with the amplitude of the IWV itself, although we consider relative amplitudes here. However, lower latitude stations also experience higher temperature contrasts over a day than higher latitude stations (Sharifnezhadazizi et al., 2019), and the IWV diurnal variability is mainly governed by the temperature diurnal variability (see Wang et al., 2016). Moreover, Fig. 7a shows that the diurnal amplitudes of GPS IWV are well correlated with station heights ($r = 0.7$). Diedrich et al. (2016) also reported the height dependence in a global analysis and attributed it to orographic circulation which enhances the temperature difference between day and night at higher altitude stations. Similar geographical patterns arise for the seasonal-averaged amplitudes (Fig. 6a-d), with identical explanations as for the overall average. An obvious feature is that the amplitudes in spring (MAM) and summer (JJA) are generally larger than those in autumn (SON) and winter (DJF), as also noted by Diedrich et al. (2016) and Steinke et al. (2019). Not only the season-dependent diurnal temperature variability plays a role in explaining this feature, but other factors also have an impact as well (Dai et al., 2002). For instance, evapotranspiration, another primary cause of the diurnal cycle of IWV, is lowest in winter (DJF) due to least transpiration of vegetation.

Concerning the phase of the IWV diurnal cycle, the GPS measurements show that most of the IWV cycles reach their minima between 5:00-12:00 LT and then peak around 16:00-24:00 LT (Fig. 6f-o). The minimum and maximum values of the yearly-averaged diurnal cycles occur around 8:00 and 19:00 LT, respectively. The result could be explained by the fact that solar insolation during the day enhances evapotranspiration and accumulates water vapor until sunset.

All the reanalyses successfully reproduce the IWV's diurnal cycle as shown in Fig. 8a-c. However, MERRA2 only scores a median KGE value of 0.62, lower than the scores of CFSR, ERAI, and JRA55 (0.71-0.75) which have a coarser original temporal resolution (6-hourly versus 3-hourly). The poor performance of MERRA2 is mostly due to its overestimation of the variability of diurnal cycle (Fig. 8a). A similar overestimation of diurnal amplitude was reported by Wang et al. (2017) in an inter-comparison of GPS and MERRA (the ancestor of MERRA2) in the southern Tibetan Plateau. In that work, the authors suggested that it could be due to an exaggerated land evaporation in MERRA (Mueller and Seneviratne, 2014), which might also exist in MERRA2 over Europe. In contrast, ERA5 reproduces the best variability (median γ=0.98). However, it only scores a median KGE of 0.72, which is at the same level of CFSR, ERAI, and JRA55. This is mainly due to its weaker correlation (Fig. 8b). Therefore, though ERA5 and MERRA2 have higher temporal resolutions than the others, future work is certainly required to improve their capabilities in reproducing the phase and amplitude of diurnal cycles of IWV, respectively.

4.3~~2~~ Diurnal anomalies

Diurnal anomaly represents high-frequency variations of IWV, associated with weather phenomena like heavy rainfall. Therefore, evaluations on the consistencies between the IWV diurnal anomalies from reanalyses with respect to GPS are

conducive to a better understanding on their performances in extreme weather, especially for ERA5 with a significantly enhanced temporal resolution of 1-hour.

We first evaluated all the reanalyses with respect to GPS at 1-hour temporal resolution. For the reanalyses with coarser resolutions (3-hour and 6-hour), we interpolated their time series to 1-hour by using cubic spline, which is slightly superior to linear interpolation. Statistics of the evaluation results are listed in Table 2. At the temporal resolution of 1-hour, ERA5 scores the highest average γ, r, and KGE with values of 0.98, 0.89, and 0.88, respectively. The results indicate that the 1-hourly ERA5 diurnal anomalies has the best agreement with GPS in variability and correlation. However, NCEP2 performs the worst, as it scores the lowest γ, r, and KGE with values of 0.75, 0.69, and 0.60, respectively. To be comparable to many other studies, we also evaluated the consistencies by using the more commonly used indicator — RMS of IWV difference (RMS_Δ) as shown in Eq. (12). Results show that ERA5 and NCEP2 score the lowest and largest average RMS_Δ values of 0.97 and 1.57 kg m^{-2}, respectively. Therefore, we drew the same conclusion as from the KGE scores. The evaluations confirm the superiority of the 1-hourly ERA5 over the other reanalyses, most likely because of its enhanced spatiotemporal resolutions and other improvements in data assimilation.

For a fairer intercomparison, we also evaluated ERA5 and the other reanalyses at their respective native resolutions. Accordingly, we extracted the ERA5 IWV every 3 and 6 hours. The comparison with MERRA2 at its native resolution of 3-hour shows that, ERA5 achieves larger KGE (0.89 versus 0.86) and smaller RMS_Δ (0.97 versus 1.15 kg m^{-2}). Moreover, the average KGE value of the 6-hourly ERA5 IWV is 0.89, which is higher than CFSR, ERAI, JRA55, and NCEP2, with values of 0.86, 0.83, 0.79, and 0.60, respectively. The results indicate that ERA5 is still superior to the other reanalyses at the coarser temporal resolutions.

Figure 9 compares the diurnal anomalies derived from reanalyses with respect to GPS. To be consistent with the temporal resolution of GPS and ERA5, the diurnal anomalies of the other reanalyses are linearly interpolated into 1-h time series. It is observed that the anomalies roughly range from −100% to 200% of the associated daily mean IWV, indicating that the diurnal variations of IWV are much stronger than the diurnal cycles. It can also be seen that the range of GPS diurnal anomalies is larger in winter than in summer, suggesting a more intensive relative variability compared to the associated daily mean IWV. It could be due to the fact that the daily mean IWV is much lower in winter than in summer.

Figure 8d-f shows the KGE scores of the reanalyses in reproducing diurnal anomaly of IWV. It can be seen that the median KGE scores of ERA5 and MERRA2 are 0.90 and 0.77, respectively. Their scores are much better than the other four reanalyses with median scores between 0.39 and 0.58. This is not surprising as ERA5 and MERRA2 have the highest initial temporal resolution (Table 1). Therefore, ERA5 is recommended in studies of high-frequency IWV variations.

5 Assessments of annual ~~and inter-annual variations~~cycle

~~5.1 Annual cycle~~

480   We ~~analyzed~~analysed the annual ~~and inter-annual variations~~cycles of IWV ~~using~~of the homogenised monthly ~~mean~~GPS IWV time series~~. The annual GPS IWV cycle~~ as shown in Fig. 11a~~, as a function of~~with increasing latitude from bottom up~~, is shown in Fig. 10a~~. ~~Most of T~~the annual IWV cycles reach their maxima ~~mostly~~ in July and August, with peak values from ~~17~~17.1 to 32.2 kg m^{-2}. In contrast, the minima of the annual cycles are ~~noted~~ typically in January and February, with values from 4.2 to 17.1 kg m^{-2}. ~~The results are consistent with those of Wypych et al. (2018).~~ The maximum and minimum values

485   of the annual cycles are generally increasing with decreasing latitude (Fig. 10a) and decreasing altitude (not shown).

Figure 11 ~~0~~b−g present the differences between the annual cycle of IWV estimated by the reanalyses with respect to GPS. It can be seen that ERA5 has the least differences. Indeed, the quantitative evaluation shows that ERA5 obtains the highest median KGE score having a value of 0.97 (Fig. 5h), indicating that it outperforms the other reanalyses. CFSR ranks last (median KGE=0.94) due to its overestimation of mean values (median β=1.04) and underestimation of variability

490   (median γ=0.96). Moreover, although the consistencies between the annual IWV signals from ~~median KGE scores of the other~~ reanalyses and GPS are ~~also~~generally rather good ~~(>0.94)~~, there could be significant discrepancies in specific seasons and regions. For example, JRA55 has an average dry bias of 0.5 kg m^{-2} with respect to the GPS IWV from May to September at the stations in the south (32 °N−48 °N, Fig. 11e), whereas NCEP has obvious wet biases (0.7−2.4 kg m^{-2}) in the annual average of IWV with respect to the GPS results at low latitudes (32 °N−40 °N, Fig. 11g). In addition, significant

495   biases (1.2−5.9 kg m^{-2}) from March to September can be seen at station BZRG in the evaluations of CFSR, ERAI, and MERRA2. The discrepancies are most likely related to the remarkable representativeness differences between the reanalyses and GPS at BZRG (Fig. 3), which is located in the Alps.

~~. The results indicate that all the reanalyses reproduce the annual cycle of IWV quite well, with ERA5 slightly outperforming the other reanalyses.~~

500   **~~5.2 Interannual variations and teleconnections~~**

~~The interannual variations of IWV are investigated by using its monthly relative anomalies. The relative anomaly of a month is calculated as the ratio between the IWV change of that month relative to the multiyear mean value of that month. The monthly relative anomaly time series of GPS IWV are presented in Fig. 11a with decreasing latitudes. It could be noted that the majority of robust IWV anomalies occurs in winter (DJF), with amplitudes as large as 50%. Those winter IWV~~

505   ~~anomalies are found to be linked to NAO, with a pattern that the NAO index and IWV anomalies are strongly positively correlated in Northern Europe and slightly negatively correlated in Southern Europe (Fig. 11d). This finding points to a wetter (drier) weather condition in Northern Europe and a drier (wetter) condition in Southern Europe when NAO is in its positive (negative) phase. The spatial pattern is in line with Trigo et al. (2002) and can be explained by the fact that during positive NAO phase, the path of moisture transport turns towards a more northeast orientation over the North Atlantic than~~

usual, and thus results in enhanced (reduced) moisture transport over Northern (Southern) Europe (Hurrell, 1995). The modulation of NAO on the IWV over Europe is also consistent with its influence on temperature and precipitation. Previous studies have demonstrated that a positive NAO phase tends to be accompanied by reinforced westerly winds over the North Atlantic, which is conducive to above-average temperature and precipitation over Northern Europe as well as below-average precipitation over Southern Europe (e.g., Hurrell 1995). During negative NAO phases, opposite patterns of temperature and precipitation anomalies are expected.

In addition, the IWV anomalies in winter are also significantly correlated to the EA pattern (Fig. 11e). The positive correlation between EA and IWV over Europe indicates a wetter (drier) condition with positive (negative) EA phase. This teleconnection could be attributed to the influence of EA on atmospheric circulation. The winter positive (negative) EA phase indicates a dominating zonal (meridional) circulation (Mikhailova and Yurovsky et al., 2016). Hence, EA can modulate heat and moisture transport. A positive EA index in winter indicates a higher likelihood of higher-than-usual temperature over Europe, enhanced precipitation in Northern Europe, and precipitation deficiency in Southern Europe. By contrast, a negative EA index is likely to result in opposite influences on temperature and precipitation.

As the winter atmospheric circulation over the Atlantic/European sector can be mostly represented by NAO and EA, the joint effects of NAO and EA on the winter IWV anomalies are investigated with four cases, namely (i) both NAO and EA are positive, (ii) NAO is positive whereas EA is negative, (iii) NAO is negative whereas EA is positive, and (iv), both NAO and EA are negative:

(i) Both NAO and EA are positive
The winters of 2013/2014 and 2015/2016 are characterized by pronounced positive IWV anomalies (Fig. 11a). The results could be explained by the positive NAO and EA indices anomalies (Fig. 11b-c), which indicate a general milder and wetter condition over Europe. For instance, the two winters are the wettest winters for the British Isles since 1850 with rainfall totals over 500 mm (McCarthy et al., 2016).

(ii) Positive NAO and negative EA
The IWV deficiencies in Southern Europe are striking in the winters of 2004/2005 and 2011/2012. This could be associated with the positive NAO and negative EA during the two winters. In this scenario, Southern Europe tends to experience colder and drier winter (Santos et al., 2013; Mellado-cano et al., 2019).

(iii) Negative NAO and positive EA
In contrast to the spatial pattern in the winter of 2011/2012, the winter of 2009/2010 witnessed pronounced IWV deficiencies in Northern Europe. The contrasting patterns of IWV anomaly could be due to the fact that the conditions of atmospheric circulations are different between these two winters, with positive NAO and negative EA in the winter of 2011/2012 but opposite phases in the winter of 2009/2010 (Santos et al., 2013). Especially the winter of 2009/2010 was marked by one of the most negative winter NAO during the last 150 years (Jung et al., 2011), which resulted in enhanced northerly surface winds towards Northern Europe from the cold and dry Arctic (Wang et al., 2010).

(iv) Both NAO and EA are negative

Northern Europe experienced a more severe IWV deficiency in the winter of 2010/2011. Comparing the December IWV anomalies of 2009 and 2010, we can find that the IWV deficiency in December 2010 is more severe. During these two December months, the NAO indices are strongly negative, indicating colder and drier-than-usual climate conditions in Northern Europe (Taws et al., 2011). However, the EA phases were slightly positive in December 2009 (Case iii here above) and negative in December 2010. Therefore, in this latter case, that negative EA strengthens the cold and dry effects due to the negative NAO, as also shown by Moore and Renfrew 2012. Therefore, the combination of negative NAO and EA indicates a more severe IWV deficiency in Northern Europe.

In addition to wintertime, the NAO and EA could also contribute to extreme IWV anomalies in other seasons. For example, Northern Europe experienced a significant negative IWV anomaly in March 2013, which could be associated with the strongly negative NAO and slightly negative EA as described in Case iv.

IWV anomalies might also be linked to other teleconnection indices (e.g., Wang et al., 2018; Thomas et al., 2021). For example, Fig. 11f illustrates that the winter IWV anomaly over Europe is well correlated with AO in a similar spatial pattern as for the NAO (Fig. 11d). This is not surprising as the AO and NAO indices are highly correlated and they are even used interchangeably in some literature (e.g., Cohen et al., 2014), albeit their definitions are different (Ambaum et al., 2001). In addition, the correlations between the winter IWV anomalies and other indices, such as the SCA, WeMO, Niño 3.4, NOI, and QBO, were also examined and displayed in Fig. 11g-k. The results show that all these indices, except for the QBO, are correlated with the winter IWV anomalies at least in some parts of Europe. However, most of their correlation coefficients are within ±0.4, hence weaker than the correlations for NAO/AO and EA. Our correlation analysis concludes that NAO/AO and EA are the dominant patterns among the teleconnection indices for the modulation of winter IWV over Europe. However, this does not mean that the other patterns might not play a role for specific extreme events. For example, the excess of IWV over Europe in the winter of 2015/2016 could also be linked to the concurrent super El Niño (ENSO) event (Stockdale et al., 2017). Moreover, although we successfully explained some of the IWV winter extremes in Europe with the four different phase combinations of NAO and EA, we must mention that the strengths and durations of the NAO and EA phase change from year to year, and that the atmospheric circulations over the Atlantic/European sector cannot be completely represented by the NAO and EA pattern. Therefore, future in-debt spatiotemporal analysis is necessary to clearly demonstrate the links between the IWV anomaly and the teleconnection indices.

The performances of the reanalyses in reproducing the interannual variations of IWV is evaluated by taking the GPS IWV anomaly as reference. The six reanalyses achieved KGE scores larger than 0.9 at most of the stations as shown in Fig. 8i. Their median KGE scores are between 0.93 and 0.97, proving that all of them are able to reproduce well the interannual IWV variations over Europe. However, the median γ scores of the six reanalyses are between 0.96 and 0.98, indicating that they slightly underestimated the variability of 1-monthly IWV anomaly. JRA55 outperforms the other reanalyses (median KGE=0.97) as it reproduces the variability of IWV anomaly the best (median γ=0.98). ERA5 only ranks second (median KGE=0.96) though it reached the highest correlation (median r=0.99). This is mostly due to its relatively lower γ (median

γ=0.96). Therefore, the performance of ERA5 in reproducing the variability of monthly IWV anomaly over Europe could be further improved.

6 Assessments of linear trends

We carried out a homogenisation of the GPS IWV time series by using the RHtestsV4 software (Wang and Feng, 2013) before the analysis. The software is dedicated to the homogenisation of climatic time series. In addition, we adopted a homogenisation strategy which allows for changepoints with and without support from metadata. We took all the six reanalyses as references and attempted to avoid the impacts of possible changepoints in specific reanalyses. However, we did not homogenise the reanalyses IWV time series because they represent the native quality of the reanalyses that we would like to assess. The homogenisation approach is detailed in Appendix A.

We then estimated the linear IWV trends from all the six reanalyses and the homogenised GPS IWV time series after the removal of annual cycle. In order to obtain realistic uncertainties of the trend estimates, we analysed the time series by using the Hector software version 1.7.2 (Bos et al.,2019). We tested four commonly used noise models, namely White Noise (WN), first-order AutoRegressive AR(1), AutoRegressive Moving Average ARMA(1,1), and Power-Law noise (PL). We then selected the optimal model of each time series by using Bayesian information criterion (BIC; Schwarz, 1978). Readers are referred to Yuan et al. (2021) for more details. The IWV trend estimates, associated uncertainties, and specific optimal noise models are listed in Table S3.

Figure 12a shows the GPS IWV trends after the homogenisation. The IWV trends generally increase from the Atlantic coasts towards southeast. The average trends of the OtherCoast, Inland, and MedCoast stations are 0.2, 0.5, and 0.9 kg m^{-2} decade^{-1}, respectively. The corresponding relative IWV trends are 1.7%, 3.1%, and 5.0% per decade (Fig. 12d), respectively. The largest trend is found at station TUBI (Gebze, Turkey, 29.5 °E, 40.8 °N), with a value of 1.6 kg m^{-2} decade^{-1} (8.7% decade^{-1}). As can be seen from Fig. 12b, AR1 is the optimal noise model at 58% of the stations (63 out of 108), which are mostly located close to sea or in Northern Europe. Most parts of Central Europe are characterised by WN, whereas Belgium and central Germany are best modelled by ARMA11. In addition, PL is superior to the other models at four stations. The optimal noise models for the monthly IWV time series of the six reanalyses show similar geographical patterns as the GPS IWV. The geographical patterns of the optimal noise models obtained in this study are different from Yuan et al. (2021), although the geographical patterns of the IWV trends are consistent to previous studies (Parracho et al., 2018; Nguyen et al., 2021; Yuan et al., 2021). It is most likely due to the difference that monthly IWV time series are used here, whereas daily IWV series were used in that work. The relative trends are characterized by a similar geographical pattern, with values from −0.5 to 8.2 % decade⁻¹. The geographical pattern and magnitudes of the GPS IWV trends are in line with earlier studies (Alshawaf et al., 2018; Yuan et al., 2021).

We evaluated the The relative IWV trends derived from the six reanalyses by taking the trends from the homogenised GPS IWV time series as reference. We compared the difference in relative IWV trend rather than their absolute trends were

compared to GPS for two reasons. One reason is~~because~~ that the relative trend is not affected by the ~~IWV~~ IWV bias in

610   individual reanalysis. ~~The other reason is that the relative IWV trend is related more directly to the temperature variation, with the well-known Clausius-Clapeyron relationship that states that water vapor holding capacity increases by 7% with a rise of 1 K in temperature (Trenberth et al. 2003).~~ As can be seen in Fig. 13, ~~Figure 13 compares the relative IWV trends from the six reanalyses against GPS. The KGE score of ERA5 is 0.76, higher than all the other reanalyses' scores. It is no wonder because the ERA5 IWV time series were used for the homogenization of the GPS time series (Yuan et al., 2021).~~

615   ~~The ERAI, JRA55, and MERRA2 also achieved rather good KGE scores, with values of 0.73, 0.72, and 0.72, respectively. The results indicate that these reanalyses are also good datasets for IWV trend reproduction. However, the KGE scores of CFSR and NCEP2 are much lower, with values of 0.48 and 0.20, respectively. This is mostly due to their deficiencies in correlation (0.55 and 0.52, respectively). Moreover, NCEP2 generally overestimated the IWV trends (β=1.61).~~ ERA5 shows the best agreement in IWV trends with respect to GPS, with a mean value and a standard deviation of 0.01% decade^{-1} and

620   0.97% decade^{-1} in their trend differences, respectively, indicating an improvement compared to its predecessor ERAI (-0.04±1.15% decade^{-1}). JRA55 also only have an average trend difference as low as 0.01% decade^{-1} but with a slightly larger standard deviation (1.12% decade^{-1}) than ERA5. Compared to the GPS IWV trends, MERRA2 has an underestimation of 0.22% decade^{-1} on average (Fig. 13e), whereas CFSR resulted in an overestimation by 0.22% decade^{-1} (Fig. 13a). The standard deviation of the CFSR-GPS IWV trend differences is as large as 1.73 % decade^{-1}, which is mainly caused by the

625   significant differences from -5.1% decade^{-1} to 4.9% decade^{-1} in South Europe (Fig. 13a). The results suggest that the CFSR IWV trends is less accurate in Southern Europe and should be carefully validated before climate change analysis.

    In addition, Fig. 13f shows that the mean value and standard deviation of NCEP2-GPS IWV trend differences are 1.61% decade^{-1} and 1.86% decade^{-1}, respectively, indicating a general overestimation of IWV trends from NCEP2 with respect to GPS. In particular, the average NCEP2-GPS IWV trend differences is as large as 2.9% decade^{-1} at 31 stations

630   located in Southern Europe (32 °N <Lat<46 °N, 10 °W <Lon<25 °E). However, NCEP2 underestimates the trends by at two stations in Eastern Mediterranean, with an average difference of -3.1% decade^{-1} compared to GPS IWV. Therefore, we concluded that the NCEP2 IWV trends are not qualified for climate change analysis in Europe.

7 Conclusions

635   In this study, Integrated Water ~~Vapor~~Vapour (IWV) time series for the period 1994−2018 were retrieved from continuous GPS observations ~~of~~ at 108 ground-based GPS stations in Europe, with an average period of 21 years for those time series. The temporal features of Europe's IWV, such as its diurnal cycle and variation, annual cycle ~~and interannual variation~~, and linear trend were then investigated. Moreover, the performances of six frequently used global atmospheric reanalyses in Europe were assessed for the first time, namely CFSR, ERA5, ERA-Interim (ERAI), JRA55, MERRA2, and

640   NCEP2. The main findings are summarised here below.

(i) The agreement between the daily GPS IWV time series and the six reanalyses are found to be best for ERA5 and worst for NCEP2, with standard deviations of IWV differences of 0.5−1.6 and 1.2~~1~~−3.0 kg m^{-2}, respectively. The standard deviations of IWV differences are well correlated with representativeness statistics of the six reanalyses, indicating that the representativeness differences contribute to the discrepancies between the reanalyses and GPS.

(ii) ~~(ii)~~ The ~~peak-to-peak~~ diurnal amplitudes are 0−1.2 kg m^{-2}~~-~~, account for 20~~%~~~~1~~8% of the associated daily mean IWV. The semidiurnal amplitudes are weaker, with values lower than 30% of the diurnal amplitudes at 88% of the stations. The peaks of the diurnal and semidiurnal harmonics are within 15−21 LST and 01−06 LST at 90% of the stations, respectively. The diurnal amplitudes are larger at the Mediterranean Coast (1.1%−4.2%), which is most likely because of stronger solar heating effect. In comparison, the diurnal amplitudes at other coastal regions in Europe are lower (0.3%−1.9%), which can be due to land-sea breeze and weaker solar heating effect. In addition, the relative diurnal and semidiurnal IWV amplitudes are correlated with altitudes with correlation coefficients of 0.66 and 0.67, respectively, which can be related to orographic circulation.

(iii) Mismatches in the diurnal cycle of ERA5 IWV product were found and evaluated between 09 and 10 UTC as well as between 21 and 22 UTC. The problem can be attributed to the edge effect in each ERA5 assimilation cycle, and it has been noticed in some other meteorological variables provided by ERA5. The average artificial shifts in ERA5 IWV are -0.08 and 0.19 kg m^{-2} at the two epochs, respectively. In contrast, the natural shifts in GPS IWV are 0.05 and -0.05 kg m^{-2}, respectively. The ERA5 shifts are dependent on seasons and locations. The ERA5 shifts are more significant in summer than in winter. Moreover, the ERA5 shifts from 09 to 10 UTC are most significant at the Alps and Eastern Europe, whereas the shifts from 21 to 22 UTC are more widespread in Central Europe. As the average diurnal IWV amplitude obtained from GPS is only 0.32 kg m^{-2}, the artificial shifts in ERA5 IWV cannot be ignored in diurnal IWV cycle analysis in these regions

(iv) Regarding diurnal IWV anomalies, ERA5 shows the best consistency with GPS at a temporal resolution of 1-hour, with an average RMS of IWV difference (RMS$_\Delta$) of 0.97 kg m^{-2}, whereas the average RMS$_\Delta$ are 1.14−1.57 kg m^{-2} for the others five reanalyses. ERA5 also outperforms the other reanalyses at their respective resolutions (3-hour and 6-hour), indicating the benefits from its enhanced spatial resolutions and other improvements in data assimilation, in addition to its higher temporal resolution.

~~The amplitudes are generally negatively correlated with station latitudes and positively correlated with station heights. Most of the diurnal cycles reach their minima between 5:00-12:00 Local Time (LT) and then peak around 16:00-24:00 LT. The diurnal IWV variations are much stronger than their cycles, with anomalies roughly ranging from −100% to 200% of the associated daily mean IWV. Owing to higher temporal resolutions, ERA5 and MERRA2 outperformed the other four reanalyses in reproducing 1-hourly diurnal anomalies of IWV with median KGE scores of 0.90 and 0.77, respectively. However, ERA5 slightly underperformed ERAI in modelling diurnal IWV cycles, and MERRA2 tended to overestimate the diurnal amplitudes. Further developments are needed for ERA5 and MERRA2 to enhance their capabilities in modelling the diurnal cycle of IWV.~~

(~~iii~~v) All the monthly IWV time series are modulated with apparent annual cycles, with minima in January and February (4–17 kg m^{-2}) and maxima in July and August (17–32 kg m^{-2}). The maxima and minima of the annual cycles show consistent geographical patterns, with larger values towards the equator and at lower altitude sites. ERA5 ranks the first in modelling the annual cycles of IWV (median KGE=0.97) with respect to GPS IWV, CFSR ranks last (median KGE=0.94) due to its overestimation of mean values (median β=1.04) and underestimation of variability (median γ=0.96).

~~(iv) The interannual variations of IWV over Europe are most significant in winter, with extreme values as large as ±50% of the associated monthly averages. The winter interannual variations are linked to many teleconnection patterns, especially the North Atlantic Oscillation (NAO) and East Atlantic (EA) pattern. The NAO positive (negative) phase in winter indicates an enhanced (deficient) IWV in Northern Europe and a deficient (enhanced) IWV in Southern Europe. The winter phase of the EA pattern is positively correlated with the IWV anomaly over Europe. All the six renalyses are capable of reproducing the interannual variations very well, with most of their KGE scores larger than 0.9. However, they slightly underestimate the magnitudes of the extreme values with median γ ranging from 0.96 to 0.99.~~

(v~~i~~) Europe's IWV is increasing as observed from more than two decades of continuous GPS observations. The trends generally increase from the Atlantic Coast towards southeast. The average trends of the Atlantic coasts, Inland Europe, and Mediterranean coasts are 0.2, 0.5, and 0.9 kg m^{-2} decade^{-1}, which are equivalent to relative values of 1.7%, 3.1%, and 5.0% per decade, respectively. The monthly IWV time series are best modelled by first-order AutoRegressive (AR1) noise at most stations located close to sea and Northern European, whereas AutoRegressive Moving Average ARMA(1,1) and White Noise (WN) and ARMA11 models are preferred at the rest stations. Power-Law noise (PL) is found to be optimal at only four stations. As for the performances of the reanalyses in reproducing IWV trends, ERA5 achieves the best consistency with GPS IWV trends, with a mean value and a standard deviation of 0.01% decade^{-1} and 0.97% decade^{-1} in their trend differences, respectively. However, CFSR is not qualified for the analysis of IWV trends in Southern Europe, due to its significant discrepancies with respect to GPS. The NCEP2 IWV trends over the whole Europe are also not recommend for the same reason.~~Europe's IWV is increasing as observed from more than two decades of continuous GPS observations. The trends are generally 0-0.4 kg m^{-2} decade^{-1} in Northern Europe, such as Iceland, British Isles, Fennoscandian Peninsula, Jutland Peninsula, and the western and northern coastal regions of the central European mainland. Stronger IWV trends (generally 0.4-1 kg m^{-2} decade^{-1}) are observed in Southern Europe, i.e., the Iberian Peninsula, the Italian Peninsula, the Balkan Peninsula, and the islands in the Mediterranean Sea. The largest trend is found at station TUBI in Gebze, Turkey (29.5°E, 40.8°N), with a value of 1.5 kg m^{-2} decade^{-1}. ERA5 achieves the best consistency with GPS IWV trends (KGE=0.76) but it has been used to homogenize the GPS IWV time series. In contrast, NCEP performs the worst in reproducing the IWV trends (KGE=0.20) primarily because of its pronounced overestimation of the IWV trends (β=1.61) and relatively poor correlation with the GPS trends (r=0.52).~~

Overall, it can be concluded that the reanalyses successfully reproduce the spatiotemporal IWV variability over Europe, as assessed ~~with~~ by using the GPS IWV dataset, with ERA5 slightly outperforming the other reanalyses at most temporal

scales. It is noteworthy that the pressure and weighted mean temperature obtained from ERA5 were used in the conversion of GPS ZTD to IWV ~~D~~due to the lack of long-term accurate and complete *in-situ* meteorological observations at the GPS stations~~, pressure and weighted mean temperature obtained from ERA5 were used in the conversion of GPS ZTD to IWV~~. This could partly contribute to the superior agreement between the IWV from ERA5 and GPS. Future studies could validate the IWV products of reanalyses using ground-based GPS when independent, quality-assured, and complete meteorological observations at the GPS stations are available. IWV measurements from other techniques could also be helpful.

Data availability. The GPS ZTD data were provided by NGL (http://geodesy.unr.edu). The ERA5 and ERAI data were downloaded from the climate data store (https://cds.climate.copernicus.eu) and ECWMF (https://www.ecmwf.int), respectively. The CFSR and JRA55 data are available in the research data archive of NCAR (https://rda.ucar.edu). MERRA2 data were derived from NASA Goddard earth sciences data and information services center (https://disc.gsfc.nasa.gov). NCEP2 data were obtained from NOAA/OAR/ESRL physical sciences laboratory (https://psl.noaa.gov). ~~The AO, EA, NAO, Niño 3.4, and SCA indices were provided by the Climate Prediction Center (CPC) of NOAA (https://www.cpc.ncep.noaa.gov). The NOI, QBO, and WeMO indices were obtained from the Environmental Research Division (ERD) of NOAA (https://oceanview.pfeg.noaa.gov), the Physical Sciences Laboratory (PSL) of NOAA (https://www.cpc.ncep.noaa.gov), and the Climatology Group of University of Barcelona (http://www.ub.edu/gc/wemo), respectively.~~ The GNSS IWV time series are available from the corresponding author upon reasonable request.

Author contributions. PY: Conceptualisation, Methodology, Formal analysis, Investigation, Writing Original Draft, and Visualisation. RV, XY, HV, WJ, JA, and BH: Investigation and Reviewing. HK: Investigation, Reviewing, Supervision, Project administration, and Funding acquisition.

Competing interests. The authors declare that they have no competing interests.

Acknowledgements. We are grateful to NGL for providing the GPS ZTD products and many institutions for sharing the continuous GPS observations. We thank ECMWF, JMA, NASA GAMO, and NCEP for providing the reanalyses products. ~~We also would like to thank the CPC, ERD, and PSL of NOAA, as well as the Climatology Group of University of Barcelona for providing the climate indices.~~ This work was performed under the German Research Foundation (DFG, project number: 321886779) and the Program for Hubei Provincial Science and Technology Innovation Talents of China (grant number: 2022EJD010).

References

Alshawaf, F., Zus, F., Balidakis, K., Deng, Z., Hoseini, M., Dick, G., and Wickert, J.: On the Statistical Significance of Climatic Trends Estimated From GPS Tropospheric Time Series, J. Geophys. Res.: Atmos., 123, 10,967-10,990, https://doi.org/10.1029/2018JD028703, 2018.

Ao, C. O., Meehan, T. K., Hajj, G. A., Mannucci, A. J., and Beyerle, G.: Lower troposphere refractivity bias in GPS occultation retrievals, J. Geophys. Res.: Atmos., 108, https://doi.org/10.1029/2002JD003216, 2003.

Awange, J.: GNSS Environmental Sensing, Springer International Publishing, Cham, https://doi.org/10.1007/978-3-319-58418-8, 2018.

Beck, H. E., Zimmermann, N. E., McVicar, T. R., Vergopolan, N., Berg, A., and Wood, E. F.: Present and future Köppen-Geiger climate classification maps at 1-km resolution, Sci Data, 5, 180214, https://doi.org/10.1038/sdata.2018.214, 2018.

Beirle, S., Lampel, J., Wang, Y., Mies, K., Dörner, S., Grossi, M., Loyola, D., Dehn, A., Danielczok, A., Schröder, M., and Wagner, T.: The ESA GOME-Evolution "Climate" water vapor product: a homogenized time series of H_2O columns from GOME, SCIAMACHY, and GOME-2, Earth Syst. Sci. Data, 10, 449–468, https://doi.org/10.5194/essd-10-449-2018, 2018.

Bernet, L., Brockmann, E., von Clarmann, T., Kämpfer, N., Mahieu, E., Mätzler, C., Stober, G., and Hocke, K.: Trends of atmospheric water vapour in Switzerland from ground-based radiometry, FTIR and GNSS data, Atmos. Chem. Phys., 20, 11223–11244, https://doi.org/10.5194/acp-20-11223-2020, 2020.

Bertiger, W., Bar-Sever, Y., Dorsey, A., Haines, B., Harvey, N., Hemberger, D., Heflin, M., Lu, W., Miller, M., Moore, A. W., Murphy, D., Ries, P., Romans, L., Sibois, A., Sibthorpe, A., Szilagyi, B., Vallisneri, M., and Willis, P.: GipsyX/RTGx, a new tool set for space geodetic operations and research, Adv. Space Res., 66, 469–489, https://doi.org/10.1016/j.asr.2020.04.015, 2020.

Bevis, M., Businger, S., Herring, T., Rocken, C., Anthes, R., and Ware, R.: GPS Meteorology: Remote Sensing of Atmospheric Water Vapor Using the Global Positioning System, J. Geophys. Res., 97, https://doi.org/10.1029/92JD01517, 1992.

Blewitt, G., Hammond, W. C., and Kreemer, C.: Harnessing the GPS data explosion for interdisciplinary science, Eos, 99, 485, https://doi.org/10.1029/2018EO104623, 2018.

Bock, O. and Parracho, A. C.: Consistency and representativeness of integrated water vapour from ground-based GPS observations and ERA-Interim reanalysis, Atmos. Chem. Phys., 19, 9453–9468, https://doi.org/10.5194/acp-19-9453-2019, 2019.

Bock, O., Keil, C., Richard, E., Flamant, C., and Bouin, M.: Validation of precipitable water from ECMWF model analyses with GPS and radiosonde data during the MAP SOP, Q. J. R. Meteorol. Soc., 131, 3013–3036, https://doi.org/10.1256/qj.05.27, 2005.

Boehm, J., Werl, B., and Schuh, H.: Troposphere mapping functions for GPS and very long baseline interferometry from European Centre for Medium-Range Weather Forecasts operational analysis data, J. Geophys. Res.: Solid Earth, 111, https://doi.org/10.1029/2005JB003629, 2006.

Bos, M., Fernandes, R., and Bastos, L.: Hector user manual version 1.7.2, Space and Earth Geodetic Analysis Laboratory: Covilhã, Portugal, 2019.

Bruyninx, C., Becker, M., and Stangl, G.: Regional densification of the IGS in europe using the EUREF permanent GPS network (EPN), Phys. Chem. Earth, Part A: Solid Earth and Geodesy, 26, 531–538, https://doi.org/10.1016/S1464-1895(01)00096-5, 2001.

Bruyninx, C., Habrich, H., Söhne, W., Kenyeres, A., Stangl, G., and Völksen, C.: Enhancement of the EUREF Permanent Network Services and Products, in: Geodesy for Planet Earth, Berlin, Heidelberg, 27–34, https://doi.org/10.1007/978-3-642-20338-1_4, 2012.

Chen, B. and Liu, Z.: Global water vapor variability and trend from the latest 36 year (1979 to 2014) data of ECMWF and NCEP reanalyses, radiosonde, GPS, and microwave satellite, J. Geophys. Res.: Atmos., 121, 11,442-11,462, https://doi.org/10.1002/2016JD024917, 2016.

Copernicus: European State of the Climate 2019 | Copernicus: https://climate.copernicus.eu/ESOTC/2019, last access: 20 September 2021.

Dai, A., Wang, J., Thorne, P. W., Parker, D. E., Haimberger, L., and Wang, X. L.: A New Approach to Homogenize Daily Radiosonde Humidity Data, J. Climate, 24, 965–991, https://doi.org/10.1175/2010JCLI3816.1, 2011.

Dai, A., Wang, J., Ware, R. H., and Hove, T. V.: Diurnal variation in water vapor over North America and its implications for sampling errors in radiosonde humidity, J. Geophys. Res.: Atmos., 107, ACL 11-1-ACL 11-14, https://doi.org/10.1029/2001JD000642, 2002.

Davis, J. L., Herring, T. A., Shapiro, I. I., Rogers, A. E. E., and Elgered, G.: Geodesy by radio interferometry: Effects of atmospheric modeling errors on estimates of baseline length, Radio Sci., 20, 1593–1607, https://doi.org/10.1029/RS020i006p01593, 1985.

Dee, D. P., Uppala, S. M., Simmons, A. J., Berrisford, P., Poli, P., Kobayashi, S., Andrae, U., Balmaseda, M. A., Balsamo, G., Bauer, P., Bechtold, P., Beljaars, A. C. M., Berg, L. van de, Bidlot, J., Bormann, N., Delsol, C., Dragani, R., Fuentes, M., Geer, A. J.,

Haimberger, L., Healy, S. B., Hersbach, H., Hólm, E. V., Isaksen, L., Kållberg, P., Köhler, M., Matricardi, M., McNally, A. P., Monge-Sanz, B. M., Morcrette, J.-J., Park, B.-K., Peubey, C., Rosnay, P. de, Tavolato, C., Thépaut, J.-N., and Vitart, F.: The ERA-Interim reanalysis: configuration and performance of the data assimilation system, Q. J. R. Meteorol. Soc., 137, 553–597, https://doi.org/10.1002/qj.828, 2011.

Diedrich, H., Wittchen, F., Preusker, R., and Fischer, J.: Representativeness of total column water vapour retrievals from instruments on polar orbiting satellites, Atmos. Chem. Phys., 16, 8331–8339, https://doi.org/10.5194/acp-16-8331-2016, 2016.

Dirksen, R. J., Sommer, M., Immler, F. J., Hurst, D. F., Kivi, R., and Vömel, H.: Reference quality upper-air measurements: GRUAN data processing for the Vaisala RS92 radiosonde, Atmos. Meas. Tech., 7, 4463–4490, https://doi.org/10.5194/amt-7-4463-2014, 2014.

Drobinski, P., Bastin, S., Arsouze, T., Béranger, K., Flaounas, E., and Stéfanon, M.: North-western Mediterranean sea-breeze circulation in a regional climate system model, Clim Dyn, 51, 1077–1093, https://doi.org/10.1007/s00382-017-3595-z, 2018.

Durre, I., Yin, X., Vose, R. S., Applequist, S., and Arnfield, J.: Enhancing the Data Coverage in the Integrated Global Radiosonde Archive, J. Atmos. Oceanic Technol., 35, 1753–1770, https://doi.org/10.1175/JTECH-D-17-0223.1, 2018.

Ejigu, Y. G., Teferle, F. N., Klos, A., Bogusz, J., and Hunegnaw, A.: Monitoring and prediction of hurricane tracks using GPS tropospheric products, GPS Solut, 25, 76, https://doi.org/10.1007/s10291-021-01104-3, 2021.

Enriquez-Alonso, A., Sanchez-Lorenzo, A., Calbó, J., González, J.-A., and Norris, J. R.: Cloud cover climatologies in the Mediterranean obtained from satellites, surface observations, reanalyses, and CMIP5 simulations: validation and future scenarios, Clim Dyn, 47, 249–269, https://doi.org/10.1007/s00382-015-2834-4, 2016.

Fadnavis, S., Müller, R., Chakraborty, T., Sabin, T. P., Laakso, A., Rap, A., Griessbach, S., Vernier, J.-P., and Tilmes, S.: The role of tropical volcanic eruptions in exacerbating Indian droughts, Sci Rep, 11, 2714, https://doi.org/10.1038/s41598-021-81566-0, 2021.

Gelaro, R., McCarty, W., Suárez, M. J., Todling, R., Molod, A., Takacs, L., Randles, C., Darmenov, A., Bosilovich, M. G., Reichle, R., Wargan, K., Coy, L., Cullather, R., Draper, C., Akella, S., Buchard, V., Conaty, A., da Silva, A., Gu, W., Kim, G.-K., Koster, R., Lucchesi, R., Merkova, D., Nielsen, J. E., Partyka, G., Pawson, S., Putman, W., Rienecker, M., Schubert, S. D., Sienkiewicz, M., and Zhao, B.: The Modern-Era Retrospective Analysis for Research and Applications, Version 2 (MERRA-2), J. Clim., Volume 30, 5419–5454, https://doi.org/10.1175/JCLI-D-16-0758.1, 2017.

Grossi, M., Valks, P., Loyola, D., Aberle, B., Slijkhuis, S., Wagner, T., Beirle, S., and Lang, R.: Total column water vapour measurements from GOME-2 MetOp-A and MetOp-B,   Atmos. Meas. Tech., 8, 1111–1133, https://doi.org/10.5194/amt-8-1111-2015, 2015.

Gupta, H. V., Kling, H., Yilmaz, K. K., and Martinez, G. F.: Decomposition of the mean squared error and NSE performance criteria: Implications for improving hydrological modelling, J. Hydrol., 377, 80–91, https://doi.org/10.1016/j.jhydrol.2009.08.003, 2009.

Hagemann, S., Bengtsson, L., and Gendt, G.: On the determination of atmospheric water vapor from GPS measurements, J. Geophys. Res.: Atmos., 108, https://doi.org/10.1029/2002JD003235, 2003.

Harries, J. E.: Atmospheric radiation and atmospheric humidity, Q. J. R. Meteorol. Soc., 123, 2173–2186, https://doi.org/10.1002/qj.49712354402, 1997.

Heise, S., Dick, G., Gendt, G., Schmidt, T., and Wickert, J.: Integrated water vapor from IGS ground-based GPS observations: initial results from a global 5-min data set,   Ann. Geophys., 27, 2851–2859, https://doi.org/10.5194/angeo-27-2851-2009, 2009.

Hersbach, H., Bell, B., Berrisford, P., Hirahara, S., Horányi, A., Muñoz-Sabater, J., Nicolas, J., Peubey, C., Radu, R., Schepers, D., Simmons, A., Soci, C., Abdalla, S., Abellan, X., Balsamo, G., Bechtold, P., Biavati, G., Bidlot, J., Bonavita, M., Chiara, G. D., Dahlgren, P., Dee, D., Diamantakis, M., Dragani, R., Flemming, J., Forbes, R., Fuentes, M., Geer, A., Haimberger, L., Healy, S., Hogan, R. J., Hólm, E., Janisková, M., Keeley, S., Laloyaux, P., Lopez, P., Lupu, C., Radnoti, G., Rosnay, P. de, Rozum, I., Vamborg, F., Villaume, S., and Thépaut, J.-N.: The ERA5 global reanalysis, Q. J. R. Meteorol. Soc., 146, 1999–2049, https://doi.org/10.1002/qj.3803, 2020.

Huang, L., Peng, H., Liu, L., Xiong, S., Xie, S., Chen, J., Li, J., and He, H.: GNSS Precipitable Water Vapor Retrieval With the Aid of NWM Data for China, Earth Space Sci., 8, e2020EA001550, https://doi.org/10.1029/2020EA001550, 2021.

Intergovernmental Panel on Climate Change: Climate Change 2014 – Impacts, Adaptation and Vulnerability: Part B: Regional Aspects: Working Group II Contribution to the IPCC Fifth Assessment Report: Volume 2: Regional Aspects, Cambridge University Press, Cambridge, https://doi.org/10.1017/CBO9781107415386, 2014.

Jade, S. and Vijayan, M. S. M.: GPS-based atmospheric precipitable water vapor estimation using meteorological parameters interpolated from NCEP global reanalysis data, J. Geophys. Res.: Atmos., 113, https://doi.org/10.1029/2007JD008758, 2008.

Jiang, W., Yuan, P., Chen, H., Cai, J., Li, Z., Chao, N., and Sneeuw, N.: Annual variations of monsoon and drought detected by GPS: A case study in Yunnan, China, Sci Rep, 7, 5874, https://doi.org/10.1038/s41598-017-06095-1, 2017.

Jones, J., Guerova, G., Douša, J., Dick, G., de Haan, S., Pottiaux, E., Bock, O., Pacione, R., and van Malderen, R. (Eds.): Advanced GNSS Tropospheric Products for Monitoring Severe Weather Events and Climate: COST Action ES1206 Final Action Dissemination Report, Springer International Publishing, Cham, https://doi.org/10.1007/978-3-030-13901-8, 2020.

Kämpfer, N. (Ed.): Monitoring Atmospheric Water Vapour: Ground-Based Remote Sensing and In-situ Methods, Springer, New York, NY, https://doi.org/10.1007/978-1-4614-3909-7, 2013.

Kanamitsu, M., Ebisuzaki, W., Woollen, J., Yang, S.-K., Hnilo, J. J., Fiorino, M., and Potter, G. L.: NCEP–DOE AMIP-II Reanalysis (R-2), Bull. Am. Meteorol. Soc., 83, 1631–1644, https://doi.org/10.1175/BAMS-83-11-1631, 2002.

Kiehl, J. T. and Trenberth, K. E.: Earth's Annual Global Mean Energy Budget, Bull. Am. Meteorol. Soc., 78, 197–208, https://doi.org/10.1175/1520-0477(1997)078<0197:EAGMEB>2.0.CO;2, 1997.

Kling, H., Fuchs, M., and Paulin, M.: Runoff conditions in the upper Danube basin under an ensemble of climate change scenarios, J. Hydrol., 424–425, 264–277, https://doi.org/10.1016/j.jhydrol.2012.01.011, 2012.

Kobayashi, S., Ota, Y., Harada, Y., Ebita, A., Moriya, M., Onoda, H., Onogi, K., Kamahori, H., Kobayashi, C., Endo, H., Miyaoka, K., and Takahashi, K.: The JRA-55 Reanalysis: General Specifications and Basic Characteristics, J. Meteorol. Soc. Jpn. Ser. II, 93, 5–48, https://doi.org/10.2151/jmsj.2015-001, 2015.

Koji, A. K., Van Malderen, R., Pottiaux, E., and Van Schaeybroeck, B.: Understanding the Present-Day Spatiotemporal Variability of Precipitable Water Vapor over Ethiopia: A Comparative Study between ERA5 and GPS, Remote Sens., 14, 686, https://doi.org/10.3390/rs14030686, 2022.

Krämer, M., Rolf, C., Spelten, N., Afchine, A., Fahey, D., Jensen, E., Khaykin, S., Kuhn, T., Lawson, P., Lykov, A., Pan, L. L., Riese, M., Rollins, A., Stroh, F., Thornberry, T., Wolf, V., Woods, S., Spichtinger, P., Quaas, J., and Sourdeval, O.: A microphysics guide to cirrus – Part 2: Climatologies of clouds and humidity from observations, Atmos. Chem. Phys., 20, 12569–12608, https://doi.org/10.5194/acp-20-12569-2020, 2020.

Kunz, A., Müller, R., Homonnai, V., M. Jánosi, I., Hurst, D., Rap, A., M. Forster, P., Rohrer, F., Spelten, N., and Riese, M.: Extending water vapor trend observations over Boulder into the tropopause region: Trend uncertainties and resulting radiative forcing, J. Geophys. Res.: Atmos., 118, 11,269-11,284, https://doi.org/10.1002/jgrd.50831, 2013.

Kunz, A., Spelten, N., Konopka, P., Müller, R., Forbes, R. M., and Wernli, H.: Comparison of Fast In situ Stratospheric Hygrometer (FISH) measurements of water vapor in the upper troposphere and lower stratosphere (UTLS) with ECMWF (re)analysis data, Atmos. Chem. Phys., 14, 10803–10822, https://doi.org/10.5194/acp-14-10803-2014, 2014.

Kursinski, E. R., Hajj, G. A., Hardy, K. R., Romans, L. J., and Schofield, J. T.: Observing tropospheric water vapor by radio occultation using the Global Positioning System, Geophys. Res. Lett., 22, 2365–2368, https://doi.org/10.1029/95GL02127, 1995.

Lavers, D. A., Pappenberger, F., Richardson, D. S., and Zsoter, E.: ECMWF Extreme Forecast Index for water vapor transport: A forecast tool for atmospheric rivers and extreme precipitation, Geophys. Res. Lett., 43, 11,852-11,858, https://doi.org/10.1002/2016GL071320, 2016.

McCarthy, M. P., Thorne, P. W., and Titchner, H. A.: An Analysis of Tropospheric Humidity Trends from Radiosondes, J. Clim., 22, 5820–5838, https://doi.org/10.1175/2009JCLI2879.1, 2009.

Müller, R., Kunz, A., Hurst, D. F., Rolf, C., Krämer, M., and Riese, M.: The need for accurate long-term measurements of water vapor in the upper troposphere and lower stratosphere with global coverage, Earths Future, 4, 25–32, https://doi.org/10.1002/2015EF000321, 2016.

Nguyen, K. N., Quarello, A., Bock, O., and Lebarbier, E.: Sensitivity of Change-Point Detection and Trend Estimates to GNSS IWV Time Series Properties, Atmosphere, 12, 1102, https://doi.org/10.3390/atmos12091102, 2021.

Nilsson, T. and Elgered, G.: Long-term trends in the atmospheric water vapor content estimated from ground-based GPS data, J. Geophys. Res.: Atmos., 113, https://doi.org/10.1029/2008JD010110, 2008.

Ning, T., Wickert, J., Deng, Z., Heise, S., Dick, G., Vey, S., and Schöne, T.: Homogenized Time Series of the Atmospheric Water Vapor Content Obtained from the GNSS Reprocessed Data, J. Clim., 29, 2443–2456, https://doi.org/10.1175/JCLI-D-15-0158.1, 2016.

Pacione, R., Araszkiewicz, E., Brockmann, E., and Dousa, J.: EPN-Repro2: A reference GNSS tropospheric data set over Europe, Atmos. Meas. Tech., 10, 1689–1705, https://doi.org/10.5194/amt-10-1689-2017, 2017.

Parracho, A. C., Bock, O., and Bastin, S.: Global IWV trends and variability in atmospheric reanalyses and GPS observations, Atmos. Chem. Phys., 18, 16213–16237, https://doi.org/10.5194/acp-18-16213-2018, 2018.

Pavlis, N. K., Holmes, S. A., Kenyon, S. C., and Factor, J. K.: The development and evaluation of the Earth Gravitational Model 2008 (EGM2008), J. Geophys. Res.: Solid Earth, 117, https://doi.org/10.1029/2011JB008916, 2012.

Price, C., Michaelides, S., Pashiardis, S., and Alpert, P.: Long term changes in diurnal temperature range in Cyprus, Atmos. Res., 51, 85–98, https://doi.org/10.1016/S0169-8095(99)00022-8, 1999.

Randel, W. J. and Wu, F.: Kelvin wave variability near the equatorial tropopause observed in GPS radio occultation measurements, J. Geophys. Res.: Atmos., 110, https://doi.org/10.1029/2004JD005006, 2005.

Randel, W. J., Wu, F., and Forster, P.: The Extratropical Tropopause Inversion Layer: Global Observations with GPS Data, and a Radiative Forcing Mechanism, J. Atmos. Sci., 64, 4489–4496, https://doi.org/10.1175/2007JAS2412.1, 2007.

Rebischung, P. and Schmid, R.: IGS14/igs14. atx: a new framework for the IGS products, in: AGU Fall Meeting 2016, 2016.

Saastamoinen, J.: Atmospheric correction for the troposphere and stratosphere in radio ranging satellites, The use of artificial satellites for geodesy, 15, 247–251, 1972.

Saha, S., Moorthi, S., Pan, H.-L., Wu, X., Wang, J., Nadiga, S., Tripp, P., Kistler, R., Woollen, J., Behringer, D., Liu, H., Stokes, D., Grumbine, R., Gayno, G., Wang, J., Hou, Y.-T., Chuang, H., Juang, H.-M. H., Sela, J., Iredell, M., Treadon, R., Kleist, D., Delst, P. V., Keyser, D., Derber, J., Ek, M., Meng, J., Wei, H., Yang, R., Lord, S., Dool, H. van den, Kumar, A., Wang, W., Long, C., Chelliah, M., Xue, Y., Huang, B., Schemm, J.-K., Ebisuzaki, W., Lin, R., Xie, P., Chen, M., Zhou, S., Higgins, W., Zou, C.-Z., Liu, Q., Chen, Y., Han, Y., Cucurull, L., Reynolds, R. W., Rutledge, G., and Goldberg, M.: The NCEP Climate Forecast System Reanalysis, Bull. Am. Meteorol. Soc., 91, 1015–1058, https://doi.org/10.1175/2010BAMS3001.1, 2010.

Saha, S., Moorthi, S., Wu, X., Wang, J., Nadiga, S., Tripp, P., Behringer, D., Hou, Y.-T., Chuang, H., Iredell, M., Ek, M., Meng, J., Yang, R., Mendez, M. P., Dool, H. van den, Zhang, Q., Wang, W., Chen, M., and Becker, E.: The NCEP Climate Forecast System Version 2, J. Clim., 27, 2185–2208, https://doi.org/10.1175/JCLI-D-12-00823.1, 2014.

Schneider, T., O'Gorman, P. A., and Levine, X. J.: Water Vapor and the Dynamics of Climate Changes, Rev. Geophys., 48, https://doi.org/10.1029/2009RG000302, 2010.

Schröder, M., Lockhoff, M., Fell, F., Forsythe, J., Trent, T., Bennartz, R., Borbas, E., Bosilovich, M. G., Castelli, E., Hersbach, H., Kachi, M., Kobayashi, S., Kursinski, E. R., Loyola, D., Mears, C., Preusker, R., Rossow, W. B., and Saha, S.: The GEWEX Water Vapor Assessment archive of water vapour products from satellite observations and reanalyses, Earth Syst. Sci. Data, 10, 1093–1117, https://doi.org/10.5194/essd-10-1093-2018, 2018.

Schröder, M., Lockhoff, M., Forsythe, J. M., Cronk, H. Q., Haar, T. H. V., and Bennartz, R.: The GEWEX Water Vapor Assessment: Results from Intercomparison, Trend, and Homogeneity Analysis of Total Column Water Vapor, J. Climatol. Appl. Meteorol., 55, 1633–1649, https://doi.org/10.1175/JAMC-D-15-0304.1, 2016.

Schüler, T.: On ground-based GPS tropospheric delay estimation (PhD Thesis), Univ. der Bundeswehr München, Fak. für Bauingenieur- und Vermessungswesen, Studiengang Geodäsie und Geoinformation, 2001.

Schwarz, G.: Estimating the dimension of a model The Annals of Statistics 6 (2), 461–464, URL: https://doi.org/10.1214/aos/1176344136, 1978.

Solomon, S., Rosenlof, K. H., Portmann, R. W., Daniel, J. S., Davis, S. M., Sanford, T. J., and Plattner, G.-K.: Contributions of Stratospheric Water Vapor to Decadal Changes in the Rate of Global Warming, Science, 327, 1219–1223, https://doi.org/10.1126/science.1182488, 2010.

Steinke, S., Wahl, S., and Crewell, S.: Benefit of high resolution COSMO reanalysis: The diurnal cycle of column-integrated water vapor over Germany, Meteorologische Zeitschrift, 165–177, https://doi.org/10.1127/metz/2019/0936, 2019.

Thébault, E., Finlay, C. C., Beggan, C. D., Alken, P., Aubert, J., Barrois, O., Bertrand, F., Bondar, T., Boness, A., Brocco, L., Canet, E., Chambodut, A., Chulliat, A., Coïsson, P., Civet, F., Du, A., Fournier, A., Fratter, I., Gillet, N., Hamilton, B., Hamoudi, M., Hulot, G., Jager, T., Korte, M., Kuang, W., Lalanne, X., Langlais, B., Léger, J.-M., Lesur, V., Lowes, F. J., Macmillan, S., Mandea, M., Manoj, C., Maus, S., Olsen, N., Petrov, V., Ridley, V., Rother, M., Sabaka, T. J., Saturnino, D., Schachtschneider, R., Sirol, O., Tangborn, A., Thomson, A., Tøffner-Clausen, L., Vigneron, P., Wardinski, I., and Zvereva, T.: International Geomagnetic Reference Field: the 12th generation, Earth, Planets Space, 67, 79, https://doi.org/10.1186/s40623-015-0228-9, 2015.

Tilmes, S., Pan, L. L., Hoor, P., Atlas, E., Avery, M. A., Campos, T., Christensen, L. E., Diskin, G. S., Gao, R.-S., Herman, R. L., Hintsa, E. J., Loewenstein, M., Lopez, J., Paige, M. E., Pittman, J. V., Podolske, J. R., Proffitt, M. R., Sachse, G. W., Schiller, C., Schlager, H., Smith, J., Spelten, N., Webster, C., Weinheimer, A., and Zondlo, M. A.: An aircraft-based upper troposphere lower stratosphere O3, CO, and H2O climatology for the Northern Hemisphere, J. Geophys. Res.: Atmos., 115, https://doi.org/10.1029/2009JD012731, 2010.

Tregoning, P. and Herring, T. A.: Impact of a priori zenith hydrostatic delay errors on GPS estimates of station heights and zenith total delays, Geophys. Res. Lett., 33, https://doi.org/10.1029/2006GL027706, 2006.

Trenberth, K. E. and Fasullo, J. T.: North American water and energy cycles, Geophys. Res. Lett., 40, 365–369, https://doi.org/10.1002/grl.50107, 2013.

Trenberth, K. E., Dai, A., Rasmussen, R. M., and Parsons, D. B.: The Changing Character of Precipitation, Bull. Am. Meteorol. Soc., 84, 1205–1218, https://doi.org/10.1175/BAMS-84-9-1205, 2003.

Trenberth, K. E.: Framing the way to relate climate extremes to climate change, Clim. Change, 115, 283–290, https://doi.org/10.1007/s10584-012-0441-5, 2012.

Turato, B., Reale, O., and Siccardi, F.: Water Vapor Sources of the October 2000 Piedmont Flood, J. Hydrometeorol., 5, 693–712, https://doi.org/10.1175/1525-7541(2004)005<0693:WVSOTO>2.0.CO;2, 2004.

Van Malderen, R., Pottiaux, E., Klos, A., Domonkos, P., Elias, M., Ning, T., Bock, O., Guijarro, J., Alshawaf, F., Hoseini, M., Quarello, A., Lebarbier, E., Chimani, B., Tornatore, V., Kazancı, S. Z., and Bogusz, J.: Homogenizing GPS Integrated Water Vapor Time Series: Benchmarking Break Detection Methods on Synthetic Data Sets, Earth and Space Science, 7, e2020EA001121, https://doi.org/10.1029/2020EA001121, 2020.

Van Malderen, R., Pottiaux, E., Stankunavicius, G., Beirle, S., Wagner, T., Brenot, H., Bruyninx, C., and Jones, J.: Global Spatiotemporal Variability of Integrated Water Vapor Derived from GPS, GOME/SCIAMACHY and ERA-Interim: Annual Cycle, Frequency Distribution and Linear Trends, Remote Sens., 14, 1050, https://doi.org/10.3390/rs14041050, 2022.

Vey, S., Dietrich, R., Rülke, A., Fritsche, M., Steigenberger, P., and Rothacher, M.: Validation of Precipitable Water Vapor within the NCEP/DOE Reanalysis Using Global GPS Observations from One Decade, J. Climate, 23, 1675–1695, https://doi.org/10.1175/2009JCLI2787.1, 2010.

Vogelmann, H. and Trickl, T.: Wide-range sounding of free-tropospheric water vapor with a differential-absorption lidar (DIAL) at a high-altitude station, Appl. Opt., AO, 47, 2116–2132, https://doi.org/10.1364/AO.47.002116, 2008.

Vonder Haar, T. H., Bytheway, J. L., and Forsythe, J. M.: Weather and climate analyses using improved global water vapor observations, Geophys. Res. Lett., 39, https://doi.org/10.1029/2012GL052094, 2012.

Wang, J. and Zhang, L.: Climate applications of a global, 2-hourly atmospheric precipitable water dataset derived from IGS tropospheric products, J Geod, 83, 209–217, https://doi.org/10.1007/s00190-008-0238-5, 2009.

Wang, J., Dai, A., and Mears, C.: Global Water Vapor Trend from 1988 to 2011 and Its Diurnal Asymmetry Based on GPS, Radiosonde, and Microwave Satellite Measurements, J. Climate, 29, 5205–5222, https://doi.org/10.1175/JCLI-D-15-0485.1, 2016.

Wang, J., Zhang, L., and Dai, A.: Global estimates of water-vapor-weighted mean temperature of the atmosphere for GPS applications, J. Geophys. Res.: Atmos., 110, https://doi.org/10.1029/2005JD006215, 2005.

Wang, S., Xu, T., Nie, W., Jiang, C., Yang, Y., Fang, Z., Li, M., and Zhang, Z.: Evaluation of Precipitable Water Vapor from Five Reanalysis Products with Ground-Based GNSS Observations, Remote Sens., 12, 1817, https://doi.org/10.3390/rs12111817, 2020.

Wang, X. L. and Y. Feng.: RHtestsV4 User Manual. Climate Research Division, Atmospheric Science and Technology Directorate, Science and Technology Branch, Environment Canada, 2013.

Wang, X. L., Wen, Q. H., and Wu, Y.: Penalized Maximal t Test for Detecting Undocumented Mean Change in Climate Data Series, J. Climatol. Appl. Meteorol., 46, 916–931, https://doi.org/10.1175/JAM2504.1, 2007.

Wang, X. L.: Accounting for Autocorrelation in Detecting Mean Shifts in Climate Data Series Using the Penalized Maximal t or F Test, J. Appl. Meteor. Climatol., 47, 2423–2444, https://doi.org/10.1175/2008JAMC1741.1, 2008.

Wang, X., Zhang, K., Wu, S., Fan, S., and Cheng, Y.: Water vapor-weighted mean temperature and its impact on the determination of precipitable water vapor and its linear trend, J. Geophys. Res.: Atmos., 121, 833–852, https://doi.org/10.1002/2015JD024181, 2016.

World Meteorological Organization: Guide to Instruments and Methods of Observation, Measurement of Meteorological Variables. (WMO-No. 8), 1, 2018.

Yuan, P., Hunegnaw, A., Alshawaf, F., Awange, J., Klos, A., Teferle, F. N., and Kutterer, H.: Feasibility of ERA5 integrated water vapor trends for climate change analysis in continental Europe: An evaluation with GPS (1994–2019) by considering statistical significance, Remote Sens. Environ., 260, 112416, https://doi.org/10.1016/j.rse.2021.112416, 2021.

Zhu, Y. and Newell, R. E.: Atmospheric rivers and bombs, Geophys. Res. Lett., 21, 1999–2002, https://doi.org/10.1029/94GL01710, 1994.

Alshawaf, F., Zus, F., Balidakis, K., Deng, Z., Hoseini, M., Dick, G., and Wickert, J.: On the statistical significance of climatic trends estimated from GPS tropospheric time series, Journal of Geophysical Research: Atmospheres, 123, 10–967, 2018.

975

Ambaum, M. H., Hoskins, B. J., and Stephenson, D. B.: Arctic oscillation or North Atlantic oscillation?, Journal of Climate, 14, 3495–3507, 2001.

Ao, C. O., Meehan, T., Hajj, G., Mannucci, A., and Beyerle, G.: Lower troposphere refractivity bias in GPS occultation retrievals, Journal of Geophysical Research: Atmospheres, 108, 2003.

980

Awange, J. L.: Environmental monitoring using GNSS: Global navigation satellite systems, . Springer-Verlag, Berlin, Heidelberge, New York., 2012.

Awange, J. L.: GNSS environmental sensing, Springer International Publishers, 2018.

Baldwin, M., Gray, L., Dunkerton, T., Hamilton, K., Haynes, P., Randel, W., Holton, J., Alexander, M., Hirota, I., and Horinouchi, T.: The quasi-biennial oscillation, Reviews of Geophysics, 39, 179–229, 2001.

985

Barnston, A. G. and Livezey, R. E.: Classification, seasonality and persistence of low-frequency atmospheric circulation patterns, Monthly weather review, 115, 1083–1126, 1987.

Bernet, L., Brockmann, E., von Clarmann, T., Kämpfer, N., Mahieu, E., Mätzler, C., Stober, G., and Hocke, K.: Trends of atmospheric water vapour in Switzerland from ground-based radiometry, FTIR and GNSS data, Atmospheric Chemistry and Physics, 20, 11 223–11 244, 2020.

990

Bertiger, W., Bar-Sever, Y., Dorsey, A., Haines, B., Harvey, N., Hemberger, D., Heflin, M., Lu, W., Miller, M., and Moore, A. W.: GipsyX/RTGx, a new tool set for space geodetic operations and research, Advances in Space Research, 66, 469–489, 2020.

Bevis, M., Businger, S., Chiswell, S., Herring, T. A., Anthes, R. A., Rocken, C., and Ware, R. H.: GPS meteorology: Mapping zenith wet delays onto precipitable water, Journal of applied meteorology, 33, 379–386, 1994.

995

Bevis, M., Businger, S., Herring, T. A., Rocken, C., Anthes, R. A., and Ware, R. H.: GPS meteorology: Remote sensing of atmospheric water vapor using the Global Positioning System, Journal of Geophysical Research: Atmospheres, 97, 15787–15801, 1992.

Blewitt, G., Hammond, W. C., and Kreemer, C.: Harnessing the GPS data explosion for interdisciplinary science, Eos, 99, 485, 2018.

1000

Bock, O. and Parracho, A. C.: Consistency and representativeness of integrated water vapour from ground-based GPS observations and ERA-Interim reanalysis, Atmospheric Chemistry and Physics, 19, 9453–9468, 2019.

Bock, O., Keil, C., Richard, E., Flamant, C., and Bouin, M.: Validation of precipitable water from ECMWF model analyses with GPS and radiosonde data during the MAP SOP, Quarterly Journal of the Royal Meteorological Society: A journal of the atmospheric sciences, applied meteorology and physical oceanography, 131, 3013–3036, 2005.

1005 Boehm, J., Werl, B., and Schuh, H.: Troposphere mapping functions for GPS and very long baseline interferometry from European Centre for Medium-Range Weather Forecasts operational analysis data, Journal of geophysical research: solid earth, 111, 2006.

Bonafoni, S., Biondi, R., Brenot, H., and Anthes, R.: Radio occultation and ground-based GNSS products for observing, understanding and predicting extreme events: A review, Atmospheric research, 230, 104624, 2019.

1010 Bruyninx, C., Habrich, H., Söhne, W., Kenyeres, A., Stangl, G., and Völksen, C.: Enhancement of the EUREF permanent network services and products, in: Geodesy for planet Earth, Springer, 27–34, 2012.

Chen, B. and Liu, Z.: Global water vapor variability and trend from the latest 36-year (1979 to 2014) data of ECMWF and NCEP reanalyses, radiosonde, GPS, and microwave satellite, Journal of Geophysical Research: Atmospheres, 121, 11 442-11 462, 2016.

1015 Cohen, J., Screen, J. A., Furtado, J. C., Barlow, M., Whittleston, D., Coumou, D., Francis, J., Dethloff, K., Entekhabi, D., and Overland, J.: Recent Arctic amplification and extreme mid-latitude weather, Nature geoscience, 7, 627–637, 2014.

Comas-Bru, L. and McDermott, F.: Impacts of the EA and SCA patterns on the European twentieth century NAO winter climate relationship, Quarterly Journal of the Royal Meteorological Society, 140, 354–363, 2014.

Copernicus: European State of the Climate 2019 | Copernicus: https://climate.copernicus.eu/ESOTC/2019, last access: 20
1020 September 2021.

Dai, A., Wang, J., Thorne, P. W., Parker, D. E., Haimberger, L., and Wang, X. L.: A new approach to homogenize daily radiosonde humidity data, Journal of Climate, 24, 965–991, 2011.

Dai, A., Wang, J., Ware, R. H., and Van Hove, T.: Diurnal variation in water vapor over North America and its implications for sampling errors in radiosonde humidity, Journal of Geophysical Research: Atmospheres, 107, ACL-11, 2002.

1025 Davis, J., Herring, T., Shapiro, I., Rogers, A., and Elgered, G.: Geodesy by radio interferometry: Effects of atmospheric modeling errors on estimates of baseline length, Radio science, 20, 1593–1607, 1985.

Dee, D. P., Uppala, S. M., Simmons, A., Berrisford, P., Poli, P., Kobayashi, S., Andrae, U., Balmaseda, M., Balsamo, G., and Bauer, d P.: The ERA-Interim reanalysis: Configuration and performance of the data assimilation system, Quarterly Journal of the royal meteorological society, 137, 553–597, 2011.

1030 Diedrich, H., Wittchen, F., Preusker, R., and Fischer, J.: Representativeness of total column water vapour retrievals from instruments on polar orbiting satellites, Atmospheric Chemistry and Physics, 16, 8331–8339, 2016.

Drobinski, P., Bastin, S., Arsouze, T., Beranger, K., Flaounas, E., and Stefanon, M.: North-western Mediterranean sea-breeze circulation in a regional climate system model, Climate Dynamics, 51, 1077–1093, 2018.

Durre, I., Williams Jr, C. N., Yin, X., and Vose, R. S.: Radiosonde-based trends in precipitable water over the Northern
1035 Hemisphere: An update, Journal of Geophysical Research: Atmospheres, 114, 2009.

Durre, I., Yin, X., Vose, R. S., Applequist, S., and Arnfield, J.: Enhancing the data coverage in the Integrated Global Radiosonde Archive, Journal of Atmospheric and Oceanic Technology, 35, 1753–1770, 2018.

Ejigu, Y. G., Teferle, F. N., Klos, A., Janusz, B., and Hunegnaw, A.: Monitoring and prediction of hurricane tracks using GPS tropospheric products, GPS Solutions, 25, 1–15, 2021.

Fadnavis, S., Müller, R., Chakraborty, T., Sabin, T. P., Laakso, A., Rap, A., Griessbach, S., Vernier, J.-P., and Tilmes, S.: The role of tropical volcanic eruptions in exacerbating Indian droughts, Scientific Reports, 11, 2714, 2021.

Field, C. B. and Barros, V. R.: Climate change 2014–Impacts, adaptation and vulnerability: Regional aspects, Cambridge University Press, 2014.

Gelaro, R., McCarty, W., Suárez, M. J., Todling, R., Molod, A., Takacs, L., Randles, C. A., Darmenov, A., Bosilovich, M. G., and Reichle, R.: The modern-era retrospective analysis for research and applications, version 2 (MERRA-2), Journal of climate, 30, 5419–5454, 2017.

Grossi, M., Valks, P., Loyola, D., Aberle, B., Slijkhuis, S., Wagner, T., Beirle, S., and Lang, R.: Total column water vapour measurements from GOME-2 MetOp-A and MetOp-B, 8, 1111–1133, Atmospheric Measurement Techniques, 2015.

Gupta, H. V., Kling, H., Yilmaz, K. K., and Martinez, G. F.: Decomposition of the mean squared error and NSE performance criteria: Implications for improving hydrological modelling, Journal of hydrology, 377, 80–91, 2009.

Hagemann, S., Bengtsson, L., and Gendt, G.: On the determination of atmospheric water vapor from GPS measurements, Journal of Geophysical Research: Atmospheres, 108, 2003.

Held, I. M. and Soden, B. J.: Water vapor feedback and global warming, Annual review of energy and the environment, 25, 441–475, 2000.

Hersbach, H., Bell, B., Berrisford, P., Hirahara, S., Horányi, A., Muñoz-Sabater, J., Nicolas, J., Peubey, C., Radu, R., and Schepers, D.: The ERA5 global reanalysis, Quarterly Journal of the Royal Meteorological Society, 146, 1999–2049, 2020.

Huang, L., Peng, H., Liu, L., Xiong, S., Xie, S., Chen, J., Li, J., and He, H.: GNSS Precipitable Water Vapor Retrieval with the Aid of NWM Data for China, Earth and Space Science, 8, e2020EA001550, 2021.

Hurrell, J. W.: Decadal trends in the North Atlantic Oscillation: Regional temperatures and precipitation, Science, 269, 676–679, 1995.

Jade, S. and Vijayan, M.: GPS-based atmospheric precipitable water vapor estimation using meteorological parameters interpolated from NCEP global reanalysis data, Journal of Geophysical Research: Atmospheres, 113, 2008.

Jiang, W., Yuan, P., Chen, H., Cai, J., Li, Z., Chao, N., and Sneeuw, N.: Annual variations of monsoon and drought detected by GPS: A case study in Yunnan, China, Scientific reports, 7, 1–10, 2017.

Jones, J., Guerova, G., Douša, J., Dick, G., de Haan, S., Pottiaux, E., Bock, O., Pacione, R., and van Malderen, R. (Eds.): Advanced GNSS Tropospheric Products for Monitoring Severe Weather Events and Climate: COST Action ES1206 Final Action Dissemination Report, Springer International Publishing, Cham, 2020.Jones, J., Guerova, G., Douša, J., Dick, G., de Haan, S., Pottiaux, E., and Van Malderen, R.: Advanced GNSS tropospheric products for monitoring severe weather events and climate, COST action ES1206 final action dissemination report, 563, 2019.

Jung, T., Vitart, F., Ferranti, L., and Morcrette, J.: Origin and predictability of the extreme negative NAO winter of 2009/10, Geophysical Research Letters, 38, 2011.

Kämpfer, N. (Ed.): Monitoring Atmospheric Water Vapour: Ground-Based Remote Sensing and In-situ Methods, ISSI Scientific Reports Series, Vol. 10, ISBN 978-1-4614-3908-0, Springer, Berlin, Heidelberg, New York, 2012.

Kanamitsu, M., Ebisuzaki, W., Woollen, J., Yang, S. K., Hnilo, J., Fiorino, M., and Potter, G.: Ncep–doe amip-ii reanalysis (r-2), Bulletin of the American Meteorological Society, 83, 1631–1644, 2002.

Khutorova, O., Khutorov, V., and Teptin, G.: Interannual variability of surface and integrated water vapor and atmospheric circulation in Europe, Atmospheric and Oceanic Optics, 31, 486–491, 2018.

Kiehl, J. T. and Trenberth, K. E.: Earth's annual global mean energy budget, Bulletin of the American meteorological society, 78, 197–208, 1997.

Kling, H., Fuchs, M., and Paulin, M.: Runoff conditions in the upper Danube basin under an ensemble of climate change scenarios, Journal of Hydrology, 424, 264–277, 2012.

Kobayashi, S., Ota, Y., Harada, Y., Ebita, A., Moriya, M., Onoda, H., Onogi, K., Kamahori, H., Kobayashi, C., and Endo, H.: The JRA-55 reanalysis: General specifications and basic characteristics, Journal of the Meteorological Society of Japan. Ser. II, 93, 5–48, 2015.

Krämer, M., Rolf, C., Spelten, N., Afchine, A., Fahey, D., Jensen, E., Khaykin, S., Kuhn, T., Lawson, P., Lykov, A., Pan, L. L., Riese, M., Rollins, A., Stroh, F., Thornberry, T., Wolf, V., Woods, S., Spichtinger, P., Quaas, J., and Sourdeval, O.: A microphysics guide to cirrus – Part 2: Climatologies of clouds and humidity from observations, Atmospheric Chemistry and Physics, 20, 12 569–12 608, 2020.

Kunz, A., Müller, R., Homonnai, V., M. Jánosi, I., Hurst, D., Rap, A., M. Forster, P., Rohrer, F., Spelten, N., and Riese, M.: Extending water vapor trend observations over Boulder into the tropopause region: Trend uncertainties and resulting radiative forcing, Journal of Geophysical Research: Atmospheres, 118, 11 269–11 284, 2013.

Kunz, A., Spelten, N., Konopka, P., Müller, R., Forbes, R. M., and Wernli, H.: Comparison of Fast In-situ Stratospheric Hygrometer (FISH) measurements of water vapor in the upper troposphere and lower stratosphere (UTLS) with ECMWF (re)analysis data, Atmospheric Chemistry and Physics, 14, 10 803–10 822, 2014.

Kursinski, E., Hajj, G., Hardy, K., Romans, L., and Schofield, J.: Observing tropospheric water vapor by radio occultation using the Global Positioning System, Geophysical Research Letters, 22, 2365–2368, 1995.

Lavers, D. A., Pappenberger, F., Richardson, D. S., and Zsoter, E.: ECMWF Extreme Forecast Index for water vapor transport: A forecast tool for atmospheric rivers and extreme precipitation, Geophysical Research Letters, 43, 11 852, 2016.

Martin-Vide, J. and Lopez-Bustins, J.: The western Mediterranean oscillation and rainfall in the Iberian Peninsula, International Journal of Climatology: A Journal of the Royal Meteorological Society, 26, 1455–1475, 2006.

McCarthy, M. P., Thorne, P., and Titchner, H. A.: An analysis of tropospheric humidity trends from radiosondes, Journal of Climate, 22, 5820–5838, 2009.

1105   McCarthy, M., Spillane, S., Walsh, S., and Kendon, M.: The meteorology of the exceptional winter of 2015/2016 across the UK and Ireland, Weather, 71, 305–313, 2016.

Mellado-Cano, J., Barriopedro, D., García-Herrera, R., Trigo, R. M., and Hernández, A.: Examining the North Atlantic oscillation, East Atlantic Pattern, and jet variability since 1685, Journal of Climate, 32, 6285–6298, 2019.

Mikhailova, N. and Yurovsky, A.: The East Atlantic oscillation: mechanism and impact on the European climate in winter,
1110   Physical Oceanography, 2016.

Moore, G. and Renfrew, I.: Cold European winters: interplay between the NAO and the East Atlantic mode, Atmospheric Science Letters, 13, 1–8, 2012.

Mueller, B. and Seneviratne, S. I.: Systematic land climate and evapotranspiration biases in CMIP5 simulations, Geophysical research letters, 41, 128–134, 2014.

1115   Müller, R., Kunz, A., Hurst, D. F., Rolf, C., Krämer, M., and Riese, M.: The need for accurate long-term measurements of water vapor in the upper troposphere and lower stratosphere with global coverage, Earth's Future, 4, 25–32, 2016.

Nilsson, T. and Elgered, G.: Long-term trends in the atmospheric water vapor content estimated from ground-based GPS data, Journal of Geophysical Research: Atmospheres, 113, 2008.

Ning, T., Wickert, J., Deng, Z., Heise, S., Dick, G., Vey, S., and Schöne, T.: Homogenized time series of the atmospheric
1120   water vapor content obtained from the GNSS reprocessed data, Journal of Climate, 29, 2443–2456, 2016.

Parracho, A. C., Bock, O., and Bastin, S.: Global IWV trends and variability in atmospheric reanalyses and GPS observations, Atmospheric Chemistry and Physics, 18, 16213–16237, 2018.

Randel, W. J. and Wu, F.: Kelvin wave variability near the equatorial tropopause observed in GPS radio occultation measurements, Journal of Geophysical Research: Atmospheres, 110, 2005.

1125   Randel, W. J., Wu, F., and Forster, P.: The Extratropical Tropopause Inversion Layer: Global Observations with GPS Data, and a Radiative Forcing Mechanism, Journal of the Atmospheric Sciences., 64, 4489–4496, 2007.

Rebischung, P. and Schmid, R.: IGS14/igs14. atx: a new framework for the IGS products, AGU Fall Meeting 2016, 2016.

Saastamoinen, J.: Atmospheric correction for the troposphere and stratosphere in radio ranging satellites, The use of artificial satellites for geodesy, 15, 247–251, 1972.

1130   Saha, S., Moorthi, S., Pan, H.-L., Wu, X., Wang, J., Nadiga, S., Tripp, P., Kistler, R., Woollen, J., and Behringer, D.: The NCEP climate forecast system reanalysis, Bulletin of the American Meteorological Society, 91, 1015–1058, 2010.

Saha, S., Moorthi, S., Wu, X., Wang, J., Nadiga, S., Tripp, P., Behringer, D., Hou, Y.-T., Chuang, H., and Iredell, M.: The NCEP climate forecast system version 2, Journal of climate, 27, 2185–2208, 2014.

Santos, J. A., Woollings, T., and Pinto, J. G.: Are the winters 2010 and 2012 archetypes exhibiting extreme opposite
1135   behavior of the North Atlantic jet stream?, Monthly Weather Review, 141, 3626–3640, 2013.

Schneider, T., O'Gorman, P. A., and Levine, X. J.: Water vapor and the dynamics of climate changes, Reviews of Geophysics, 48, 2010.

Schröder, M., Lockhoff, M., Fell, F., Forsythe, J., Trent, T., Bennartz, R., Borbas, E., Bosilovich, M. G., Castelli, E., and Hersbach, H.: The GEWEX Water Vapor Assessment archive of water vapour products from satellite observations and reanalyses, Earth system science data, 10, 1093–1117, 2018.

Schröder, M., Lockhoff, M., Forsythe, J. M., Cronk, H. Q., Vonder Haar, T. H., and Bennartz, R.: The GEWEX water vapor assessment: Results from intercomparison, trend, and homogeneity analysis of total column water vapor, Journal of Applied Meteorology and Climatology, 55, 1633–1649, 2016.

Schüler, T.: On ground based GPS tropospheric delay estimation (PhD Thesis), Univ. der Bundeswehr München, Fak. für Bauingenieur- und Vermessungswesen, Studiengang Geodäsie und Geoinformation, 2001.

Schwing, F., Murphree, T., and Green, P.: The Northern Oscillation Index (NOI): a new climate index for the northeast Pacific, Progress in Oceanography, 53, 115–139, 2002.

Sharifnezhadazizi, Z., Norouzi, H., Prakash, S., Beale, C., and Khanbilvardi, R.: A global analysis of land surface temperature diurnal cycle using MODIS observations, Journal of Applied Meteorology and Climatology, 58, 1279–1291, 2019.

Steinke, S., Wahl, S., and Crewell, S.: Benefit of high resolution COSMO reanalysis: The diurnal cycle of column-integrated water vapor over Germany, Meteorol. Z, 28, 165–177, 2019.

Stockdale, T., Balmaseda, M., and Ferranti, L.: The 2015/2016 El Niño and beyond. ECMWF Newsletter 151, 464–465, 2017.

Taws, S. L., Marsh, R., Wells, N. C., and Hirschi, J.: Re-emerging ocean temperature anomalies in late-2010 associated with a repeat negative NAO, Geophysical Research Letters, 38, 2011.

Thébault, E., Finlay, C. C., Beggan, C. D., Alken, P., Aubert, J., Barrois, O., Bertrand, F., Bondar, T., Boness, A., and Brocco, L.: International geomagnetic reference field: the 12th generation, Earth, Planets and Space, 67, 1–19, 2015.

Thompson, D. W. and Wallace, J. M.: The Arctic Oscillation signature in the wintertime geopotential height and temperature fields, Geophysical research letters, 25, 1297–1300, 1998.

Tilmes, S., Pan, L. L., Hoor, P., Atlas, E., Avery, M. A., Campos, T., Christensen, L. E., Diskin, G. S., Gao, R.-S., Herman, R. L., Hintsa, E. J., Loewenstein, M., Lopez, J., Paige, M. E., Pittman, J. V., Podolske, J. R., Proffitt, M. R., Sachse, G. W., Schiller, C., Schlager, H., Smith, J., Spelten, N., Webster, C., Weinheimer, A., and Zondlo, M. A.: An aircraft based upper troposphere lower stratosphere O3, CO, and H2O climatology for the Northern Hemisphere, Journal of Geophysical Research: Atmospheres, 115, D14303, 2010.

Trenberth, K. E. and Fasullo, J. T.: North American water and energy cycles, Geophysical research letters, 40, 365–369, 2013.

Trenberth, K. E., Dai, A., Rasmussen, R. M., and Parsons, D. B.: The changing character of precipitation, Bulletin of the American Meteorological Society, 84, 1205–1218, 2003.

Trenberth, K. E.: Framing the way to relate climate extremes to climate change, Climatic change, 115, 283–290, 2012.

Trenberth, K. E.: The definition of el nino, Bulletin of the American Meteorological Society, 78, 2771–2778, 1997.

Trigo, R. M., Osborn, T. J., and Corte-Real, J. M.: The North Atlantic Oscillation influence on Europe: climate impacts and associated physical mechanisms, Climate research, 20, 9–17, 2002.

Turato, B., Reale, O., and Siccardi, F.: Water vapor sources of the October 2000 Piedmont flood, Journal of Hydrometeorology, 5, 693–712, 2004.

1175

Van Malderen, R., Pottiaux, E., Klos, A., Domonkos, P., Elias, M., Ning, T., Bock, O., Guijarro, J., Alshawaf, F., and Hoseini, M.: Homogenizing GPS integrated water vapor time series: Benchmarking break detection methods on synthetic data sets, Earth and Space Science, 7, e2020EA001121, 2020.

Vey, S., Dietrich, R., Rülke, A., Fritsche, M., Steigenberger, P., and Rothacher, M.: Validation of precipitable water vapor within the NCEP/DOE reanalysis using global GPS observations from one decade, Journal of Climate, 23, 1675–1695, 2010.

1180

Vogelmann, H., Sussmann, R., Trickl, T., and Reichert, A.: Spatiotemporal variability of water vapor investigated using lidar and FTIR vertical soundings above the Zugspitze, Atmospheric Chemistry and Physics, 15, 3135–3148, 2015.

Vonder Haar, T. H., Bytheway, J. L., and Forsythe, J. M.: Weather and climate analyses using improved global water vapor observations, Geophysical Research Letters, 39, 2012.

1185

Wagner, T., Beirle, S., Dörner, S., Borger, C., and Van Malderen, R.: Identification of atmospheric and oceanic teleconnection patterns in a 20-year global data set of the atmospheric water vapour column measured from satellites in the visible spectral range, Atmospheric Chemistry and Physics, 21, 5315–5353, 2021.

Wang, C., Liu, H., and Lee, S.: The record-breaking cold temperatures during the winter of 2009/2010 in the Northern Hemisphere, Atmospheric Science Letters, 11, 161–168, 2010.

1190

Wang, J. and Zhang, L.: Climate applications of a global, 2-hourly atmospheric precipitable water dataset derived from IGS tropospheric products, Journal of Geodesy, 83, 209–217, 2009.

Wang, J., Dai, A., and Mears, C.: Global water vapor trend from 1988 to 2011 and its diurnal asymmetry based on GPS, radiosonde, and microwave satellite measurements, Journal of Climate, 29, 5205–5222, 2016.

1195

Wang, J., Zhang, L., and Dai, A.: Global estimates of water-vapor-weighted mean temperature of the atmosphere for GPS applications, Journal of Geophysical Research: Atmospheres, 110, 2005.

Wang, S., Xu, T., Nie, W., Jiang, C., Yang, Y., Fang, Z., Li, M., and Zhang, Z.: Evaluation of precipitable water vapor from five reanalysis products with Ground-Based GNSS observations, Remote Sensing, 12, 1817, 2020.

Wang, X., Zhang, K., Wu, S., Li, Z., Cheng, Y., Li, L., and Yuan, H.: The correlation between GNSS-derived precipitable water vapor and sea surface temperature and its responses to El Niño Southern Oscillation, Remote Sensing of Environment, 216, 1–12, 2018.

1200

Wang, Y., Yang, K., Pan, Z., Qin, J., Chen, D., Lin, C., Chen, Y., Tang, W., Han, M., and Lu, N.: Evaluation of precipitable water vapor from four satellite products and four reanalysis datasets against GPS measurements on the Southern Tibetan Plateau, Journal of Climate, 30, 5699–5713, 2017.

1205 Wypych, A., Bochenek, B., and Różycki, M.: Atmospheric moisture content over Europe and the Northern Atlantic, Atmosphere, 9, 18, 2018.

Yuan, P., Hunegnaw, A., Alshawaf, F., Awange, J., Klos, A., Teferle, F. N., and Kutterer, H.: Feasibility of ERA5 integrated water vapor trends for climate change analysis in continental Europe: An evaluation with GPS (1994 2019) by considering statistical significance, Remote Sensing of Environment, 260, 112416, 2021.

1210   Zhu, Y. and Newell, R. E.: Atmospheric rivers and bombs, Geophysical Research Letters, 21, 1999–2002, 1994.
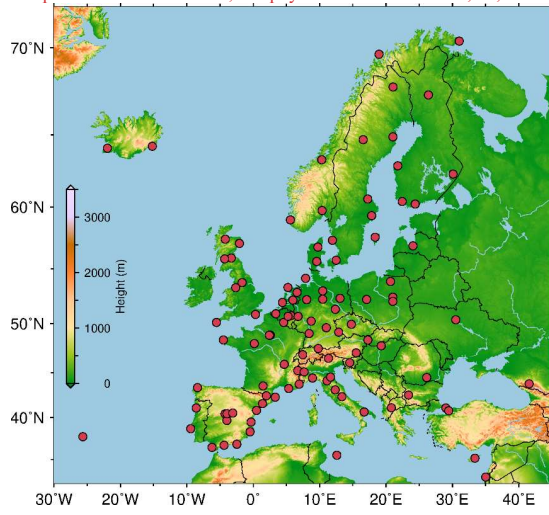
Figure 1. Geographical distribution of the 108 GPS stations (red dots). An enlarged version of this figure with station names is provided in ~~Figure~~ Fig. S1 in the supplementary material. The coordinates of the stations and their time lengths are provided in Table S1.

1215
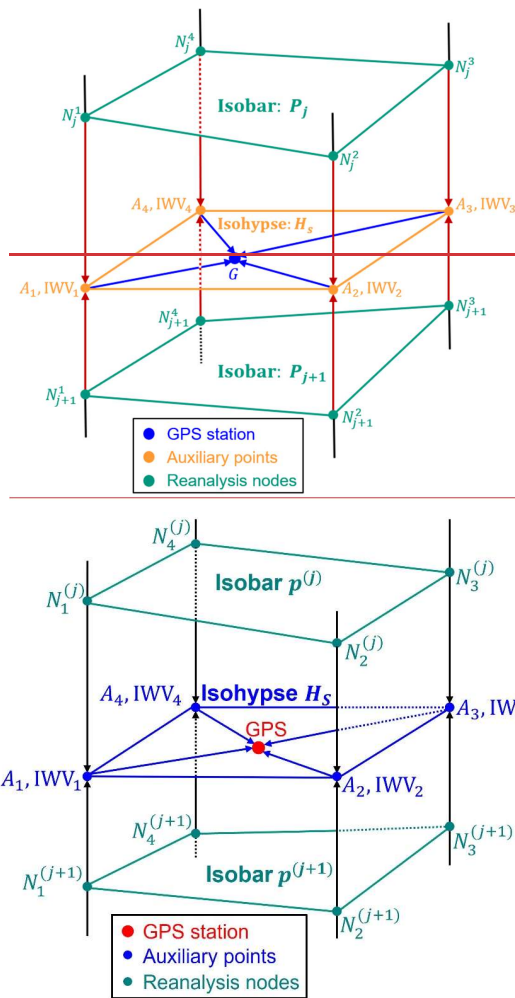
Figure 2. Schematic plot of the vertical and horizontal interpolation of the reanalysis pressure level products. The IWV at each auxiliary point (A_i; orange dots) is calculated with vertical interpolation or extrapolation of the adjacent reanalysis

1220   nodes ($N_i^{(j)}$ and $N_i^{(j+1)}$; green dots). The IWV at the GPS station (red dot) is then estimated with horizontal interpolation of the auxiliary points.
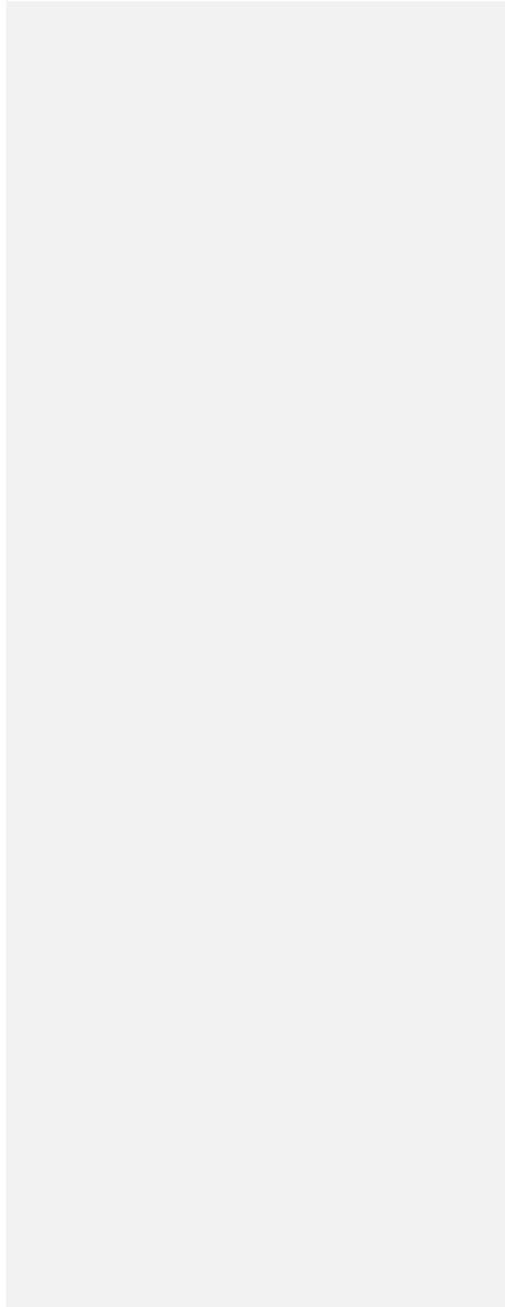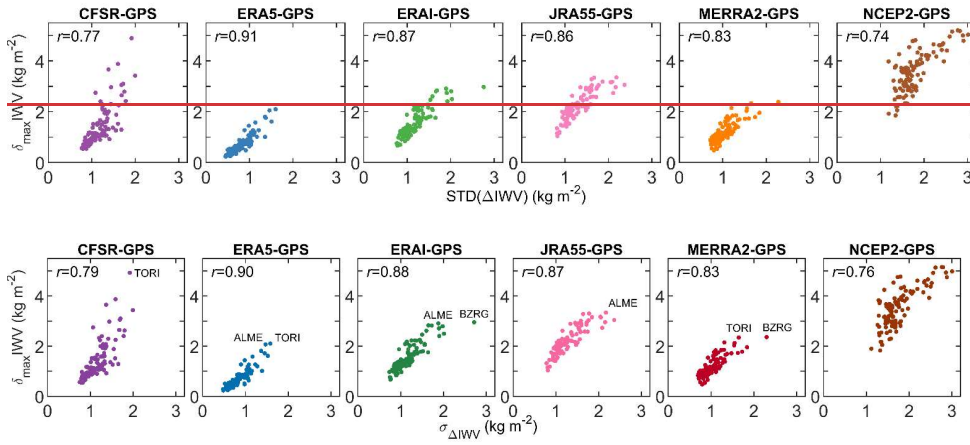
1225 **Figure 3.** Scatterplots showing the relationships between the standard deviations of daily IWV difference (σ_Δ) and the representativeness error statistic (δ_{max}) for the 108 GPS stations.
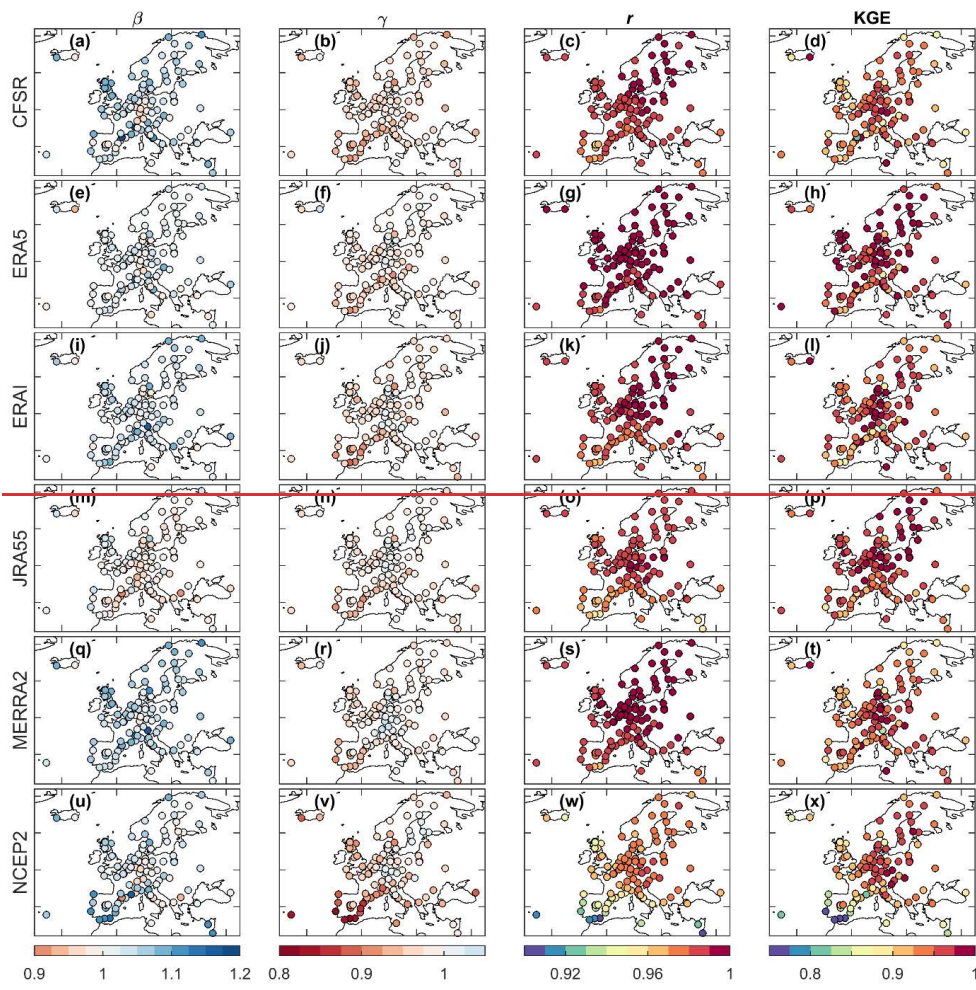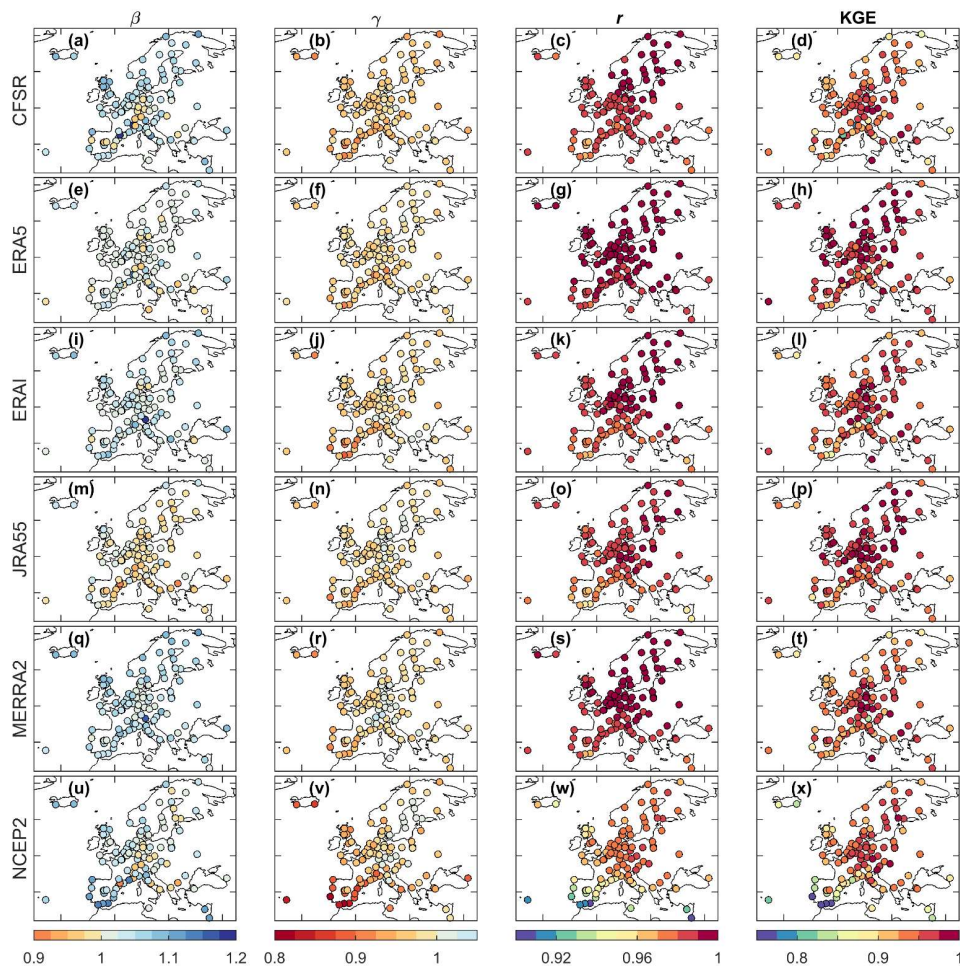
1230   **Figure 4.** Plots of the KGE parameters for the daily IWV time series of the 108 GPS stations. The β and γ indicate the consistencies in the mean and variability, respectively. The r indicates the Pearson correlation coefficient between the GPS and reanalyses time series. With perfect consistencies in mean, variability, and correlation, the β, γ, and r are identical to 1, respectively. When the β, γ, and r are identical to 1, the KGE score will reach its maximum value of 1.

Formatted: Check spelling and grammar

Formatted: Check spelling and grammar

Formatted: Check spelling and grammar

Formatted: Check spelling and grammar

Formatted: Check spelling and grammar

Formatted: Check spelling and grammar

Formatted: Check spelling and grammar
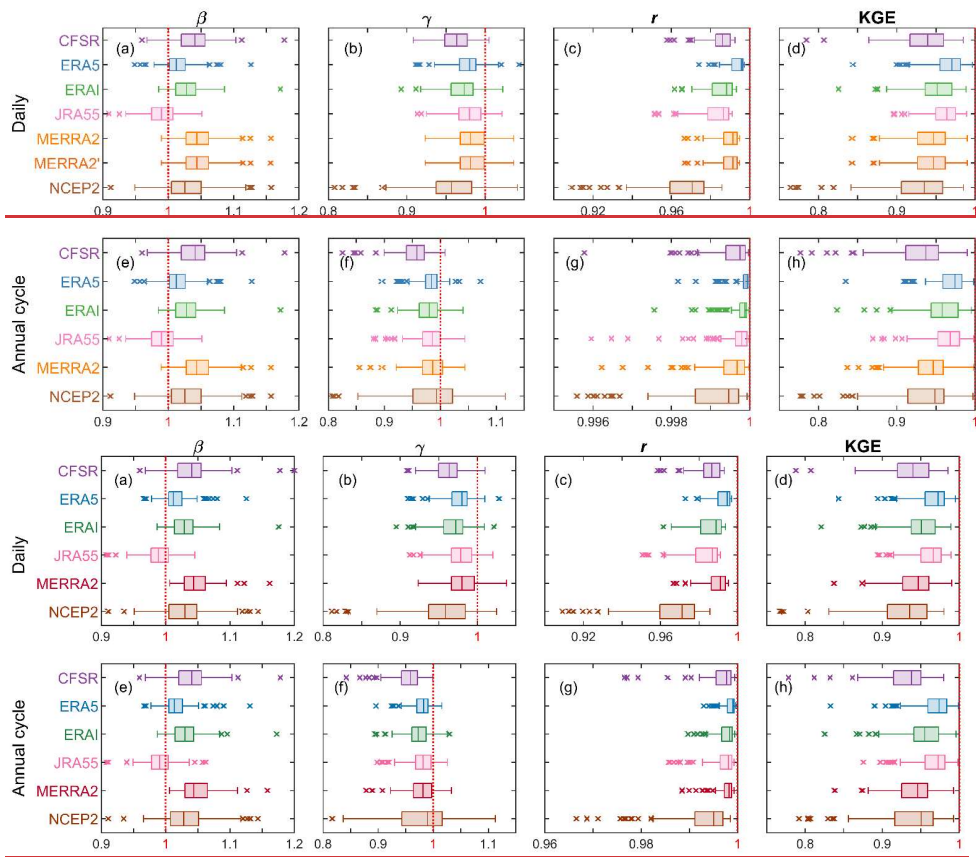
Figure 5. Box-whisker plots of the KGE parameters for the daily time series (a−d) and monthly annual cycle of IWV (e−h) from the reanalyses compared to GPS for the 108 stations.

1235
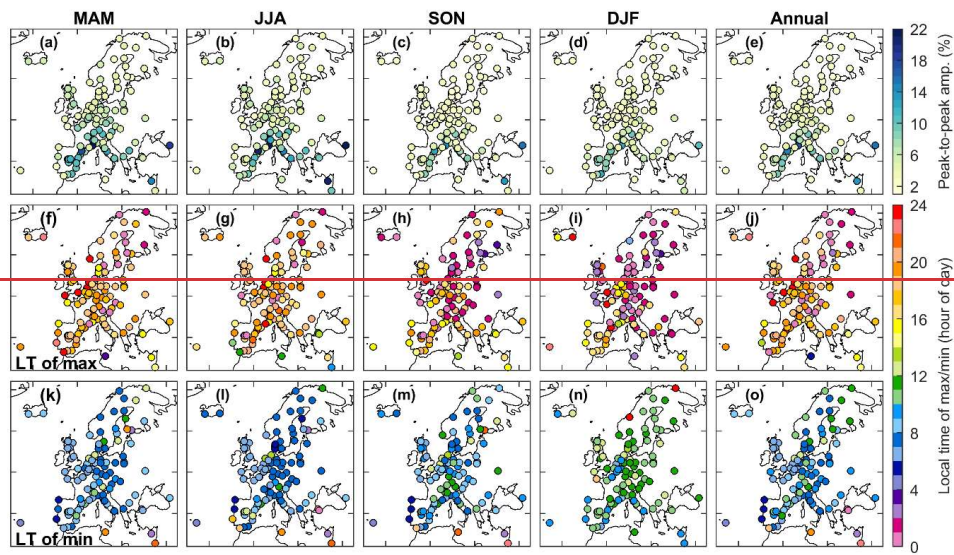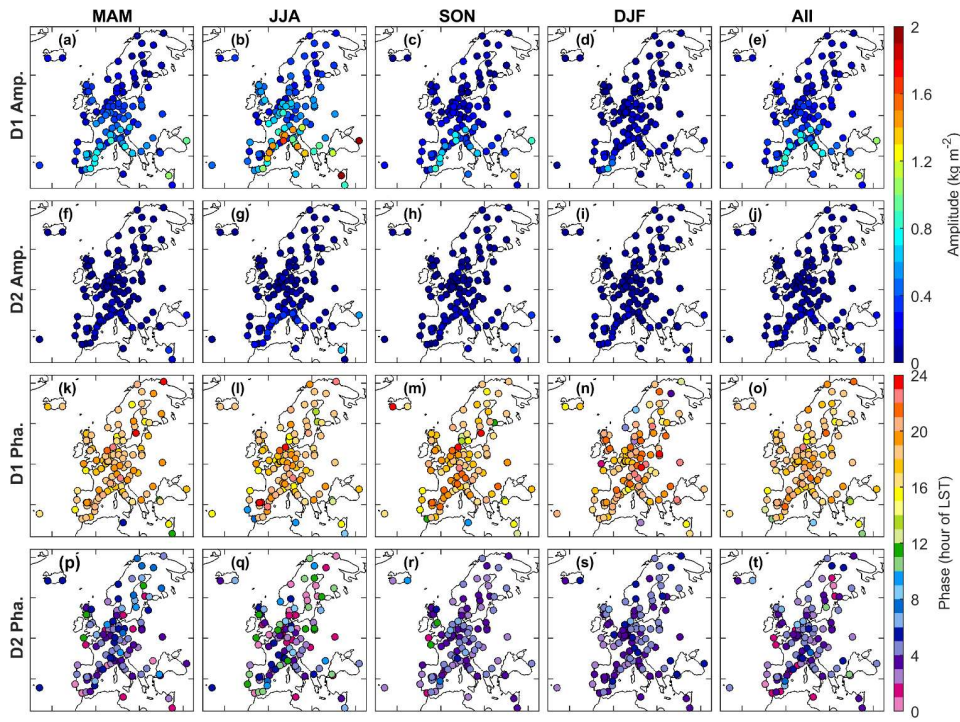
Figure 6. Plots of the amplitudes (a and f) and phases (k and p) for the first (D1) and second (D2) harmonics of diurnal GPS IWV cycle averaged in MAM (spring) at each station, respectively. relative peak-to-peak amplitude (a), local time of occurrence of the maximum (f) and minimum (k) of the diurnal cycle of GPS IWV averaged in MAM (spring) for the 108 GPS stations. The other subplots are for JJA (summer), SON (autumn), DJF (winter), and annual, from left to right, respectively. The phases are in Local Solar Time (LST) at the peak of associated harmonics.
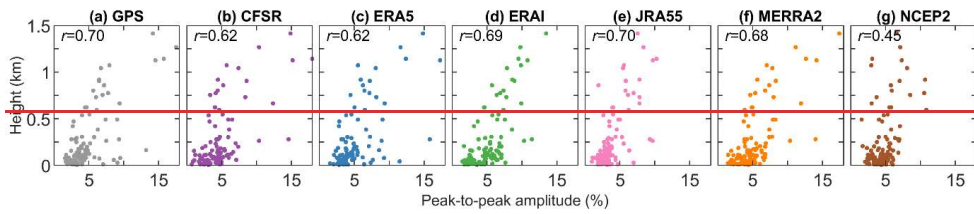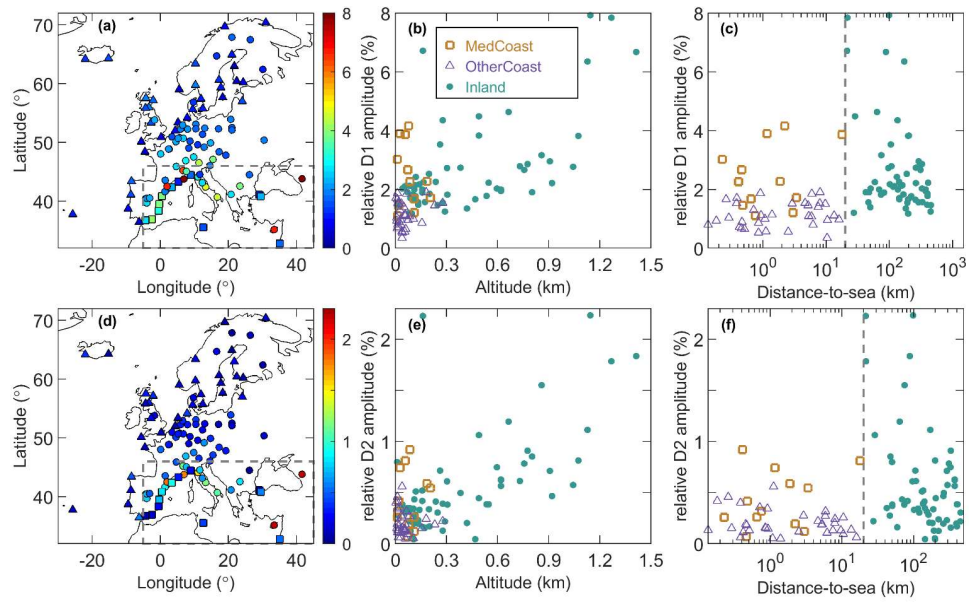
Figure 7. (a) relative amplitudes of the first harmonic (D_1) of diurnal GPS IWV cycle. (b) and (c) are the variations of the relative D_1 amplitudes with respect to station altitude and distance-to-sea, respectively. (d−f) are the same as (a−c) but for the second harmonic (D_2). The stations are classified into three types, namely Inland, MedCoast and OtherCoast. The type of Inland includes 62 stations with their distance to sea (SeaDist) no shorter than 20 km. The type of MedCoast contains 12 stations located at the coastal region of Mediterranean (SeaDist<20 km, 32 °N <Lat<46 °N, 5 °W<Lon<45 °E). The rest 34 stations are classified as OtherCoast.

260
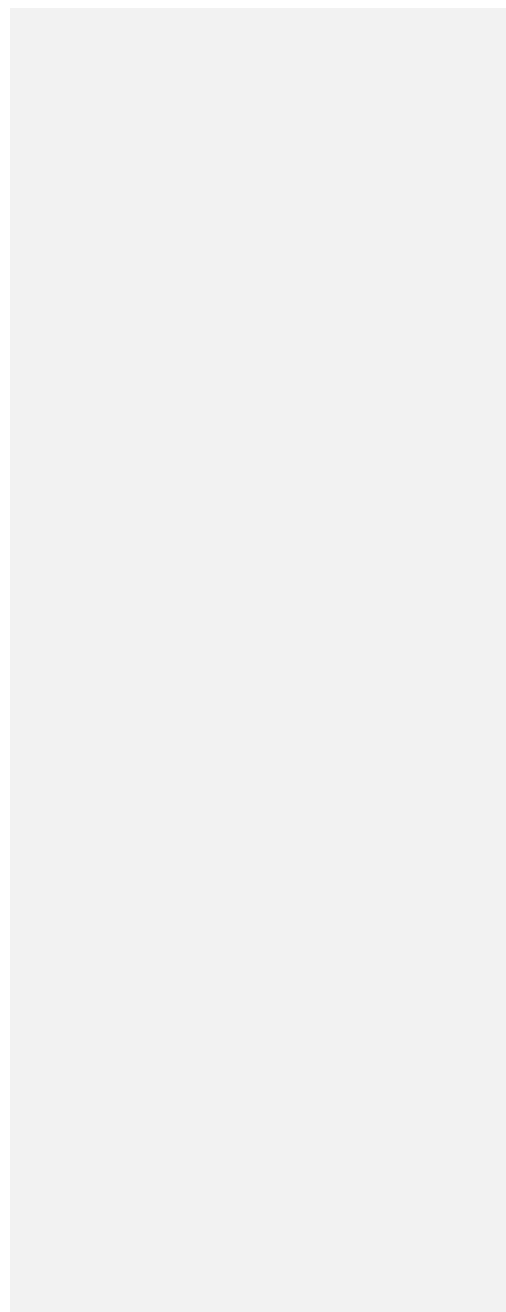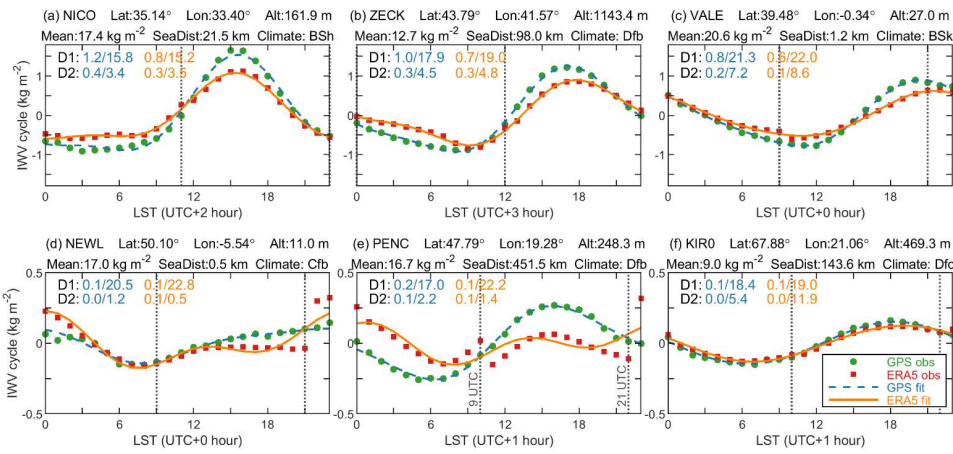
Figure 8. Diurnal IWV cycles at selected six stations obtained from 1-hourly GPS (green dots) and ERA5 (red squares). The stations are selected with the consideration of different altitudes, distance-to-sea (SeaDist), and climate zones classified according to Köppen Climate Classification (Beck et al., 2018). The data points are fitted with diurnal (D1) and semidiurnal (D2) harmonics (blue dashed curve for GPS and orange curve for ERA5). The amplitudes and phases of the D1 and D2 harmonics are also given. The phases are shown as the Local Solar Time (LST) at the peak of associated harmonics. For instance, the D1 amplitude and phase of GPS IWV at station NICO are 1.2 kg m^{-2} and 15.8 LST, respectively. By comparison, the values of its ERA5 IWV are 0.8 kg m^{-2} and 15.2 LST, respectively. The vertical black dotted lines at 09 and 12 UTC indicate the time of possible mismatches in the ERA5 IWV cycle.
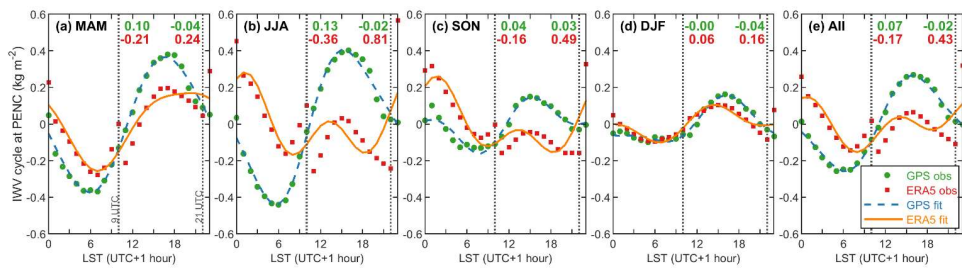
Figure 9. (a) Similar to Fig. 8 but for the seasonal and all-time averaged diurnal IWV cycles at station PENC. The green and red numbers are the IWV shifts from ERA5 and GPS, respectively. The numbers on the left and right are the IWV shifts from 09 to 10 UTC and from 21 to 22 UTC, respectively.
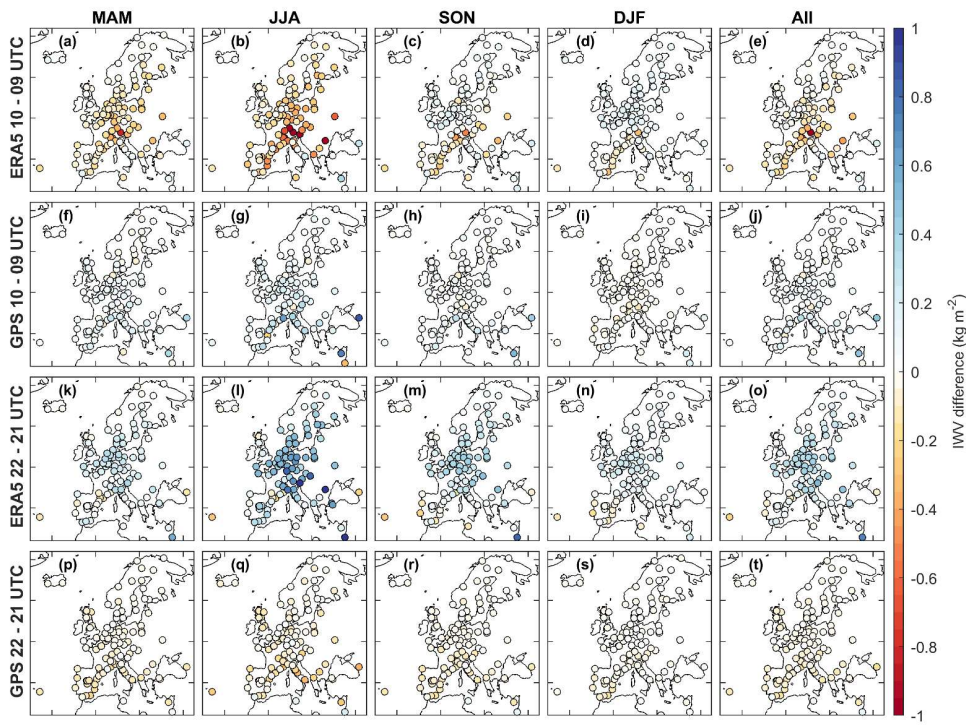
Figure 10. Seasonal and all-time averaged IWV shifts in the GPS and ERA5 diurnal cycles from 09 to 10 UTC and from 21 to 22 UTC.
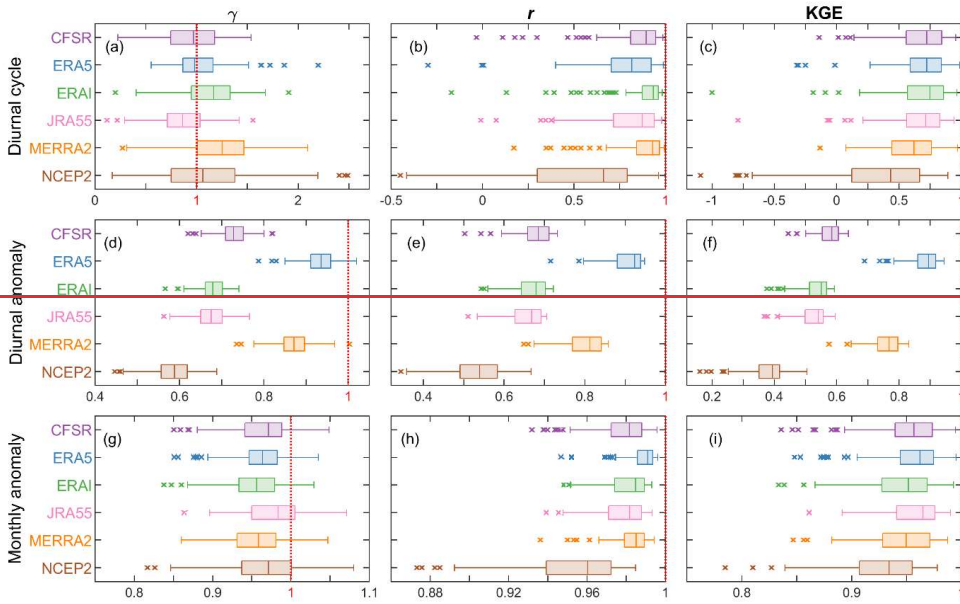
Figure 8. Box-whisker plots of the KGE parameters for the relative diurnal cycle (a-c), diurnal anomaly (d-f), and monthly anomaly (g-i) of IWV from the reanalyses compared to GPS for the 108 stations.
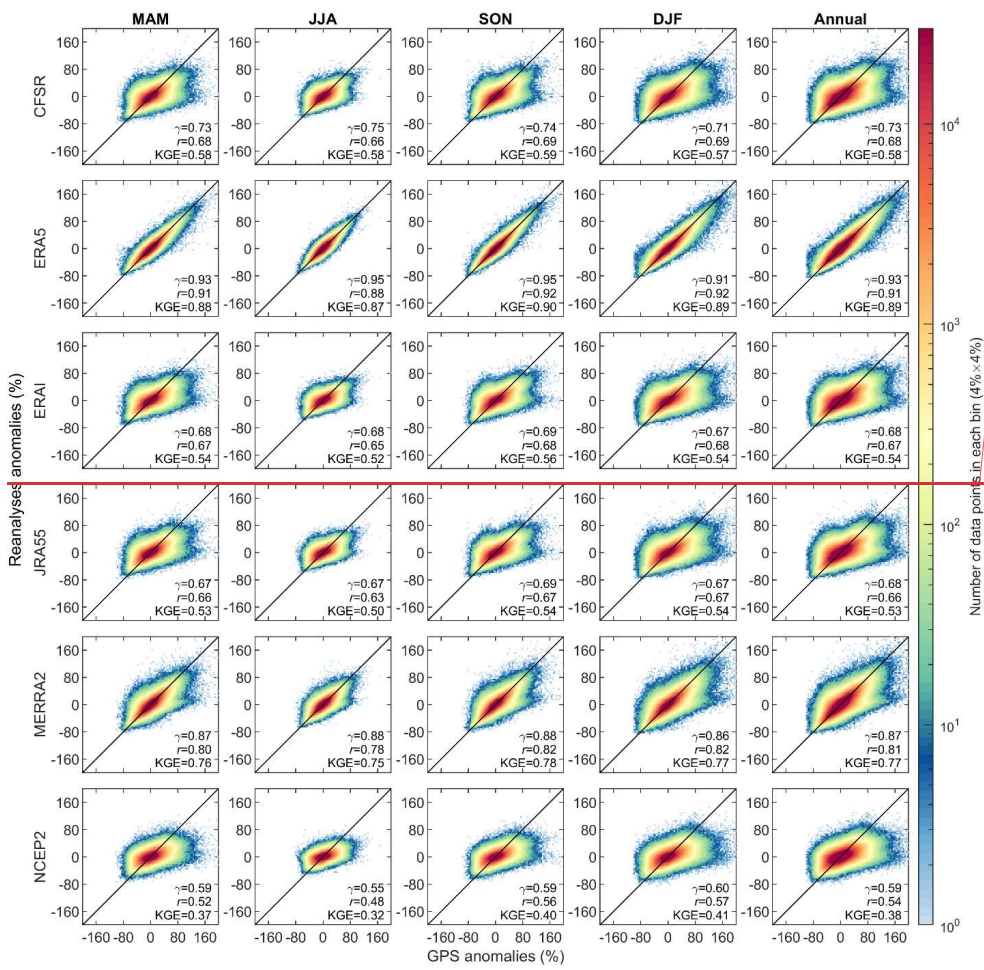
1285 **Figure 9.** Scatter plot of the hourly relative anomalies from the daily mean IWV in percentage for the 108 GPS stations. The KGE parameters of the intercomparison are also given.

Formatted: Figure, Justified

Formatted: Figure, Justified
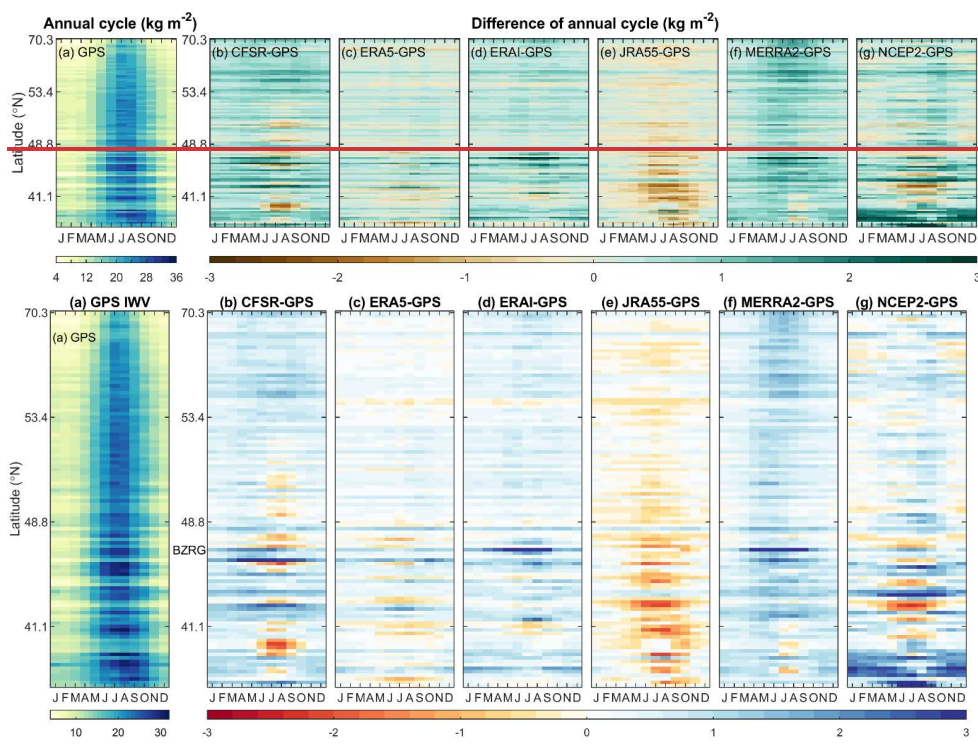
1290   **Figure ~~10~~11.** (a) Monthly annual cycle of GPS IWV in kg m⁻² for the 108 GPS stations with increasing latitude from bottom up. ~~The stations are shown with descending latitudes.~~ (b–g) are the differences of annual cycle from the various reanalyses compared to the GPS.

1295
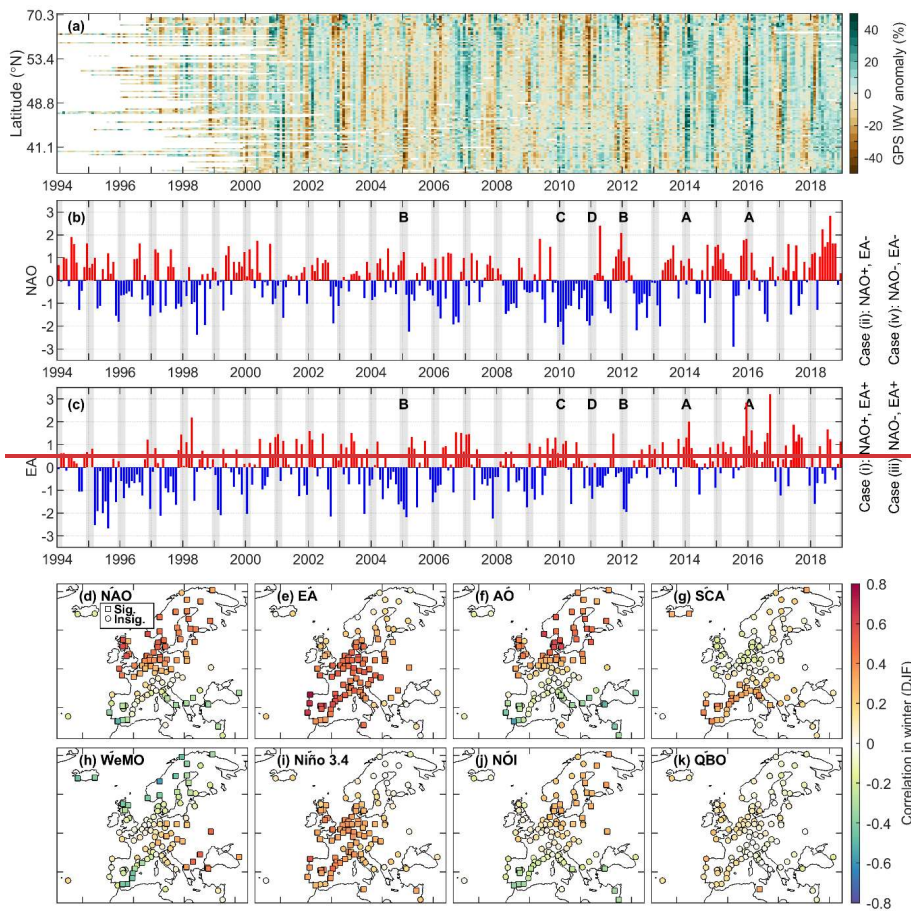
Figure 11. (a) Monthly relative anomalies of GPS IWV for the 108 GPS stations with descending latitudes. (b) and (c) are monthly NAO and EA indices, respectively. The gray bars in (b) and (c) indicates the winter months, i.e., DJF. The winters typically characterized with the four cases (i, ii, iii, and iv) are labelled. (d-k) Spatial correlations between the GPS IWV
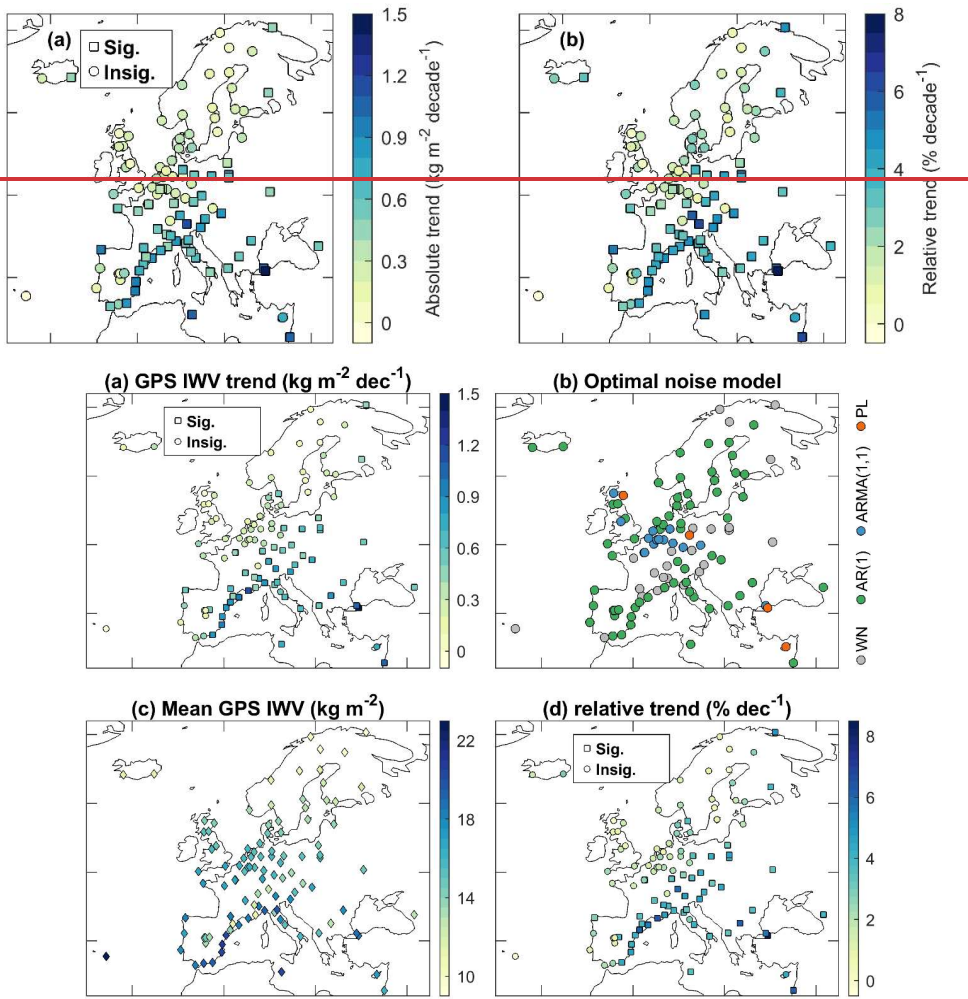
1305 **Figure 12.** (a) Map of the absolute trends of the homogenised monthly GPS IWV anomaly time series. The squares and circles indicate the trend estimates being significant and insignificant at 95% confidence level, respectively. The trend uncertainties are estimated based on optimal noise models (b). The relative trends (d) are calculated as the absolute trends (a) divided by the associated average IWV (c).

Maps for the absolute (a) and relative (b) trends of the monthly IWV anomaly time series. The relative trend of each station
1310 was calculated as the absolute trends divided by the associated average IWV. The squares and circles indicate the trend estimates being significant and insignificant at 95% confidence level, respectively.
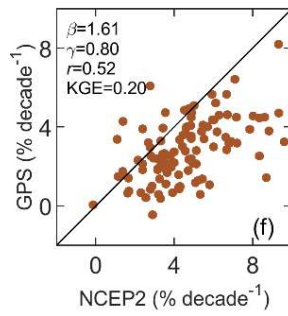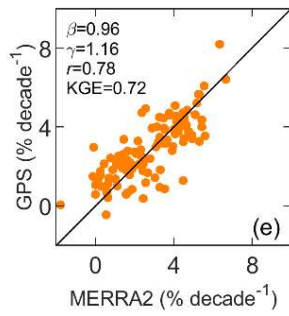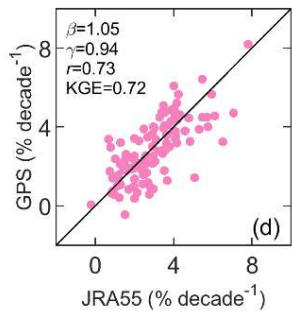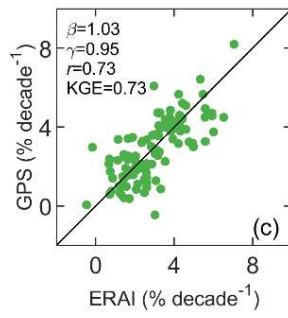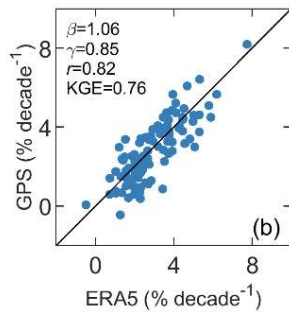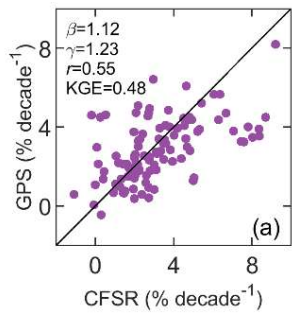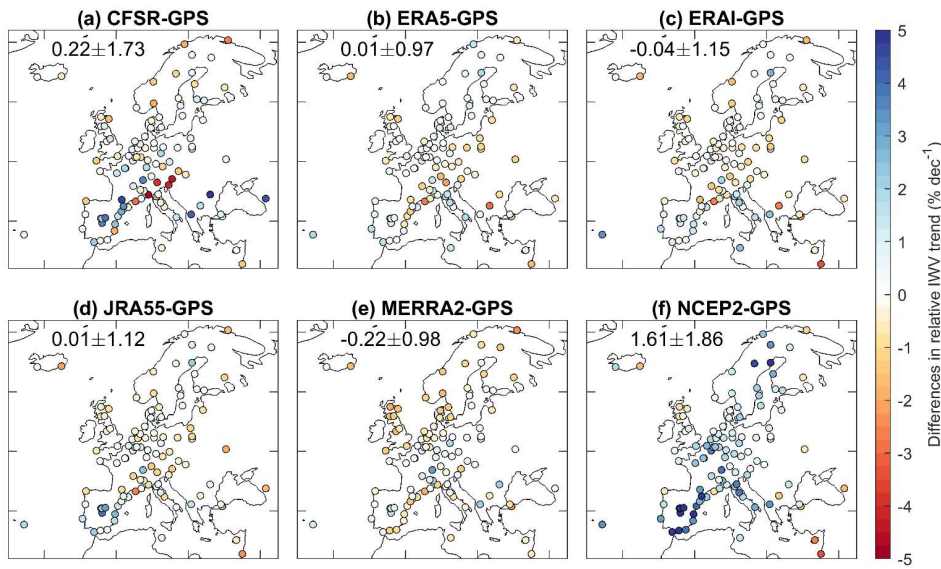
Figure 13. Comparison of the relative IWV trends differences (% decade^{-1}) from for various reanalyses against with respect to GPS, respectively. The numbers in each subplot indicate the mean value and standard deviation of the associated relative IWV trend differences, respectively.

Table 1. Six atmospheric reanalyses used in this study and their characteristics.

Reanalysis	CFSR	ERA5	ERAI	JRA55	MERRA2	NCEP2
Source	NCEP	ECMWF	ECMWF	JMA	GMAO	NCEP
Assimilation	3DVAR	4DVAR	4DVAR	4DVAR	3DVAR	3DVAR
Time range	1979−present	1979−present	1979−Aug. 2019	1958−present	1980−present	1979−present
Temporal res. (hour)	6	1	6	6	3	6
Horizontal res. (lat.×lon.)	0.5°×0.5°	0.25°×0.25°	0.75°×0.75°	1.25°×1.25°	0.5°×0.625°	2.5°×2.5°
Pressure levels	37	37	37	37	42	17
References	Saha et al., 2010, 2014	Hersbach et al., 2020	Dee et al., 2011	Kobayashi et al., 2015	Gelaro et al., 2017	Kanamitsu et al., 2002

1320

Table 2. Statistics of the consistencies in diurnal IWV anomalies from reanalyses compared to GPS.

	Temporal resolution	CFSR	ERA5	ERAI	JRA55	MERRA2	NCEP2
γ	1 h	0.98±0.04	0.98±0.03	0.91±0.04	0.86±0.04	1.02±0.04	0.75±0.05
	3 h	–	0.97±0.03	–	–	1.02±0.04	–
	6 h	0.99±0.03	0.96±0.03	0.92±0.04	0.87±0.04	–	0.76±0.05
r	1 h	0.85±0.05	0.89±0.05	0.85±0.06	0.83±0.06	0.86±0.06	0.69±0.08
	3 h	–	0.89±0.05	–	–	0.86±0.06	–
	6 h	0.87±0.05	0.90±0.06	0.86±0.07	0.84±0.07	–	0.69±0.08
KGE	1 h	0.85±0.05	0.88±0.06	0.82±0.07	0.78±0.07	0.85±0.06	0.60±0.09
	3 h	–	0.89±0.06	–	–	0.86±0.06	–
	6 h	0.86±0.06	0.89±0.06	0.83±0.07	0.79±0.07	–	0.60±0.08
RMS (kg m^{-2})	1 h	1.14±0.19	0.97±0.21	1.14±0.22	1.20±0.21	1.14±0.22	1.57±0.24
	3 h	–	0.97±0.21	–	–	1.15±0.22	–
	6 h	1.09±0.21	0.94±0.21	1.09±0.24	1.16±0.22	–	1.59±0.24

Appendix A: Homogenisation of GNSS IWV time series

Long-term IWV time series often suffer from inhomogeneities due to changes in instrumentation, data processing methods, and local environmental conditions (Van Malderen et al., 2020; Nguyen et al., 2021 and references therein). These inhomogeneities can manifest themselves as changes in the mean of the time series ("biases") at specific epochs, i.e., breaks or changepoints. If such changepoints are not properly corrected, they can significantly modify the estimations of long-term linear trend and multi-temporal-scale variabilities (e.g., Ning et al., 2016; Van Malderen et al., 2020; Yuan et al., 2021). Therefore, the homogenisation of the IWV time series is essential for a sound understanding and proper interpretation of IWV variability under climate change.

In this work, we examined the homogeneity of the monthly GPS IWV time series by using the RHtestsV4 software (Wang and Feng, 2013). This software is developed especially for the detection and adjustment of changepoints in climatic time series, and it has been used in the homogenisation of IWV time series in previous studies (Ning et al., 2016; Schröder et al., 2016; Van Malderen et al., 2020). The software is based on a penalized maximal t test with the consideration of linear trend, annual cycle, and AR(1) noise in the time series (Wang et al., 2007; Wang 2008).

We took all the six reanalyses as references for the homogenisation of the GNSS IWV time series, meaning that we inspected the monthly IWV difference time series between the GNSS and each of the reanalysis IWV. It is noteworthy that the reanalyses may also contain changepoints (e.g., Ning et al., 2016; Schröder et al, 2016). However, we did not homogenise the reanalyses IWV time series because they represent the native quality of the reanalyses that we would like to assess in this work. Also, by taking all six reanalyses as references, we are confident to minimise the impact of inhomogeneities in either reanalysis on the homogenisation process of the GNSS IWV time series. Practically, we used the following strategy to avoid the impacts of changepoints in specific reanalyses on the homogenisation of the GPS IWV time series:

(1) We examined the GPS IWV and metadata (station log file and IGSMAIL) carefully. If there is an instrumentation change within the first (or the last) year, we removed the several months before (or after) the epoch of change. Moreover, we also inspected the station up-coordinate time series and excluded periods with quality problem, as it is well-known that they are strongly correlated with the GPS tropospheric delay estimates (Tregoning and Herring, 2006). An example is given in Fig. A1 and will be described later in this appendix.

(2) We used the *FindU.wRef* command of the RHtestsV4 software to identify all possible changepoints in each GPS-reanalysis IWV monthly mean difference time series, which can be significant at a confidence level of 99% no matter they are documented in metadata or not.

(3) If a changepoint is within three months before or after a documented change in instrumentation, we adjusted its epoch according to the metadata and set it as Type-0. The rest changepoints are set as Type-1.

(4) If identical Type-1 changepoints are reported within six months in at least four GPS-reanalysis IWV differences, but not supported by metadata, we recognised them as a single Type-1 changepoint at the median of the epochs.

(5) We estimated the amplitudes of the Type-0 and Type-1 changepoints and tested their amplitude significances at a confidence level of 99% with the *StepSize.wRef* command of the RHtestsV4 software.

(6) We calculated the amplitude of each changepoint as the average of all the significant amplitude estimates from the six GPS-reanalysis IWV differences.

(7) We removed a changepoint if its amplitude is only significant in less than four GPS-reanalysis comparisons or its amplitude is less than three times of its standard deviation. Then, we repeated the steps of (5) and (6) until all the rest changepoints are significant.

The changepoint identification is finished after one or two iterations for most stations. In the end, we identified 44 Type-0 and 9 Type-1 changepoints as listed in Table A1. The total number of 53 changepoints is consistent to a previous global GPS IWV homogenisation work carried out by Ning et al. (2016), which identified 45 changepoints in total at 101 stations.

As the changepoint detection was carried out on monthly level, the specific dates of the Type-0 changepoint are fixed as documented. However, for the Type-1 changepoints without supports from metadata, their time of occurrences are fixed to the 15th day of associated month. We adjusted the GPS IWV time series by adding the amplitude of each changepoint to the GPS IWV data points before its time of occurrence. Note that five out of the nine Type-1 changepoints are significant in all the six GPS-reanalyses comparisons. Although we tried to minimize the impacts of changepoints in specific reanalyses on the results here, we cannot completely rule out that identical changepoints appear in all the six reanalyses by ingesting the same observational datasets through data assimilation.

Figure A1 and A2 show the homogenisation results at two stations. Station HERS (Herstmonceux, UK, 0.34 °E, 50.87 °N) is characterised with abnormal variations in its up-coordinate time series before the changes of antenna and receiver on 1998-2-18 as shown in Fig. A1h, indicating low-quality observations related to the instrumentation. In addition, obvious abnormal variations can be seen in all the GPS-reanalysis comparisons before 2001 September. We checked IGSMAIL-3503 (https://lists.igs.org/pipermail/igsmail/2001/004876.html) which reported a repair of antenna at station HERS until 2001-9-3. Therefore, we excluded the GPS IWV data before the date of repair. Then, we used the RHtestsV4 software to identify the changepoints in the rest GPS

IWV time series and found one on 2010-8-19, which is significant at a confidence level of 99%. It is a Type-0 changepoint due to an antenna and receiver changes as recorded in the station log file. After the homogenisation, the linear trend of the GPS IWV time series at station HERS has been reduced from 0.71 to 0.27 kg m^{-2} decade^{-1}, which generally agrees better with the trend estimates from reanalyses, which are 0.15, 0.43, 0.33, 0.37, 0.10, and 0.59 kg m^{-2} decade^{-1} for CFSR, ERA5, ERAI, JRA55, MERRA2, and NCEP2, respectively.

Station ERLA (Erlangen, Germany, 11.01 °E, 49.59 °N) has a Type-1 changepoint in 2015 July for unknown reason, in addition to a Type-0 one due to antenna and radome changes on 2010-8-18 (Fig. A2). The date of the Type-1 changepoint was fixed to 2005-7-15. With the homogenisation, the linear trend of the GPS IWV time series at station ERLA has been increased from 0.14 to 0.40 kg m^{-2} decade^{-1}, which is closer to the trend estimates from reanalyses, which are 0.43, 0.36, 0.41, 0.43, 0.52, and 0.68 kg m^{-2} decade^{-1} for CFSR, ERA5, ERAI, JRA55, MERRA2, and NCEP2, respectively. Moreover, we compared the GPS IWV trend to three nearby stations (KARL, KLOP, and WTZR) with values of 0.56, 0.32, and 0.66 kg m^{-2} decade^{-1} and their distances to ERLA of 198.6, 177.5, and 144.4 km, respectively. The results indicate an improved spatial consistency in the GPS IWV trends from the homogenised time series. Therefore, the homogenisation at station ERLA is considered to be reasonable.
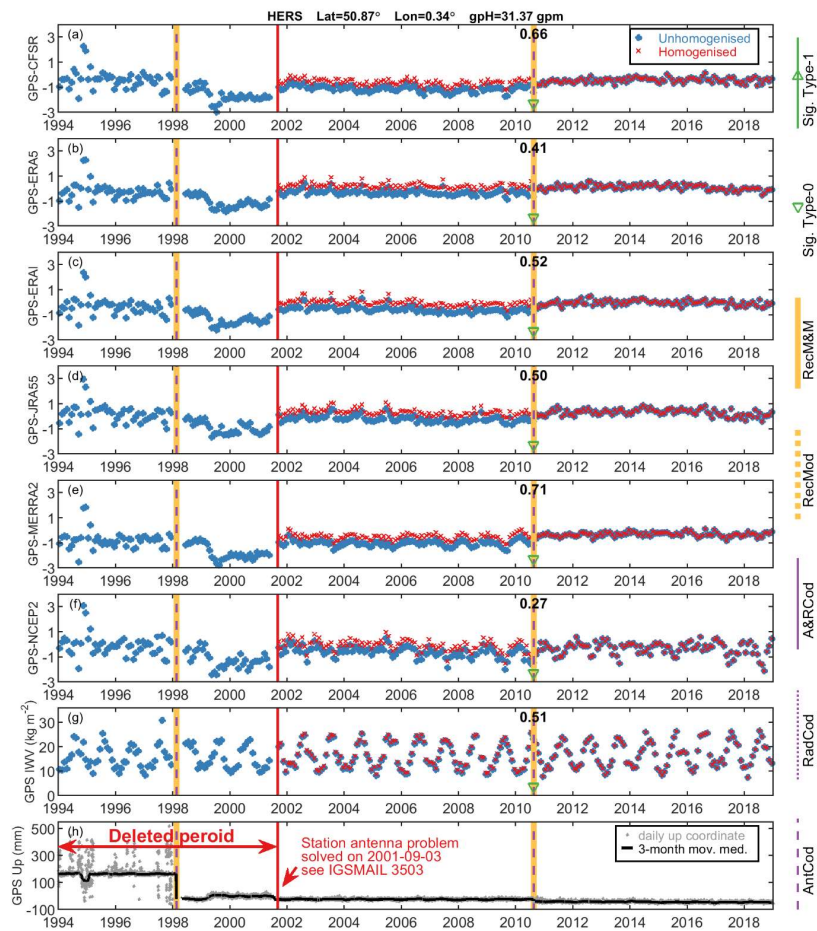
Figure A1. Monthly GPS-reanalysis IWV difference (a–f), monthly GPS IWV (g), and daily up-coordinate time series at station HERS. The GPS data before 2001-9-3 were deleted due to a problem in station antenna (see IGSMAIL 3503). The IWV time series before and after the homogenisation are labelled as blue dots and red crosses in (a)–(g). The types of instrumentation changes are listed in Table A2. The Type-0 changepoint on 2010-8-19 is significant at a confidence level of

1410
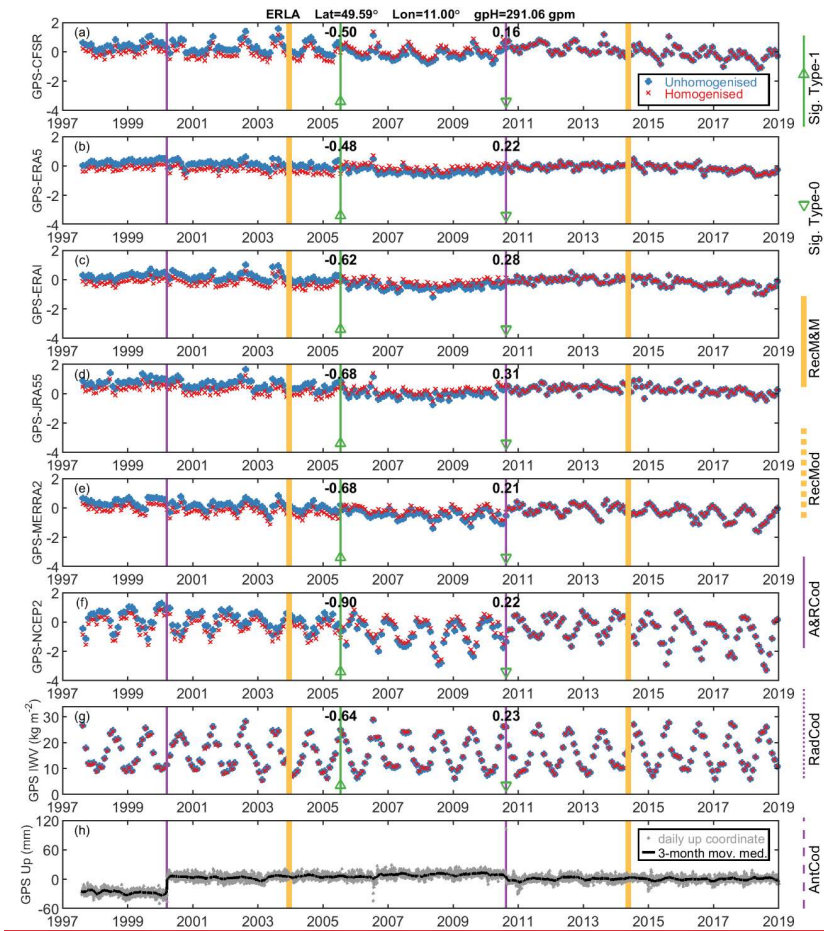
Figure A2. The same as Fig. A1 but for station ERLA. A Type-0 changepoint is significant on 2010-8-18 (green triangle) due to changes in antenna and radome at the station. A Type-1 changepoint in 2005 July (green vertical line and upward-pointing triangle) is significant but without support from metadata, and hence its date was fixed to 2005-7-15.

Table A1. The identified changepoints in GPS IWV time series. The Type-0 and Type-1 are changepoints with and without changes in instrumentation as documented in GPS station log files, respectively. The full names of the Type-0 changepoint events are shown in Table A2, and the Type-1 changepoints are labelled as Unknown. The G-C, G-E, G-I, G-J, G-M, and G-N indicate the GPS IWV changepoints in kg m^{-2} estimated by compared to CFSR, ERA5, ERAI, JRA55, MERRA2, and NCEP2, respectively. The NaN indicates that the changepoint in the specific GPS-reanalysis comparison is insignificant at a confidence level of 99%. The mean and SD are the mean value and standard deviation of each changepoint.

Station	Type	Date	Mean	SD	G-C	G-E	G-I	G-J	G-M	G-N	Events
APEL	1	2006-09-15	-0.31	0.10	-0.26	-0.30	-0.32	-0.22	-0.26	-0.50	Unknown
APEL	0	2013-06-19	0.36	0.10	0.36	0.32	0.40	0.44	0.47	0.20	RecM&M
APEL	1	2016-04-15	-0.33	0.04	-0.37	-0.29	NaN	-0.32	-0.33	NaN	Unknown
BELL	0	2012-01-26	1.22	0.30	0.67	1.43	1.30	1.34	1.47	1.11	AntCod
BELL	0	2014-09-22	-0.47	0.13	-0.36	-0.49	-0.49	-0.32	-0.46	-0.69	AntCod
BELL	0	2016-05-12	-1.61	0.05	-1.56	-1.57	-1.59	-1.71	-1.63	-1.63	AntCod and RecM&M
BRST	0	2011-10-26	0.36	0.08	0.45	0.28	0.39	0.41	0.37	0.25	AntCod and RecM&M
CREU	0	2016-05-17	-1.03	0.17	-0.81	-1.11	-1.08	-1.04	-0.87	-1.28	AntCod and RecM&M
DELF	0	2000-07-23	0.23	0.05	NaN	0.26	0.27	0.20	0.18	NaN	A&RCod and RecM&M
DOUR	0	2015-03-02	0.37	0.03	0.40	0.35	0.35	0.34	0.39	NaN	AntCod
EIJS	0	2000-04-28	0.22	0.07	0.33	0.25	0.19	0.18	0.15	NaN	A&RCod and RecM&M
ERLA	1	2005-07-15	-0.64	0.15	-0.50	-0.48	-0.62	-0.68	-0.68	-0.90	Unknown
ERLA	0	2010-08-18	0.23	0.05	0.16	0.22	0.28	0.31	0.21	0.22	A&RCod
EUSK	0	2001-05-09	-0.74	0.13	-0.56	-0.74	-0.76	-0.73	-0.71	-0.97	A&RCod
GOPE	0	1999-11-04	0.27	0.03	0.25	0.24	NaN	NaN	0.31	0.28	A&RCod and RecM&M
GOPE	0	2000-07-24	-0.96	0.07	-1.06	-0.86	-0.97	-1.00	-0.98	-0.92	A&RCod and RecM&M
GOPE	1	2001-09-15	-0.51	0.10	-0.52	-0.57	-0.34	-0.51	-0.65	-0.49	Unknown
GOPE	0	2006-07-14	-0.39	0.09	-0.39	-0.30	-0.32	-0.33	-0.47	-0.52	A&RCod
GOPE	0	2009-12-14	0.35	0.10	0.17	0.33	0.40	0.43	0.33	0.42	A&RCod and RecM&M
GOPE	1	2016-05-15	-0.36	0.06	NaN	-0.29	-0.36	-0.33	-0.35	-0.46	Unknown
HELG	0	2008-09-02	0.19	0.06	0.23	0.15	0.11	0.19	0.27	0.18	A&RCod and RecM&M
HELG	0	2014-09-09	-0.14	0.04	NaN	-0.19	-0.10	-0.11	NaN	-0.17	A&RCod and RecM&M
HERS	0	2010-08-19	0.51	0.16	0.66	0.41	0.52	0.50	0.71	0.27	AntCod and RecM&M
HOBU	0	2007-02-28	-0.31	0.08	-0.23	-0.24	-0.33	-0.40	-0.24	-0.40	A&RCod and RecM&M

HOBU	0	2010-11-22	0.40	0.08	0.34	0.28	0.44	0.50	0.40	0.45	A&RCod
HOBU	0	2015-05-27	-0.22	0.06	-0.27	-0.19	-0.20	-0.13	-0.21	-0.30	RecM&M
HOFN	0	2001-09-21	-0.95	0.09	-1.11	-0.91	-0.92	-0.85	-0.98	-0.91	A&RCod
KARL	0	2001-05-10	-0.64	0.14	-0.64	-0.47	-0.54	-0.65	-0.68	-0.89	A&RCod
KLOP	0	2001-05-08	-0.60	0.11	-0.40	-0.55	-0.65	-0.67	-0.62	-0.72	A&RCod
LAMP	1	2013-03-15	0.99	0.17	1.05	0.70	NaN	1.00	1.10	1.10	Unknown
LAMP	0	2014-04-11	-1.75	0.18	-1.53	-1.60	-1.94	-1.82	-1.66	-1.95	AntCod and RecM&M
LAMP	0	2017-09-26	0.52	0.13	0.48	0.36	0.69	0.47	0.59	NaN	AntCod
LEED	0	2008-11-11	0.38	0.11	0.24	0.38	0.39	0.46	0.53	0.29	A&RCod
LEIJ	0	2010-07-01	0.25	0.06	NaN	0.23	0.31	0.29	NaN	0.17	A&RCod
MAN2	0	2008-01-23	0.29	0.04	NaN	0.24	0.32	0.32	0.28	NaN	AntCod and RecMod
MODA	0	2007-07-12	1.54	0.08	NaN	1.45	1.64	1.60	1.56	1.47	RecM&M
MODA	0	2008-01-08	-1.60	0.28	-1.11	-1.53	-1.69	-1.68	-1.92	-1.70	RecM&M
MOPI	1	2004-08-15	-0.53	0.09	-0.43	-0.54	-0.51	-0.44	-0.65	-0.62	Unknown
OSNA	0	2004-04-22	0.38	0.07	0.47	0.41	0.32	0.31	0.37	NaN	AntCod
OSNA	0	2007-04-23	-0.61	0.06	-0.60	-0.57	-0.62	-0.59	-0.57	-0.73	A&RCod and RecM&M
OSNA	0	2011-04-05	0.23	0.06	0.18	0.14	0.28	0.29	0.24	0.26	A&RCod
OSNA	0	2015-06-11	-0.18	0.06	-0.17	-0.20	-0.12	-0.16	-0.18	-0.28	RecM&M
PENC	0	2003-05-22	0.55	0.10	0.54	0.57	0.56	0.59	0.37	0.68	AntCod
PENC	0	2007-06-26	-0.32	0.06	-0.29	-0.30	-0.29	-0.29	-0.34	-0.43	RecM&M
PTBB	1	2014-06-15	-0.50	0.11	-0.57	-0.49	-0.39	-0.36	-0.53	-0.65	Unknown
REYK	1	2003-03-15	0.31	0.03	NaN	0.35	0.34	0.28	0.29	NaN	Unknown
REYK	0	2008-03-13	-0.30	0.08	-0.19	-0.28	-0.36	-0.31	-0.25	-0.42	A&RCod
REYK	0	2013-05-02	0.27	0.09	0.24	0.13	0.34	0.33	0.28	NaN	A&RCod and RecM&M
SULD	0	2005-06-14	-0.53	0.11	-0.54	-0.52	-0.56	-0.55	-0.32	-0.67	AntCod
TERS	0	2008-09-16	-0.20	0.06	-0.29	-0.18	-0.20	-0.14	-0.13	-0.26	RecM&M
TERS	0	2013-08-29	0.35	0.05	0.30	0.37	0.39	0.36	0.41	0.28	RecM&M
TRDS	0	2007-05-07	0.25	0.06	0.27	0.20	0.27	0.18	0.32	NaN	A&RCod
WSRA	0	2000-01-06	0.14	0.02	NaN	0.15	0.16	0.11	0.13	NaN	RecM&M

Table A2. Types of changes in GPS instrumentation.

Abbreviation	Type of change
1 AntCod	Antenna Code
2 RadCod	Radome Code

3	A&RCod	Antenna and Radome Code
4	RecMod	Receiver Model
5	RecM&M	Receiver Make and Model

Page 9: [1] Formatted	Yuan, Peng (GIK)	12/23/2022 11:27:00 AM

Font: (Default) Times New Roman, 10 pt, Check spelling and grammar

Page 9: [2] Formatted	Yuan, Peng (GIK)	1/8/2023 3:57:00 PM

Check spelling and grammar

Page 9: [3] Formatted	Yuan, Peng (GIK)	1/8/2023 3:57:00 PM

Font: 10 pt

Page 9: [4] Formatted	Yuan, Peng (GIK)	1/8/2023 3:57:00 PM

Font: 10 pt

Page 9: [5] Formatted	Yuan, Peng (GIK)	1/8/2023 3:57:00 PM

Font: 10 pt

Page 9: [6] Formatted	Yuan, Peng (GIK)	1/8/2023 3:57:00 PM

Font: (Default) +Headings (Calibri Light), 10 pt

Page 9: [7] Formatted	Yuan, Peng (GIK)	1/8/2023 3:57:00 PM

Font: (Default) +Headings (Calibri Light), 10 pt, Font color: Auto, Pattern: Clear

Page 9: [8] Formatted	Yuan, Peng (GIK)	1/8/2023 3:57:00 PM

Font: (Default) +Headings (Calibri Light)

Page 9: [9] Formatted	Yuan, Peng (GIK)	1/8/2023 3:57:00 PM

Font: 10 pt

Page 60: [10] Formatted	Yuan, Peng (GIK)	12/21/2022 4:36:00 PM

Space Before: 3 pt, After: 3 pt

Page 60: [11] Formatted	Yuan, Peng (GIK)	12/23/2022 11:27:00 AM

English (United Kingdom)

Page 60: [12] Formatted	Yuan, Peng (GIK)	12/23/2022 11:27:00 AM

English (United Kingdom)

Page 60: [13] Formatted	Yuan, Peng (GIK)	12/23/2022 11:27:00 AM

English (United Kingdom)

Page 60: [14] Formatted	Yuan, Peng (GIK)	12/23/2022 11:27:00 AM

English (United Kingdom)

Page 60: [15] Formatted	Yuan, Peng (GIK)	12/23/2022 11:27:00 AM

English (United Kingdom)

Page 60: [16] Formatted	Yuan, Peng (GIK)	12/23/2022 11:27:00 AM

English (United Kingdom)

Page 60: [17] Formatted	Yuan, Peng (GIK)	12/23/2022 11:27:00 AM

English (United Kingdom)

Page 60: [18] Formatted   Yuan, Peng (GIK)   12/21/2022 4:36:00 PM

Space Before: 3 pt, After: 3 pt

Page 60: [19] Formatted   Yuan, Peng (GIK)   12/23/2022 11:27:00 AM

English (United Kingdom)

Page 60: [20] Formatted   Yuan, Peng (GIK)   12/23/2022 11:27:00 AM

English (United Kingdom)

Page 60: [21] Formatted   Yuan, Peng (GIK)   12/23/2022 11:27:00 AM

English (United Kingdom)

Page 60: [22] Formatted   Yuan, Peng (GIK)   12/23/2022 11:27:00 AM

English (United Kingdom)

Page 60: [23] Formatted   Yuan, Peng (GIK)   12/23/2022 11:27:00 AM

English (United Kingdom)

Page 60: [24] Formatted   Yuan, Peng (GIK)   12/23/2022 11:27:00 AM

English (United Kingdom)

Page 60: [25] Formatted   Yuan, Peng (GIK)   12/23/2022 11:27:00 AM

English (United Kingdom)

Page 60: [26] Formatted   Yuan, Peng (GIK)   12/21/2022 4:36:00 PM

Space Before: 3 pt, After: 3 pt

Page 60: [27] Formatted   Yuan, Peng (GIK)   12/23/2022 11:27:00 AM

English (United Kingdom)

Page 60: [28] Formatted   Yuan, Peng (GIK)   12/23/2022 11:27:00 AM

English (United Kingdom)

Page 60: [29] Formatted   Yuan, Peng (GIK)   12/23/2022 11:27:00 AM

English (United Kingdom)

Page 60: [30] Formatted   Yuan, Peng (GIK)   12/23/2022 11:27:00 AM

English (United Kingdom)

Page 60: [31] Formatted   Yuan, Peng (GIK)   12/23/2022 11:27:00 AM

English (United Kingdom)

Page 60: [32] Formatted   Yuan, Peng (GIK)   12/23/2022 11:27:00 AM

English (United Kingdom)

Page 60: [33] Formatted   Yuan, Peng (GIK)   12/23/2022 11:27:00 AM

English (United Kingdom)

Page 60: [34] Formatted   Yuan, Peng (GIK)   12/21/2022 4:36:00 PM

Space Before: 3 pt, After: 3 pt

Page 60: [35] Formatted   Yuan, Peng (GIK)   **12/23/2022 11:27:00 AM**
English (United Kingdom)

Page 60: [36] Formatted   Yuan, Peng (GIK)   **12/23/2022 11:27:00 AM**
English (United Kingdom)

Page 60: [37] Formatted   Yuan, Peng (GIK)   **12/23/2022 11:27:00 AM**
English (United Kingdom)

Page 60: [38] Formatted   Yuan, Peng (GIK)   **12/23/2022 11:27:00 AM**
English (United Kingdom)

Page 60: [39] Formatted   Yuan, Peng (GIK)   **12/23/2022 11:27:00 AM**
English (United Kingdom)

Page 60: [40] Formatted   Yuan, Peng (GIK)   **12/23/2022 11:27:00 AM**
English (United Kingdom)

Page 60: [41] Formatted   Yuan, Peng (GIK)   **12/23/2022 11:27:00 AM**
English (United Kingdom)

Page 60: [42] Formatted   Yuan, Peng (GIK)   **12/21/2022 4:36:00 PM**
Space Before: 3 pt, After: 3 pt

Page 60: [43] Formatted   Yuan, Peng (GIK)   **12/23/2022 11:27:00 AM**
English (United Kingdom)

Page 60: [44] Formatted   Yuan, Peng (GIK)   **12/23/2022 11:27:00 AM**
English (United Kingdom)

Page 60: [45] Formatted   Yuan, Peng (GIK)   **12/23/2022 11:27:00 AM**
English (United Kingdom)

Page 60: [46] Formatted   Yuan, Peng (GIK)   **12/23/2022 11:27:00 AM**
English (United Kingdom)

Page 60: [47] Formatted   Yuan, Peng (GIK)   **12/23/2022 11:27:00 AM**
English (United Kingdom)

Page 60: [48] Formatted   Yuan, Peng (GIK)   **12/23/2022 11:27:00 AM**
English (United Kingdom)

Page 60: [49] Formatted   Yuan, Peng (GIK)   **12/23/2022 11:27:00 AM**
English (United Kingdom)

Page 60: [50] Formatted   Yuan, Peng (GIK)   **12/21/2022 4:36:00 PM**
Space Before: 3 pt, After: 3 pt

Page 60: [51] Formatted   Yuan, Peng (GIK)   12/23/2022 11:27:00 AM

English (United Kingdom)

Page 60: [52] Formatted   Yuan, Peng (GIK)   12/23/2022 11:27:00 AM

English (United Kingdom)

Page 60: [53] Formatted   Yuan, Peng (GIK)   12/23/2022 11:27:00 AM

English (United Kingdom)

Page 60: [54] Formatted   Yuan, Peng (GIK)   12/23/2022 11:27:00 AM

English (United Kingdom)

Page 60: [55] Formatted   Yuan, Peng (GIK)   12/23/2022 11:27:00 AM

English (United Kingdom)

Page 60: [56] Formatted   Yuan, Peng (GIK)   12/23/2022 11:27:00 AM

English (United Kingdom)

Page 60: [57] Formatted   Yuan, Peng (GIK)   12/23/2022 11:27:00 AM

English (United Kingdom)

Page 60: [58] Formatted   Yuan, Peng (GIK)   12/21/2022 4:36:00 PM

Space Before: 3 pt, After: 3 pt

Page 60: [59] Formatted   Yuan, Peng (GIK)   12/23/2022 11:27:00 AM

English (United Kingdom)

Page 60: [60] Formatted   Yuan, Peng (GIK)   12/23/2022 11:27:00 AM

English (United Kingdom)

Page 60: [61] Formatted   Yuan, Peng (GIK)   12/23/2022 11:27:00 AM

English (United Kingdom)

Page 60: [62] Formatted   Yuan, Peng (GIK)   12/23/2022 11:27:00 AM

English (United Kingdom)

Page 60: [63] Formatted   Yuan, Peng (GIK)   12/23/2022 11:27:00 AM

English (United Kingdom)

Page 60: [64] Formatted   Yuan, Peng (GIK)   12/23/2022 11:27:00 AM

English (United Kingdom)

Page 60: [65] Formatted   Yuan, Peng (GIK)   12/23/2022 11:27:00 AM

English (United Kingdom)

Page 60: [66] Formatted   Yuan, Peng (GIK)   12/21/2022 4:36:00 PM

Space Before: 3 pt, After: 3 pt

Page 60: [67] Formatted   Yuan, Peng (GIK)   12/23/2022 11:27:00 AM

English (United Kingdom)

English (United Kingdom)

Page 61: [101] Formatted	Yuan, Peng (GIK)	12/23/2022 11:27:00 AM

English (United Kingdom)

Page 61: [102] Formatted	Yuan, Peng (GIK)	12/23/2022 11:27:00 AM

English (United Kingdom)

Page 61: [103] Formatted	Yuan, Peng (GIK)	12/23/2022 11:27:00 AM

English (United Kingdom)

Page 61: [104] Formatted	Yuan, Peng (GIK)	12/23/2022 11:27:00 AM

English (United Kingdom)

Page 61: [105] Formatted	Yuan, Peng (GIK)	12/23/2022 11:27:00 AM

English (United Kingdom)

Page 61: [106] Formatted	Yuan, Peng (GIK)	12/23/2022 11:27:00 AM

English (United Kingdom)

Page 61: [107] Formatted	Yuan, Peng (GIK)	12/23/2022 11:27:00 AM

English (United Kingdom)

Page 61: [108] Formatted	Yuan, Peng (GIK)	12/23/2022 11:27:00 AM

English (United Kingdom)

Page 61: [109] Formatted	Yuan, Peng (GIK)	12/23/2022 11:27:00 AM

English (United Kingdom)

Page 61: [110] Formatted	Yuan, Peng (GIK)	12/23/2022 11:27:00 AM

English (United Kingdom)

Page 61: [111] Formatted	Yuan, Peng (GIK)	12/23/2022 11:27:00 AM

English (United Kingdom)

Page 61: [112] Formatted	Yuan, Peng (GIK)	12/23/2022 11:27:00 AM

English (United Kingdom)

Page 61: [113] Formatted	Yuan, Peng (GIK)	12/23/2022 11:27:00 AM

English (United Kingdom)

Page 61: [114] Formatted	Yuan, Peng (GIK)	12/23/2022 11:27:00 AM

English (United Kingdom)

Page 61: [115] Formatted	Yuan, Peng (GIK)	12/23/2022 11:27:00 AM

English (United Kingdom)

Page 61: [116] Formatted	Yuan, Peng (GIK)	12/23/2022 11:27:00 AM

English (United Kingdom)

Page 61: [117] Formatted	Yuan, Peng (GIK)	12/23/2022 11:27:00 AM

English (United Kingdom)

Page 61: [118] Formatted	Yuan, Peng (GIK)	12/23/2022 11:27:00 AM

English (United Kingdom)

Page 61: [119] Formatted	Yuan, Peng (GIK)	12/23/2022 11:27:00 AM

English (United Kingdom)

Page 61: [120] Formatted	Yuan, Peng (GIK)	12/23/2022 11:27:00 AM

English (United Kingdom)

Page 61: [121] Formatted	Yuan, Peng (GIK)	12/23/2022 11:27:00 AM

English (United Kingdom)

Page 61: [122] Formatted	Yuan, Peng (GIK)	12/23/2022 11:27:00 AM

English (United Kingdom)

Page 61: [123] Formatted	Yuan, Peng (GIK)	12/23/2022 11:27:00 AM

English (United Kingdom)

Page 61: [124] Formatted	Yuan, Peng (GIK)	12/23/2022 11:27:00 AM

English (United Kingdom)

Page 61: [125] Formatted	Yuan, Peng (GIK)	12/23/2022 11:27:00 AM

English (United Kingdom)

Page 61: [126] Formatted	Yuan, Peng (GIK)	12/23/2022 11:27:00 AM

English (United Kingdom)

Page 61: [127] Formatted	Yuan, Peng (GIK)	12/23/2022 11:27:00 AM

English (United Kingdom)

Page 61: [128] Formatted	Yuan, Peng (GIK)	12/23/2022 11:27:00 AM

English (United Kingdom)

Page 61: [129] Formatted	Yuan, Peng (GIK)	12/23/2022 11:27:00 AM

English (United Kingdom)

Page 61: [130] Formatted	Yuan, Peng (GIK)	12/23/2022 11:27:00 AM

English (United Kingdom)

Page 61: [131] Formatted	Yuan, Peng (GIK)	12/23/2022 11:27:00 AM

English (United Kingdom)

Page 61: [132] Formatted	Yuan, Peng (GIK)	12/23/2022 11:27:00 AM

English (United Kingdom)

Page 61: [133] Formatted	Yuan, Peng (GIK)	12/23/2022 11:27:00 AM

English (United Kingdom)

Page 61: [134] Formatted	Yuan, Peng (GIK)	12/23/2022 11:27:00 AM

English (United Kingdom)

Page 61: [135] Formatted	Yuan, Peng (GIK)	12/23/2022 11:27:00 AM

English (United Kingdom)

Page 61: [136] Formatted	Yuan, Peng (GIK)	12/23/2022 11:27:00 AM

English (United Kingdom)

Page 61: [137] Formatted	Yuan, Peng (GIK)	12/23/2022 11:27:00 AM

English (United Kingdom)

Page 61: [138] Formatted	Yuan, Peng (GIK)	12/23/2022 11:27:00 AM

English (United Kingdom)

Page 61: [139] Formatted	Yuan, Peng (GIK)	12/23/2022 11:27:00 AM

English (United Kingdom)

Page 61: [140] Formatted	Yuan, Peng (GIK)	12/23/2022 11:27:00 AM

English (United Kingdom)

Page 61: [141] Formatted	Yuan, Peng (GIK)	12/23/2022 11:27:00 AM

English (United Kingdom)

Page 61: [142] Formatted	Yuan, Peng (GIK)	12/23/2022 11:27:00 AM

English (United Kingdom)

Page 61: [143] Formatted	Yuan, Peng (GIK)	12/23/2022 11:27:00 AM

English (United Kingdom)

Page 61: [144] Formatted	Yuan, Peng (GIK)	12/23/2022 11:27:00 AM

English (United Kingdom)

Page 61: [145] Formatted	Yuan, Peng (GIK)	12/23/2022 11:27:00 AM

English (United Kingdom)

Page 61: [146] Formatted	Yuan, Peng (GIK)	12/23/2022 11:27:00 AM

English (United Kingdom)

Page 61: [147] Formatted	Yuan, Peng (GIK)	12/23/2022 11:27:00 AM

English (United Kingdom)

Page 61: [148] Formatted	Yuan, Peng (GIK)	12/23/2022 11:27:00 AM

English (United Kingdom)

Page 61: [149] Formatted	Yuan, Peng (GIK)	12/23/2022 11:27:00 AM

English (United Kingdom)

Page 61: [150] Formatted	Yuan, Peng (GIK)	12/23/2022 11:27:00 AM

English (United Kingdom)

Page 61: [151] Formatted	Yuan, Peng (GIK)	12/23/2022 11:27:00 AM

English (United Kingdom)

Page 61: [152] Formatted	Yuan, Peng (GIK)	12/23/2022 11:27:00 AM

English (United Kingdom)

Page 61: [153] Formatted	Yuan, Peng (GIK)	12/23/2022 11:27:00 AM

English (United Kingdom)

Page 61: [154] Formatted	Yuan, Peng (GIK)	12/23/2022 11:27:00 AM

English (United Kingdom)

Page 61: [155] Formatted	Yuan, Peng (GIK)	12/23/2022 11:27:00 AM

English (United Kingdom)

Page 61: [156] Formatted	Yuan, Peng (GIK)	12/23/2022 11:27:00 AM

English (United Kingdom)

Page 61: [157] Formatted	Yuan, Peng (GIK)	12/23/2022 11:27:00 AM

English (United Kingdom)

Page 61: [158] Formatted	Yuan, Peng (GIK)	12/23/2022 11:27:00 AM

English (United Kingdom)

Page 61: [159] Formatted	Yuan, Peng (GIK)	12/23/2022 11:27:00 AM

English (United Kingdom)

Page 61: [160] Formatted	Yuan, Peng (GIK)	12/23/2022 11:27:00 AM

English (United Kingdom)

Page 61: [161] Formatted	Yuan, Peng (GIK)	12/23/2022 11:27:00 AM

English (United Kingdom)

Page 61: [162] Formatted	Yuan, Peng (GIK)	12/23/2022 11:27:00 AM

English (United Kingdom)

Page 61: [163] Formatted	Yuan, Peng (GIK)	12/23/2022 11:27:00 AM

English (United Kingdom)

Page 61: [164] Formatted	Yuan, Peng (GIK)	12/23/2022 11:27:00 AM

English (United Kingdom)

Page 61: [165] Formatted	Yuan, Peng (GIK)	12/23/2022 11:27:00 AM

English (United Kingdom)

Page 61: [166] Formatted	Yuan, Peng (GIK)	12/23/2022 11:27:00 AM

English (United Kingdom)

Page 61: [167] Formatted	Yuan, Peng (GIK)	12/23/2022 11:27:00 AM

English (United Kingdom)

Page 61: [168] Formatted	Yuan, Peng (GIK)	12/23/2022 11:27:00 AM

English (United Kingdom)

Page 61: [169] Formatted	Yuan, Peng (GIK)	12/23/2022 11:27:00 AM

English (United Kingdom)

Page 61: [170] Formatted	Yuan, Peng (GIK)	12/23/2022 11:27:00 AM

English (United Kingdom)

Page 67: [171] Formatted	Yuan, Peng (GIK)	12/23/2022 3:41:00 PM

Superscript

Page 67: [172] Formatted Table	Yuan, Peng (GIK)	12/22/2022 5:09:00 PM

Formatted Table

Page 67: [173] Formatted	Yuan, Peng (GIK)	12/23/2022 11:27:00 AM

English (United Kingdom)

Page 67: [174] Formatted	Yuan, Peng (GIK)	12/23/2022 11:27:00 AM

English (United Kingdom)

Page 67: [175] Formatted	Yuan, Peng (GIK)	12/23/2022 11:27:00 AM

English (United Kingdom)

Page 67: [176] Formatted	Yuan, Peng (GIK)	12/23/2022 11:27:00 AM

English (United Kingdom)

Page 67: [177] Formatted	Yuan, Peng (GIK)	12/23/2022 11:27:00 AM

English (United Kingdom)

Page 67: [178] Formatted	Yuan, Peng (GIK)	12/23/2022 11:27:00 AM

English (United Kingdom)

Page 67: [179] Formatted	Yuan, Peng (GIK)	12/23/2022 11:27:00 AM

English (United Kingdom)

Page 67: [180] Formatted	Yuan, Peng (GIK)	12/23/2022 11:27:00 AM

English (United Kingdom)

Page 67: [181] Formatted	Yuan, Peng (GIK)	12/23/2022 11:27:00 AM

English (United Kingdom)

Page 67: [182] Formatted	Yuan, Peng (GIK)	12/23/2022 11:27:00 AM

English (United Kingdom)

Page 67: [183] Formatted	Yuan, Peng (GIK)	12/23/2022 11:27:00 AM

English (United Kingdom)

Page 67: [184] Formatted	Yuan, Peng (GIK)	12/23/2022 11:27:00 AM

English (United Kingdom)

Page 67: [185] Formatted	Yuan, Peng (GIK)	12/23/2022 11:27:00 AM

Font: Bold

Page 67: [185] Formatted	Yuan, Peng (GIK)	12/23/2022 11:27:00 AM

Font: Bold

Page 67: [186] Formatted	Yuan, Peng (GIK)	12/23/2022 11:27:00 AM

English (United Kingdom)

Page 67: [187] Formatted	Yuan, Peng (GIK)	12/23/2022 11:27:00 AM

English (United Kingdom)

Page 67: [188] Formatted	Yuan, Peng (GIK)	12/23/2022 11:27:00 AM

English (United Kingdom)

Page 67: [189] Formatted	Yuan, Peng (GIK)	12/23/2022 11:27:00 AM

English (United Kingdom)

Page 67: [190] Formatted	Yuan, Peng (GIK)	12/23/2022 11:27:00 AM

English (United Kingdom)

Page 67: [191] Formatted	Yuan, Peng (GIK)	12/23/2022 11:27:00 AM

English (United Kingdom)

Page 67: [192] Formatted	Yuan, Peng (GIK)	12/23/2022 11:27:00 AM

English (United Kingdom)

Page 67: [193] Formatted	Yuan, Peng (GIK)	12/23/2022 11:27:00 AM

English (United Kingdom)

Page 67: [194] Formatted	Yuan, Peng (GIK)	12/23/2022 11:27:00 AM

English (United Kingdom)

Page 67: [195] Formatted	Yuan, Peng (GIK)	12/23/2022 11:27:00 AM

English (United Kingdom)

Page 67: [196] Formatted	Yuan, Peng (GIK)	12/23/2022 11:27:00 AM

English (United Kingdom)

Page 67: [197] Formatted	Yuan, Peng (GIK)	12/23/2022 11:27:00 AM

Font: Bold

Page 67: [197] Formatted	Yuan, Peng (GIK)	12/23/2022 11:27:00 AM

Font: Bold

Page 67: [198] Formatted	Yuan, Peng (GIK)	12/23/2022 11:27:00 AM

English (United Kingdom)

Page 67: [199] Formatted	Yuan, Peng (GIK)	12/23/2022 11:27:00 AM

English (United Kingdom)

Page 67: [200] Formatted	Yuan, Peng (GIK)	12/23/2022 11:27:00 AM

English (United Kingdom)

Page 67: [201] Formatted	Yuan, Peng (GIK)	12/23/2022 11:27:00 AM

English (United Kingdom)

Page 67: [202] Formatted	Yuan, Peng (GIK)	12/23/2022 11:27:00 AM

English (United Kingdom)

Page 67: [203] Formatted	Yuan, Peng (GIK)	12/23/2022 11:27:00 AM

English (United Kingdom)

Page 67: [204] Formatted	Yuan, Peng (GIK)	12/23/2022 11:27:00 AM

English (United Kingdom)

Page 67: [205] Formatted	Yuan, Peng (GIK)	12/23/2022 11:27:00 AM

English (United Kingdom)

Page 67: [206] Formatted	Yuan, Peng (GIK)	12/23/2022 11:27:00 AM

English (United Kingdom)

Page 67: [207] Formatted	Yuan, Peng (GIK)	12/23/2022 11:27:00 AM

English (United Kingdom)

Page 67: [208] Formatted	Yuan, Peng (GIK)	12/23/2022 11:27:00 AM

English (United Kingdom)

Page 67: [209] Formatted	Yuan, Peng (GIK)	12/23/2022 11:27:00 AM

Font: Bold

Page 67: [209] Formatted	Yuan, Peng (GIK)	12/23/2022 11:27:00 AM

Font: Bold

Page 67: [210] Formatted	Yuan, Peng (GIK)	12/23/2022 11:27:00 AM

English (United Kingdom)

Page 67: [211] Formatted	Yuan, Peng (GIK)	12/23/2022 11:27:00 AM

English (United Kingdom)

Page 67: [212] Formatted	Yuan, Peng (GIK)	12/23/2022 11:27:00 AM

English (United Kingdom)

Page 67: [213] Formatted	Yuan, Peng (GIK)	12/23/2022 11:27:00 AM

English (United Kingdom)

Page 67: [214] Formatted	Yuan, Peng (GIK)	12/23/2022 11:27:00 AM

English (United Kingdom)

Page 67: [215] Formatted	Yuan, Peng (GIK)	12/23/2022 11:27:00 AM

English (United Kingdom)

Page 67: [216] Formatted	Yuan, Peng (GIK)	12/23/2022 11:27:00 AM

English (United Kingdom)

Page 67: [217] Formatted	Yuan, Peng (GIK)	12/23/2022 11:27:00 AM

English (United Kingdom)

Page 67: [218] Formatted	Yuan, Peng (GIK)	12/23/2022 11:27:00 AM

English (United Kingdom)

Page 67: [219] Formatted	Yuan, Peng (GIK)	12/23/2022 11:27:00 AM

English (United Kingdom)

Page 67: [220] Formatted	Yuan, Peng (GIK)	12/23/2022 11:27:00 AM

English (United Kingdom)

Page 67: [221] Formatted	Yuan, Peng (GIK)	12/23/2022 11:27:00 AM

Font: Bold

Page 67: [221] Formatted	Yuan, Peng (GIK)	12/23/2022 11:27:00 AM

Font: Bold

Page 67: [222] Formatted	Yuan, Peng (GIK)	12/23/2022 11:27:00 AM

English (United Kingdom)

Page 67: [223] Formatted	Yuan, Peng (GIK)	12/23/2022 11:27:00 AM

English (United Kingdom)

Page 67: [224] Formatted	Yuan, Peng (GIK)	12/23/2022 11:27:00 AM

English (United Kingdom)

Page 67: [225] Formatted	Yuan, Peng (GIK)	12/23/2022 11:27:00 AM

English (United Kingdom)

Page 67: [226] Formatted	Yuan, Peng (GIK)	12/23/2022 11:27:00 AM

English (United Kingdom)

Page 67: [227] Formatted	Yuan, Peng (GIK)	12/23/2022 11:27:00 AM

English (United Kingdom)

Page 67: [228] Formatted	Yuan, Peng (GIK)	12/23/2022 11:27:00 AM

English (United Kingdom)

Page 67: [229] Formatted	Yuan, Peng (GIK)	12/23/2022 11:27:00 AM

English (United Kingdom)

Page 67: [230] Formatted	Yuan, Peng (GIK)	12/23/2022 11:27:00 AM

English (United Kingdom)

Page 67: [231] Formatted	Yuan, Peng (GIK)	12/23/2022 11:27:00 AM

English (United Kingdom)

Page 67: [232] Formatted	Yuan, Peng (GIK)	12/23/2022 11:27:00 AM

English (United Kingdom)

Page 67: [233] Formatted	Yuan, Peng (GIK)	12/23/2022 11:27:00 AM

Font: Bold

Page 67: [233] Formatted	Yuan, Peng (GIK)	12/23/2022 11:27:00 AM

Font: Bold

Page 67: [234] Formatted	Yuan, Peng (GIK)	12/23/2022 11:27:00 AM

English (United Kingdom)

Page 67: [235] Formatted	Yuan, Peng (GIK)	12/23/2022 11:27:00 AM

English (United Kingdom)

Page 67: [236] Formatted	Yuan, Peng (GIK)	12/23/2022 11:27:00 AM

English (United Kingdom)

Page 67: [237] Formatted	Yuan, Peng (GIK)	12/23/2022 11:27:00 AM

English (United Kingdom)

Page 67: [238] Formatted	Yuan, Peng (GIK)	12/23/2022 11:27:00 AM

English (United Kingdom)

Page 67: [239] Formatted	Yuan, Peng (GIK)	12/23/2022 11:27:00 AM

English (United Kingdom)

Page 67: [240] Formatted	Yuan, Peng (GIK)	12/23/2022 11:27:00 AM

English (United Kingdom)

Page 67: [241] Formatted	Yuan, Peng (GIK)	12/23/2022 11:27:00 AM

English (United Kingdom)

Page 67: [242] Formatted	Yuan, Peng (GIK)	12/23/2022 11:27:00 AM

English (United Kingdom)

Page 67: [243] Formatted	Yuan, Peng (GIK)	12/23/2022 11:27:00 AM

English (United Kingdom)

Page 67: [244] Formatted	Yuan, Peng (GIK)	12/23/2022 11:27:00 AM

English (United Kingdom)

Page 67: [245] Formatted	Yuan, Peng (GIK)	12/23/2022 11:27:00 AM

Font: Bold

Page 67: [245] Formatted	Yuan, Peng (GIK)	12/23/2022 11:27:00 AM

Font: Bold

Page 67: [246] Formatted	Yuan, Peng (GIK)	12/23/2022 11:27:00 AM

English (United Kingdom)

Page 67: [247] Formatted	Yuan, Peng (GIK)	12/23/2022 11:27:00 AM

English (United Kingdom)

Page 67: [248] Formatted	Yuan, Peng (GIK)	12/23/2022 11:27:00 AM

English (United Kingdom)

Page 67: [249] Formatted	Yuan, Peng (GIK)	12/23/2022 11:27:00 AM

English (United Kingdom)

Page 67: [250] Formatted	Yuan, Peng (GIK)	12/23/2022 11:27:00 AM

English (United Kingdom)

Page 67: [251] Formatted	Yuan, Peng (GIK)	12/23/2022 11:27:00 AM

English (United Kingdom)

Page 67: [252] Formatted	Yuan, Peng (GIK)	12/23/2022 11:27:00 AM

English (United Kingdom)

Page 67: [253] Formatted	Yuan, Peng (GIK)	12/23/2022 11:27:00 AM

English (United Kingdom)

Page 67: [254] Formatted	Yuan, Peng (GIK)	12/23/2022 11:27:00 AM

English (United Kingdom)

Page 67: [255] Formatted	Yuan, Peng (GIK)	12/23/2022 11:27:00 AM

English (United Kingdom)

Page 67: [256] Formatted	Yuan, Peng (GIK)	12/23/2022 11:27:00 AM

English (United Kingdom)

Page 67: [257] Formatted	Yuan, Peng (GIK)	12/23/2022 11:27:00 AM

Font: Bold

Page 67: [257] Formatted	Yuan, Peng (GIK)	12/23/2022 11:27:00 AM

Font: Bold

Page 67: [258] Formatted	Yuan, Peng (GIK)	12/23/2022 11:27:00 AM

English (United Kingdom)

Page 67: [259] Formatted	Yuan, Peng (GIK)	12/23/2022 11:27:00 AM

English (United Kingdom)

Page 67: [260] Formatted	Yuan, Peng (GIK)	12/23/2022 11:27:00 AM

English (United Kingdom)

Page 67: [261] Formatted	Yuan, Peng (GIK)	12/23/2022 11:27:00 AM

English (United Kingdom)

Page 67: [262] Formatted	Yuan, Peng (GIK)	12/23/2022 11:27:00 AM

English (United Kingdom)

Page 67: [263] Formatted	Yuan, Peng (GIK)	12/23/2022 11:27:00 AM

English (United Kingdom)

Page 67: [264] Formatted	Yuan, Peng (GIK)	12/23/2022 11:27:00 AM

English (United Kingdom)

Page 67: [265] Formatted	Yuan, Peng (GIK)	12/23/2022 11:27:00 AM

English (United Kingdom)

Page 67: [266] Formatted	Yuan, Peng (GIK)	12/23/2022 11:27:00 AM

English (United Kingdom)

Page 67: [267] Formatted	Yuan, Peng (GIK)	12/23/2022 11:27:00 AM

English (United Kingdom)

Page 67: [268] Formatted	Yuan, Peng (GIK)	12/23/2022 11:27:00 AM

English (United Kingdom)

Page 67: [269] Formatted	Yuan, Peng (GIK)	12/23/2022 11:27:00 AM

Font: Bold

Page 67: [269] Formatted	Yuan, Peng (GIK)	12/23/2022 11:27:00 AM

Font: Bold

Page 67: [270] Formatted	Yuan, Peng (GIK)	12/23/2022 11:27:00 AM

English (United Kingdom)

Page 67: [271] Formatted	Yuan, Peng (GIK)	12/23/2022 11:27:00 AM

English (United Kingdom)

Page 67: [272] Formatted	Yuan, Peng (GIK)	12/23/2022 11:27:00 AM

English (United Kingdom)

Page 67: [273] Formatted	Yuan, Peng (GIK)	12/23/2022 11:27:00 AM

English (United Kingdom)

Page 67: [274] Formatted	Yuan, Peng (GIK)	12/23/2022 11:27:00 AM

English (United Kingdom)

Page 67: [275] Formatted	Yuan, Peng (GIK)	12/23/2022 11:27:00 AM

English (United Kingdom)

Page 67: [276] Formatted	Yuan, Peng (GIK)	12/23/2022 11:27:00 AM

English (United Kingdom)

Page 67: [277] Formatted	Yuan, Peng (GIK)	12/23/2022 11:27:00 AM

English (United Kingdom)

Page 67: [278] Formatted	Yuan, Peng (GIK)	12/23/2022 11:27:00 AM

English (United Kingdom)

Page 67: [279] Formatted	Yuan, Peng (GIK)	12/23/2022 11:27:00 AM

English (United Kingdom)

Page 67: [280] Formatted	Yuan, Peng (GIK)	12/23/2022 11:27:00 AM

English (United Kingdom)

Page 67: [281] Formatted	Yuan, Peng (GIK)	12/23/2022 11:27:00 AM

Font: Bold

Page 67: [281] Formatted	Yuan, Peng (GIK)	12/23/2022 11:27:00 AM

Font: Bold

Page 67: [282] Formatted	Yuan, Peng (GIK)	12/23/2022 11:27:00 AM

English (United Kingdom)

Page 67: [283] Formatted	Yuan, Peng (GIK)	12/23/2022 11:27:00 AM

English (United Kingdom)

Page 67: [284] Formatted	Yuan, Peng (GIK)	12/23/2022 11:27:00 AM

English (United Kingdom)

Page 67: [285] Formatted	Yuan, Peng (GIK)	12/23/2022 11:27:00 AM

English (United Kingdom)

Page 67: [286] Formatted	Yuan, Peng (GIK)	12/23/2022 11:27:00 AM

English (United Kingdom)

Page 67: [287] Formatted	Yuan, Peng (GIK)	12/23/2022 11:27:00 AM

English (United Kingdom)

Page 67: [288] Formatted	Yuan, Peng (GIK)	12/23/2022 11:27:00 AM

English (United Kingdom)

Page 67: [289] Formatted	Yuan, Peng (GIK)	12/23/2022 11:27:00 AM

English (United Kingdom)

Page 67: [290] Formatted	Yuan, Peng (GIK)	12/23/2022 11:27:00 AM

English (United Kingdom)

Page 67: [291] Formatted	Yuan, Peng (GIK)	12/23/2022 11:27:00 AM

English (United Kingdom)

Page 67: [292] Formatted	Yuan, Peng (GIK)	12/23/2022 11:27:00 AM

English (United Kingdom)

Page 67: [293] Formatted	Yuan, Peng (GIK)	12/23/2022 11:27:00 AM

Font: Bold

Page 67: [293] Formatted	Yuan, Peng (GIK)	12/23/2022 11:27:00 AM

Font: Bold

Page 67: [294] Formatted	Yuan, Peng (GIK)	12/23/2022 11:27:00 AM

English (United Kingdom)

Page 67: [295] Formatted	Yuan, Peng (GIK)	12/23/2022 11:27:00 AM

English (United Kingdom)

Page 67: [296] Formatted	Yuan, Peng (GIK)	12/23/2022 11:27:00 AM

English (United Kingdom)

Page 67: [297] Formatted	Yuan, Peng (GIK)	12/23/2022 11:27:00 AM

English (United Kingdom)

Page 67: [298] Formatted	Yuan, Peng (GIK)	12/23/2022 11:27:00 AM

English (United Kingdom)

Page 67: [299] Formatted	Yuan, Peng (GIK)	12/23/2022 11:27:00 AM

English (United Kingdom)

Page 67: [300] Formatted	Yuan, Peng (GIK)	12/23/2022 11:27:00 AM

English (United Kingdom)

Page 67: [301] Formatted	Yuan, Peng (GIK)	12/23/2022 11:27:00 AM

English (United Kingdom)

Page 67: [302] Formatted	Yuan, Peng (GIK)	12/23/2022 11:27:00 AM

English (United Kingdom)

Page 67: [303] Formatted	Yuan, Peng (GIK)	12/23/2022 11:27:00 AM

English (United Kingdom)

Page 67: [304] Formatted	Yuan, Peng (GIK)	12/23/2022 11:27:00 AM

English (United Kingdom)

Page 67: [305] Formatted	Yuan, Peng (GIK)	12/23/2022 11:27:00 AM

Font: Bold

Page 67: [305] Formatted	Yuan, Peng (GIK)	12/23/2022 11:27:00 AM

Font: Bold

Page 67: [306] Formatted	Yuan, Peng (GIK)	12/23/2022 11:27:00 AM

English (United Kingdom)

Page 67: [307] Formatted	Yuan, Peng (GIK)	12/23/2022 11:27:00 AM

English (United Kingdom)

Page 67: [308] Formatted	Yuan, Peng (GIK)	12/23/2022 11:27:00 AM

English (United Kingdom)

Page 67: [309] Formatted	Yuan, Peng (GIK)	12/23/2022 11:27:00 AM

English (United Kingdom)

Page 67: [310] Formatted	Yuan, Peng (GIK)	12/23/2022 11:27:00 AM

English (United Kingdom)

Page 67: [311] Formatted	Yuan, Peng (GIK)	12/23/2022 11:27:00 AM

English (United Kingdom)

Page 67: [312] Formatted	Yuan, Peng (GIK)	12/23/2022 11:27:00 AM

English (United Kingdom)

Page 67: [313] Formatted	Yuan, Peng (GIK)	12/23/2022 11:27:00 AM

English (United Kingdom)

Page 67: [314] Formatted	Yuan, Peng (GIK)	12/23/2022 11:27:00 AM

English (United Kingdom)

Page 67: [315] Formatted	Yuan, Peng (GIK)	12/23/2022 11:27:00 AM

English (United Kingdom)

Page 67: [316] Formatted	Yuan, Peng (GIK)	12/23/2022 11:27:00 AM

English (United Kingdom)

Page 67: [317] Formatted	Yuan, Peng (GIK)	12/23/2022 11:27:00 AM

Font: Bold

Page 67: [317] Formatted	Yuan, Peng (GIK)	12/23/2022 11:27:00 AM

Font: Bold

Page 67: [318] Formatted	Yuan, Peng (GIK)	12/23/2022 11:27:00 AM

English (United Kingdom)

Page 67: [319] Formatted	Yuan, Peng (GIK)	12/23/2022 11:27:00 AM

English (United Kingdom)

Page 67: [320] Formatted	Yuan, Peng (GIK)	12/23/2022 11:27:00 AM

English (United Kingdom)

Page 67: [321] Formatted	Yuan, Peng (GIK)	12/23/2022 11:27:00 AM

English (United Kingdom)

Page 67: [322] Formatted	Yuan, Peng (GIK)	12/23/2022 11:27:00 AM

English (United Kingdom)

Page 67: [323] Formatted	Yuan, Peng (GIK)	12/23/2022 11:27:00 AM

English (United Kingdom)

Page 67: [324] Formatted	Yuan, Peng (GIK)	12/23/2022 11:27:00 AM

English (United Kingdom)

Page 67: [325] Formatted	Yuan, Peng (GIK)	12/23/2022 11:27:00 AM

English (United Kingdom)

Page 67: [326] Formatted	Yuan, Peng (GIK)	12/23/2022 11:27:00 AM

English (United Kingdom)

Page 67: [327] Formatted	Yuan, Peng (GIK)	12/23/2022 11:27:00 AM

English (United Kingdom)

Page 67: [328] Formatted	Yuan, Peng (GIK)	12/23/2022 11:27:00 AM

English (United Kingdom)

Page 67: [329] Formatted	Yuan, Peng (GIK)	12/23/2022 11:27:00 AM

Font: Bold

Page 67: [329] Formatted	Yuan, Peng (GIK)	12/23/2022 11:27:00 AM

Font: Bold

Page 67: [330] Formatted	Yuan, Peng (GIK)	12/23/2022 11:27:00 AM

English (United Kingdom)

Page 67: [331] Formatted	Yuan, Peng (GIK)	12/23/2022 11:27:00 AM

English (United Kingdom)

Page 67: [332] Formatted	Yuan, Peng (GIK)	12/23/2022 11:27:00 AM

English (United Kingdom)

Page 67: [333] Formatted	Yuan, Peng (GIK)	12/23/2022 11:27:00 AM

English (United Kingdom)

Page 67: [334] Formatted	Yuan, Peng (GIK)	12/23/2022 11:27:00 AM

English (United Kingdom)

Page 67: [335] Formatted	Yuan, Peng (GIK)	12/23/2022 11:27:00 AM

English (United Kingdom)

Page 67: [336] Formatted	Yuan, Peng (GIK)	12/23/2022 11:27:00 AM

English (United Kingdom)

Page 67: [337] Formatted	Yuan, Peng (GIK)	12/23/2022 11:27:00 AM

English (United Kingdom)

Page 67: [338] Formatted	Yuan, Peng (GIK)	12/23/2022 11:27:00 AM

English (United Kingdom)

Page 67: [339] Formatted	Yuan, Peng (GIK)	12/23/2022 11:27:00 AM

English (United Kingdom)

Page 67: [340] Formatted	Yuan, Peng (GIK)	12/23/2022 11:27:00 AM

English (United Kingdom)

Page 67: [341] Formatted	Yuan, Peng (GIK)	12/23/2022 11:27:00 AM

Font: Bold

Page 67: [341] Formatted	Yuan, Peng (GIK)	12/23/2022 11:27:00 AM

Font: Bold

Page 67: [342] Formatted	Yuan, Peng (GIK)	12/23/2022 11:27:00 AM

English (United Kingdom)

Page 67: [343] Formatted	Yuan, Peng (GIK)	12/23/2022 11:27:00 AM

English (United Kingdom)

Page 67: [344] Formatted	Yuan, Peng (GIK)	12/23/2022 11:27:00 AM

English (United Kingdom)

Page 67: [345] Formatted	Yuan, Peng (GIK)	12/23/2022 11:27:00 AM

English (United Kingdom)

Page 67: [346] Formatted	Yuan, Peng (GIK)	12/23/2022 11:27:00 AM

English (United Kingdom)

Page 67: [347] Formatted	Yuan, Peng (GIK)	12/23/2022 11:27:00 AM

English (United Kingdom)

Page 67: [348] Formatted	Yuan, Peng (GIK)	12/23/2022 11:27:00 AM

English (United Kingdom)

Page 67: [349] Formatted	Yuan, Peng (GIK)	12/23/2022 11:27:00 AM

English (United Kingdom)

Page 67: [350] Formatted	Yuan, Peng (GIK)	12/23/2022 11:27:00 AM

English (United Kingdom)

Page 67: [351] Formatted	Yuan, Peng (GIK)	12/23/2022 11:27:00 AM

English (United Kingdom)

Page 67: [352] Formatted	Yuan, Peng (GIK)	12/23/2022 11:27:00 AM

English (United Kingdom)

Page 67: [353] Formatted	Yuan, Peng (GIK)	12/23/2022 11:27:00 AM

Font: Bold

Page 67: [353] Formatted	Yuan, Peng (GIK)	12/23/2022 11:27:00 AM

Font: Bold

Page 67: [354] Formatted	Yuan, Peng (GIK)	12/23/2022 11:27:00 AM

English (United Kingdom)

Page 67: [355] Formatted	Yuan, Peng (GIK)	12/23/2022 11:27:00 AM

English (United Kingdom)

Page 67: [356] Formatted	Yuan, Peng (GIK)	12/23/2022 11:27:00 AM

English (United Kingdom)

Page 67: [357] Formatted	Yuan, Peng (GIK)	12/23/2022 11:27:00 AM

English (United Kingdom)

Page 67: [358] Formatted	Yuan, Peng (GIK)	12/23/2022 11:27:00 AM

English (United Kingdom)

Page 67: [359] Formatted	Yuan, Peng (GIK)	12/23/2022 11:27:00 AM

English (United Kingdom)

Page 67: [360] Formatted	Yuan, Peng (GIK)	12/23/2022 11:27:00 AM

English (United Kingdom)

Page 67: [361] Formatted	Yuan, Peng (GIK)	12/23/2022 11:27:00 AM

English (United Kingdom)

Page 67: [362] Formatted	Yuan, Peng (GIK)	12/23/2022 11:27:00 AM

English (United Kingdom)

Page 67: [363] Formatted	Yuan, Peng (GIK)	12/23/2022 11:27:00 AM

English (United Kingdom)

Page 67: [364] Formatted	Yuan, Peng (GIK)	12/23/2022 11:27:00 AM

English (United Kingdom)

Page 67: [365] Formatted	Yuan, Peng (GIK)	12/23/2022 11:27:00 AM

Font: Bold

Page 67: [365] Formatted	Yuan, Peng (GIK)	12/23/2022 11:27:00 AM

Font: Bold

Page 67: [366] Formatted	Yuan, Peng (GIK)	12/23/2022 11:27:00 AM

English (United Kingdom)

Page 67: [367] Formatted	Yuan, Peng (GIK)	12/23/2022 11:27:00 AM

English (United Kingdom)

Page 67: [368] Formatted	Yuan, Peng (GIK)	12/23/2022 11:27:00 AM

English (United Kingdom)

Page 67: [369] Formatted	Yuan, Peng (GIK)	12/23/2022 11:27:00 AM

English (United Kingdom)

Page 67: [370] Formatted	Yuan, Peng (GIK)	12/23/2022 11:27:00 AM

English (United Kingdom)

Page 67: [371] Formatted	Yuan, Peng (GIK)	12/23/2022 11:27:00 AM

English (United Kingdom)

Page 67: [372] Formatted	Yuan, Peng (GIK)	12/23/2022 11:27:00 AM

English (United Kingdom)

Page 67: [373] Formatted	Yuan, Peng (GIK)	12/23/2022 11:27:00 AM

English (United Kingdom)

Page 67: [374] Formatted	Yuan, Peng (GIK)	12/23/2022 11:27:00 AM

English (United Kingdom)

Page 67: [375] Formatted	Yuan, Peng (GIK)	12/23/2022 11:27:00 AM

English (United Kingdom)

Page 67: [376] Formatted	Yuan, Peng (GIK)	12/23/2022 11:27:00 AM

English (United Kingdom)

Page 67: [377] Formatted	Yuan, Peng (GIK)	12/23/2022 11:27:00 AM

Font: Bold

Page 67: [377] Formatted	Yuan, Peng (GIK)	12/23/2022 11:27:00 AM

Font: Bold

Page 67: [378] Formatted	Yuan, Peng (GIK)	12/23/2022 11:27:00 AM

English (United Kingdom)

Page 67: [379] Formatted	Yuan, Peng (GIK)	12/23/2022 11:27:00 AM

English (United Kingdom)

Page 67: [380] Formatted	Yuan, Peng (GIK)	12/23/2022 11:27:00 AM

English (United Kingdom)

Page 67: [381] Formatted	Yuan, Peng (GIK)	12/23/2022 11:27:00 AM

English (United Kingdom)

Page 67: [382] Formatted	Yuan, Peng (GIK)	12/23/2022 11:27:00 AM

English (United Kingdom)

Page 67: [383] Formatted	Yuan, Peng (GIK)	12/23/2022 11:27:00 AM

English (United Kingdom)

Page 67: [384] Formatted	Yuan, Peng (GIK)	12/23/2022 11:27:00 AM

English (United Kingdom)

Page 67: [385] Formatted	Yuan, Peng (GIK)	12/23/2022 11:27:00 AM

English (United Kingdom)

Page 67: [386] Formatted	Yuan, Peng (GIK)	12/23/2022 11:27:00 AM

English (United Kingdom)

Page 67: [387] Formatted	Yuan, Peng (GIK)	12/23/2022 11:27:00 AM

English (United Kingdom)

Page 67: [388] Formatted	Yuan, Peng (GIK)	12/23/2022 11:27:00 AM

English (United Kingdom)

Page 67: [389] Formatted	Yuan, Peng (GIK)	12/23/2022 11:27:00 AM

Font: Bold

Page 67: [389] Formatted	Yuan, Peng (GIK)	12/23/2022 11:27:00 AM

Font: Bold

Page 67: [390] Formatted	Yuan, Peng (GIK)	12/23/2022 11:27:00 AM

English (United Kingdom)

Page 67: [391] Formatted	Yuan, Peng (GIK)	12/23/2022 11:27:00 AM

English (United Kingdom)

Page 67: [392] Formatted	Yuan, Peng (GIK)	12/23/2022 11:27:00 AM

English (United Kingdom)

Page 67: [393] Formatted	Yuan, Peng (GIK)	12/23/2022 11:27:00 AM

English (United Kingdom)

Page 67: [394] Formatted	Yuan, Peng (GIK)	12/23/2022 11:27:00 AM

English (United Kingdom)

Page 67: [395] Formatted	Yuan, Peng (GIK)	12/23/2022 11:27:00 AM

English (United Kingdom)

Page 67: [396] Formatted	Yuan, Peng (GIK)	12/23/2022 11:27:00 AM

English (United Kingdom)

Page 67: [397] Formatted	Yuan, Peng (GIK)	12/23/2022 11:27:00 AM

English (United Kingdom)

Page 67: [398] Formatted	Yuan, Peng (GIK)	12/23/2022 11:27:00 AM

English (United Kingdom)

Page 67: [399] Formatted	Yuan, Peng (GIK)	12/23/2022 11:27:00 AM

English (United Kingdom)

Page 67: [400] Formatted	Yuan, Peng (GIK)	12/23/2022 11:27:00 AM

English (United Kingdom)

Page 67: [401] Formatted	Yuan, Peng (GIK)	12/23/2022 11:27:00 AM

Font: Bold

Page 67: [401] Formatted	Yuan, Peng (GIK)	12/23/2022 11:27:00 AM

Font: Bold

Page 67: [402] Formatted	Yuan, Peng (GIK)	12/23/2022 11:27:00 AM

English (United Kingdom)

Page 67: [403] Formatted	Yuan, Peng (GIK)	12/23/2022 11:27:00 AM

English (United Kingdom)

Page 67: [404] Formatted	Yuan, Peng (GIK)	12/23/2022 11:27:00 AM

English (United Kingdom)

Page 67: [405] Formatted	Yuan, Peng (GIK)	12/23/2022 11:27:00 AM

English (United Kingdom)

Page 67: [406] Formatted	Yuan, Peng (GIK)	12/23/2022 11:27:00 AM

English (United Kingdom)

Page 67: [407] Formatted	Yuan, Peng (GIK)	12/23/2022 11:27:00 AM

English (United Kingdom)

Page 67: [408] Formatted	Yuan, Peng (GIK)	12/23/2022 11:27:00 AM

English (United Kingdom)

Page 67: [409] Formatted	Yuan, Peng (GIK)	12/23/2022 11:27:00 AM

English (United Kingdom)

Page 67: [410] Formatted	Yuan, Peng (GIK)	12/23/2022 11:27:00 AM

English (United Kingdom)

Page 67: [411] Formatted	Yuan, Peng (GIK)	12/23/2022 11:27:00 AM

English (United Kingdom)

Page 67: [412] Formatted	Yuan, Peng (GIK)	12/23/2022 11:27:00 AM

English (United Kingdom)

Page 67: [413] Formatted	Yuan, Peng (GIK)	12/23/2022 11:27:00 AM

Font: Bold

Page 67: [413] Formatted	Yuan, Peng (GIK)	12/23/2022 11:27:00 AM

Font: Bold

Page 67: [414] Formatted	Yuan, Peng (GIK)	12/23/2022 11:27:00 AM

English (United Kingdom)

Page 67: [415] Formatted	Yuan, Peng (GIK)	12/23/2022 11:27:00 AM

English (United Kingdom)

Page 67: [416] Formatted	Yuan, Peng (GIK)	12/23/2022 11:27:00 AM

English (United Kingdom)

Page 67: [417] Formatted	Yuan, Peng (GIK)	12/23/2022 11:27:00 AM

English (United Kingdom)

Page 67: [418] Formatted	Yuan, Peng (GIK)	12/23/2022 11:27:00 AM

English (United Kingdom)

Page 67: [419] Formatted	Yuan, Peng (GIK)	12/23/2022 11:27:00 AM

English (United Kingdom)

Page 67: [420] Formatted	Yuan, Peng (GIK)	12/23/2022 11:27:00 AM

English (United Kingdom)

Page 67: [421] Formatted	Yuan, Peng (GIK)	12/23/2022 11:27:00 AM

English (United Kingdom)

Page 67: [422] Formatted	Yuan, Peng (GIK)	12/23/2022 11:27:00 AM

English (United Kingdom)

Page 67: [423] Formatted	Yuan, Peng (GIK)	12/23/2022 11:27:00 AM

English (United Kingdom)

Page 67: [424] Formatted	Yuan, Peng (GIK)	12/23/2022 11:27:00 AM

English (United Kingdom)

Page 67: [425] Formatted	Yuan, Peng (GIK)	12/23/2022 11:27:00 AM

Font: Bold

Page 67: [425] Formatted	Yuan, Peng (GIK)	12/23/2022 11:27:00 AM

Font: Bold

Page 67: [426] Formatted	Yuan, Peng (GIK)	12/23/2022 11:27:00 AM

English (United Kingdom)

Page 67: [427] Formatted	Yuan, Peng (GIK)	12/23/2022 11:27:00 AM

English (United Kingdom)

Page 67: [428] Formatted	Yuan, Peng (GIK)	12/23/2022 11:27:00 AM

English (United Kingdom)

Page 67: [429] Formatted	Yuan, Peng (GIK)	12/23/2022 11:27:00 AM

English (United Kingdom)

Page 67: [430] Formatted	Yuan, Peng (GIK)	12/23/2022 11:27:00 AM

English (United Kingdom)

Page 67: [431] Formatted	Yuan, Peng (GIK)	12/23/2022 11:27:00 AM

English (United Kingdom)

Page 67: [432] Formatted	Yuan, Peng (GIK)	12/23/2022 11:27:00 AM

English (United Kingdom)

Page 67: [433] Formatted	Yuan, Peng (GIK)	12/23/2022 11:27:00 AM

English (United Kingdom)

Page 67: [434] Formatted	Yuan, Peng (GIK)	12/23/2022 11:27:00 AM

English (United Kingdom)

Page 67: [435] Formatted	Yuan, Peng (GIK)	12/23/2022 11:27:00 AM

English (United Kingdom)

Page 67: [436] Formatted	Yuan, Peng (GIK)	12/23/2022 11:27:00 AM

English (United Kingdom)

Page 67: [437] Formatted	Yuan, Peng (GIK)	12/23/2022 11:27:00 AM

Font: Bold

Page 67: [437] Formatted	Yuan, Peng (GIK)	12/23/2022 11:27:00 AM

Font: Bold

Page 67: [438] Formatted	Yuan, Peng (GIK)	12/23/2022 11:27:00 AM

English (United Kingdom)

Page 67: [439] Formatted	Yuan, Peng (GIK)	12/23/2022 11:27:00 AM

English (United Kingdom)

Page 67: [440] Formatted	Yuan, Peng (GIK)	12/23/2022 11:27:00 AM

English (United Kingdom)

Page 67: [441] Formatted	Yuan, Peng (GIK)	12/23/2022 11:27:00 AM

English (United Kingdom)

Page 67: [442] Formatted	Yuan, Peng (GIK)	12/23/2022 11:27:00 AM

English (United Kingdom)

Page 67: [443] Formatted	Yuan, Peng (GIK)	12/23/2022 11:27:00 AM

English (United Kingdom)

Page 67: [444] Formatted	Yuan, Peng (GIK)	12/23/2022 11:27:00 AM

English (United Kingdom)

Page 67: [445] Formatted	Yuan, Peng (GIK)	12/23/2022 11:27:00 AM

English (United Kingdom)

Page 67: [446] Formatted	Yuan, Peng (GIK)	12/23/2022 11:27:00 AM

English (United Kingdom)

Page 67: [447] Formatted	Yuan, Peng (GIK)	12/23/2022 11:27:00 AM

English (United Kingdom)

Page 67: [448] Formatted	Yuan, Peng (GIK)	12/23/2022 11:27:00 AM

English (United Kingdom)

Page 67: [449] Formatted	Yuan, Peng (GIK)	12/23/2022 11:27:00 AM

Font: Bold

Page 67: [449] Formatted	Yuan, Peng (GIK)	12/23/2022 11:27:00 AM

Font: Bold

Page 67: [450] Formatted	Yuan, Peng (GIK)	12/23/2022 11:27:00 AM

English (United Kingdom)

Page 67: [451] Formatted	Yuan, Peng (GIK)	12/23/2022 11:27:00 AM

English (United Kingdom)

Page 67: [452] Formatted	Yuan, Peng (GIK)	12/23/2022 11:27:00 AM

English (United Kingdom)

Page 67: [453] Formatted	Yuan, Peng (GIK)	12/23/2022 11:27:00 AM

English (United Kingdom)

Page 67: [454] Formatted	Yuan, Peng (GIK)	12/23/2022 11:27:00 AM

English (United Kingdom)

Page 67: [455] Formatted	Yuan, Peng (GIK)	12/23/2022 11:27:00 AM

English (United Kingdom)

Page 67: [456] Formatted	Yuan, Peng (GIK)	12/23/2022 11:27:00 AM

English (United Kingdom)

Page 67: [457] Formatted	Yuan, Peng (GIK)	12/23/2022 11:27:00 AM

English (United Kingdom)

Page 67: [458] Formatted	Yuan, Peng (GIK)	12/23/2022 11:27:00 AM

English (United Kingdom)

Page 67: [459] Formatted	Yuan, Peng (GIK)	12/23/2022 11:27:00 AM

English (United Kingdom)

Page 67: [460] Formatted	Yuan, Peng (GIK)	12/23/2022 11:27:00 AM

English (United Kingdom)

Page 67: [461] Formatted	Yuan, Peng (GIK)	12/23/2022 11:27:00 AM

Font: Bold

Page 67: [461] Formatted	Yuan, Peng (GIK)	12/23/2022 11:27:00 AM

Font: Bold

Page 67: [462] Formatted	Yuan, Peng (GIK)	12/23/2022 11:27:00 AM

English (United Kingdom)

Page 67: [463] Formatted	Yuan, Peng (GIK)	12/23/2022 11:27:00 AM

English (United Kingdom)

Page 67: [464] Formatted	Yuan, Peng (GIK)	12/23/2022 11:27:00 AM

English (United Kingdom)

Page 67: [465] Formatted	Yuan, Peng (GIK)	12/23/2022 11:27:00 AM

English (United Kingdom)

Page 67: [466] Formatted	Yuan, Peng (GIK)	12/23/2022 11:27:00 AM

English (United Kingdom)

Page 67: [467] Formatted	Yuan, Peng (GIK)	12/23/2022 11:27:00 AM

English (United Kingdom)

Page 67: [468] Formatted	Yuan, Peng (GIK)	12/23/2022 11:27:00 AM

English (United Kingdom)

Page 67: [469] Formatted	Yuan, Peng (GIK)	12/23/2022 11:27:00 AM

English (United Kingdom)

Page 67: [470] Formatted	Yuan, Peng (GIK)	12/23/2022 11:27:00 AM

English (United Kingdom)

Page 67: [471] Formatted	Yuan, Peng (GIK)	12/23/2022 11:27:00 AM

English (United Kingdom)

Page 67: [472] Formatted	Yuan, Peng (GIK)	12/23/2022 11:27:00 AM

English (United Kingdom)

Page 68: [473] Formatted	Yuan, Peng (GIK)	12/23/2022 11:27:00 AM

Font: Bold

Page 68: [473] Formatted	Yuan, Peng (GIK)	12/23/2022 11:27:00 AM

Font: Bold

Page 68: [474] Formatted	Yuan, Peng (GIK)	12/23/2022 11:27:00 AM

English (United Kingdom)

Page 68: [475] Formatted	Yuan, Peng (GIK)	12/23/2022 11:27:00 AM

English (United Kingdom)

Page 68: [476] Formatted	Yuan, Peng (GIK)	12/23/2022 11:27:00 AM

English (United Kingdom)

Page 68: [477] Formatted	Yuan, Peng (GIK)	12/23/2022 11:27:00 AM

English (United Kingdom)

Page 68: [478] Formatted	Yuan, Peng (GIK)	12/23/2022 11:27:00 AM

English (United Kingdom)

Page 68: [479] Formatted	Yuan, Peng (GIK)	12/23/2022 11:27:00 AM

English (United Kingdom)

Page 68: [480] Formatted	Yuan, Peng (GIK)	12/23/2022 11:27:00 AM

English (United Kingdom)

Page 68: [481] Formatted	Yuan, Peng (GIK)	12/23/2022 11:27:00 AM

English (United Kingdom)

Page 68: [482] Formatted	Yuan, Peng (GIK)	12/23/2022 11:27:00 AM

English (United Kingdom)

Page 68: [483] Formatted	Yuan, Peng (GIK)	12/23/2022 11:27:00 AM

English (United Kingdom)

Page 68: [484] Formatted	Yuan, Peng (GIK)	12/23/2022 11:27:00 AM

English (United Kingdom)

Page 68: [485] Formatted	Yuan, Peng (GIK)	12/23/2022 11:27:00 AM

Font: Bold

Page 68: [485] Formatted	Yuan, Peng (GIK)	12/23/2022 11:27:00 AM

Font: Bold

Page 68: [486] Formatted	Yuan, Peng (GIK)	12/23/2022 11:27:00 AM

English (United Kingdom)

Page 68: [487] Formatted	Yuan, Peng (GIK)	12/23/2022 11:27:00 AM

English (United Kingdom)

Page 68: [488] Formatted	Yuan, Peng (GIK)	12/23/2022 11:27:00 AM

English (United Kingdom)

Page 68: [489] Formatted	Yuan, Peng (GIK)	12/23/2022 11:27:00 AM

English (United Kingdom)

Page 68: [490] Formatted	Yuan, Peng (GIK)	12/23/2022 11:27:00 AM

English (United Kingdom)

Page 68: [491] Formatted	Yuan, Peng (GIK)	12/23/2022 11:27:00 AM

English (United Kingdom)

Page 68: [492] Formatted	Yuan, Peng (GIK)	12/23/2022 11:27:00 AM

English (United Kingdom)

Page 68: [493] Formatted	Yuan, Peng (GIK)	12/23/2022 11:27:00 AM

English (United Kingdom)

Page 68: [494] Formatted	Yuan, Peng (GIK)	12/23/2022 11:27:00 AM

English (United Kingdom)

Page 68: [495] Formatted	Yuan, Peng (GIK)	12/23/2022 11:27:00 AM

English (United Kingdom)

Page 68: [496] Formatted	Yuan, Peng (GIK)	12/23/2022 11:27:00 AM

English (United Kingdom)

Page 68: [497] Formatted	Yuan, Peng (GIK)	12/23/2022 11:27:00 AM

Font: Bold

Page 68: [497] Formatted	Yuan, Peng (GIK)	12/23/2022 11:27:00 AM

Font: Bold

Page 68: [498] Formatted	Yuan, Peng (GIK)	12/23/2022 11:27:00 AM

English (United Kingdom)

Page 68: [499] Formatted	Yuan, Peng (GIK)	12/23/2022 11:27:00 AM

English (United Kingdom)

Page 68: [500] Formatted	Yuan, Peng (GIK)	12/23/2022 11:27:00 AM

English (United Kingdom)

Page 68: [501] Formatted	Yuan, Peng (GIK)	12/23/2022 11:27:00 AM

English (United Kingdom)

Page 68: [502] Formatted	Yuan, Peng (GIK)	12/23/2022 11:27:00 AM

English (United Kingdom)

Page 68: [503] Formatted	Yuan, Peng (GIK)	12/23/2022 11:27:00 AM

English (United Kingdom)

Page 68: [504] Formatted	Yuan, Peng (GIK)	12/23/2022 11:27:00 AM

English (United Kingdom)

Page 68: [505] Formatted	Yuan, Peng (GIK)	12/23/2022 11:27:00 AM

English (United Kingdom)

Page 68: [506] Formatted	Yuan, Peng (GIK)	12/23/2022 11:27:00 AM

English (United Kingdom)

Page 68: [507] Formatted	Yuan, Peng (GIK)	12/23/2022 11:27:00 AM

English (United Kingdom)

Page 68: [508] Formatted	Yuan, Peng (GIK)	12/23/2022 11:27:00 AM

English (United Kingdom)

Page 68: [509] Formatted	Yuan, Peng (GIK)	12/23/2022 11:27:00 AM

Font: Bold

Page 68: [509] Formatted	Yuan, Peng (GIK)	12/23/2022 11:27:00 AM

Font: Bold

Page 68: [510] Formatted	Yuan, Peng (GIK)	12/23/2022 11:27:00 AM

English (United Kingdom)

Page 68: [511] Formatted	Yuan, Peng (GIK)	12/23/2022 11:27:00 AM

English (United Kingdom)

Page 68: [512] Formatted	Yuan, Peng (GIK)	12/23/2022 11:27:00 AM

English (United Kingdom)

Page 68: [513] Formatted	Yuan, Peng (GIK)	12/23/2022 11:27:00 AM

English (United Kingdom)

Page 68: [514] Formatted	Yuan, Peng (GIK)	12/23/2022 11:27:00 AM

English (United Kingdom)

Page 68: [515] Formatted	Yuan, Peng (GIK)	12/23/2022 11:27:00 AM

English (United Kingdom)

Page 68: [516] Formatted	Yuan, Peng (GIK)	12/23/2022 11:27:00 AM

English (United Kingdom)

Page 68: [517] Formatted	Yuan, Peng (GIK)	12/23/2022 11:27:00 AM

English (United Kingdom)

Page 68: [518] Formatted	Yuan, Peng (GIK)	12/23/2022 11:27:00 AM

English (United Kingdom)

Page 68: [519] Formatted	Yuan, Peng (GIK)	12/23/2022 11:27:00 AM

English (United Kingdom)

Page 68: [520] Formatted	Yuan, Peng (GIK)	12/23/2022 11:27:00 AM

English (United Kingdom)

Page 68: [521] Formatted	Yuan, Peng (GIK)	12/23/2022 11:27:00 AM

Font: Bold

Page 68: [521] Formatted	Yuan, Peng (GIK)	12/23/2022 11:27:00 AM

Font: Bold

Page 68: [522] Formatted	Yuan, Peng (GIK)	12/23/2022 11:27:00 AM

English (United Kingdom)

Page 68: [523] Formatted	Yuan, Peng (GIK)	12/23/2022 11:27:00 AM

English (United Kingdom)

Page 68: [524] Formatted	Yuan, Peng (GIK)	12/23/2022 11:27:00 AM

English (United Kingdom)

Page 68: [525] Formatted	Yuan, Peng (GIK)	12/23/2022 11:27:00 AM

English (United Kingdom)

Page 68: [526] Formatted	Yuan, Peng (GIK)	12/23/2022 11:27:00 AM

English (United Kingdom)

Page 68: [527] Formatted	Yuan, Peng (GIK)	12/23/2022 11:27:00 AM

English (United Kingdom)

Page 68: [528] Formatted	Yuan, Peng (GIK)	12/23/2022 11:27:00 AM

English (United Kingdom)

Page 68: [529] Formatted	Yuan, Peng (GIK)	12/23/2022 11:27:00 AM

English (United Kingdom)

Page 68: [530] Formatted	Yuan, Peng (GIK)	12/23/2022 11:27:00 AM

English (United Kingdom)

Page 68: [531] Formatted	Yuan, Peng (GIK)	12/23/2022 11:27:00 AM

English (United Kingdom)

Page 68: [532] Formatted	Yuan, Peng (GIK)	12/23/2022 11:27:00 AM

English (United Kingdom)

Page 68: [533] Formatted	Yuan, Peng (GIK)	12/23/2022 11:27:00 AM

Font: Bold

Page 68: [533] Formatted	Yuan, Peng (GIK)	12/23/2022 11:27:00 AM

Font: Bold

Page 68: [534] Formatted	Yuan, Peng (GIK)	12/23/2022 11:27:00 AM

English (United Kingdom)

Page 68: [535] Formatted	Yuan, Peng (GIK)	12/23/2022 11:27:00 AM

English (United Kingdom)

Page 68: [536] Formatted	Yuan, Peng (GIK)	12/23/2022 11:27:00 AM

English (United Kingdom)

Page 68: [537] Formatted	Yuan, Peng (GIK)	12/23/2022 11:27:00 AM

English (United Kingdom)

| Page 68: [538] Formatted | Yuan, Peng (GIK) | 12/23/2022 11:27:00 AM |

English (United Kingdom)

| Page 68: [539] Formatted | Yuan, Peng (GIK) | 12/23/2022 11:27:00 AM |

English (United Kingdom)

| Page 68: [540] Formatted | Yuan, Peng (GIK) | 12/23/2022 11:27:00 AM |

English (United Kingdom)

| Page 68: [541] Formatted | Yuan, Peng (GIK) | 12/23/2022 11:27:00 AM |

English (United Kingdom)

| Page 68: [542] Formatted | Yuan, Peng (GIK) | 12/23/2022 11:27:00 AM |

English (United Kingdom)

| Page 68: [543] Formatted | Yuan, Peng (GIK) | 12/23/2022 11:27:00 AM |

English (United Kingdom)

| Page 68: [544] Formatted | Yuan, Peng (GIK) | 12/23/2022 11:27:00 AM |

English (United Kingdom)

| Page 68: [545] Formatted | Yuan, Peng (GIK) | 12/23/2022 11:27:00 AM |

Font: Bold

| Page 68: [545] Formatted | Yuan, Peng (GIK) | 12/23/2022 11:27:00 AM |

Font: Bold

| Page 68: [546] Formatted | Yuan, Peng (GIK) | 12/23/2022 11:27:00 AM |

English (United Kingdom)

| Page 68: [547] Formatted | Yuan, Peng (GIK) | 12/23/2022 11:27:00 AM |

English (United Kingdom)

| Page 68: [548] Formatted | Yuan, Peng (GIK) | 12/23/2022 11:27:00 AM |

English (United Kingdom)

| Page 68: [549] Formatted | Yuan, Peng (GIK) | 12/23/2022 11:27:00 AM |

English (United Kingdom)

| Page 68: [550] Formatted | Yuan, Peng (GIK) | 12/23/2022 11:27:00 AM |

English (United Kingdom)

| Page 68: [551] Formatted | Yuan, Peng (GIK) | 12/23/2022 11:27:00 AM |

English (United Kingdom)

| Page 68: [552] Formatted | Yuan, Peng (GIK) | 12/23/2022 11:27:00 AM |

English (United Kingdom)

| Page 68: [553] Formatted | Yuan, Peng (GIK) | 12/23/2022 11:27:00 AM |

English (United Kingdom)

Page 68: [554] Formatted	Yuan, Peng (GIK)	12/23/2022 11:27:00 AM

English (United Kingdom)

Page 68: [555] Formatted	Yuan, Peng (GIK)	12/23/2022 11:27:00 AM

English (United Kingdom)

Page 68: [556] Formatted	Yuan, Peng (GIK)	12/23/2022 11:27:00 AM

English (United Kingdom)

Page 68: [557] Formatted	Yuan, Peng (GIK)	12/23/2022 11:27:00 AM

Font: Bold

Page 68: [557] Formatted	Yuan, Peng (GIK)	12/23/2022 11:27:00 AM

Font: Bold

Page 68: [558] Formatted	Yuan, Peng (GIK)	12/23/2022 11:27:00 AM

English (United Kingdom)

Page 68: [559] Formatted	Yuan, Peng (GIK)	12/23/2022 11:27:00 AM

English (United Kingdom)

Page 68: [560] Formatted	Yuan, Peng (GIK)	12/23/2022 11:27:00 AM

English (United Kingdom)

Page 68: [561] Formatted	Yuan, Peng (GIK)	12/23/2022 11:27:00 AM

English (United Kingdom)

Page 68: [562] Formatted	Yuan, Peng (GIK)	12/23/2022 11:27:00 AM

English (United Kingdom)

Page 68: [563] Formatted	Yuan, Peng (GIK)	12/23/2022 11:27:00 AM

English (United Kingdom)

Page 68: [564] Formatted	Yuan, Peng (GIK)	12/23/2022 11:27:00 AM

English (United Kingdom)

Page 68: [565] Formatted	Yuan, Peng (GIK)	12/23/2022 11:27:00 AM

English (United Kingdom)

Page 68: [566] Formatted	Yuan, Peng (GIK)	12/23/2022 11:27:00 AM

English (United Kingdom)

Page 68: [567] Formatted	Yuan, Peng (GIK)	12/23/2022 11:27:00 AM

English (United Kingdom)

Page 68: [568] Formatted	Yuan, Peng (GIK)	12/23/2022 11:27:00 AM

English (United Kingdom)

Page 68: [569] Formatted	Yuan, Peng (GIK)	12/23/2022 11:27:00 AM

Font: Bold

Page 68: [569] Formatted	Yuan, Peng (GIK)	12/23/2022 11:27:00 AM

Font: Bold

Page 68: [570] Formatted	Yuan, Peng (GIK)	12/23/2022 11:27:00 AM

English (United Kingdom)

Page 68: [571] Formatted	Yuan, Peng (GIK)	12/23/2022 11:27:00 AM

English (United Kingdom)

Page 68: [572] Formatted	Yuan, Peng (GIK)	12/23/2022 11:27:00 AM

English (United Kingdom)

Page 68: [573] Formatted	Yuan, Peng (GIK)	12/23/2022 11:27:00 AM

English (United Kingdom)

Page 68: [574] Formatted	Yuan, Peng (GIK)	12/23/2022 11:27:00 AM

English (United Kingdom)

Page 68: [575] Formatted	Yuan, Peng (GIK)	12/23/2022 11:27:00 AM

English (United Kingdom)

Page 68: [576] Formatted	Yuan, Peng (GIK)	12/23/2022 11:27:00 AM

English (United Kingdom)

Page 68: [577] Formatted	Yuan, Peng (GIK)	12/23/2022 11:27:00 AM

English (United Kingdom)

Page 68: [578] Formatted	Yuan, Peng (GIK)	12/23/2022 11:27:00 AM

English (United Kingdom)

Page 68: [579] Formatted	Yuan, Peng (GIK)	12/23/2022 11:27:00 AM

English (United Kingdom)

Page 68: [580] Formatted	Yuan, Peng (GIK)	12/23/2022 11:27:00 AM

English (United Kingdom)

Page 68: [581] Formatted	Yuan, Peng (GIK)	12/23/2022 11:27:00 AM

Font: Bold

Page 68: [581] Formatted	Yuan, Peng (GIK)	12/23/2022 11:27:00 AM

Font: Bold

Page 68: [582] Formatted	Yuan, Peng (GIK)	12/23/2022 11:27:00 AM

English (United Kingdom)

Page 68: [583] Formatted	Yuan, Peng (GIK)	12/23/2022 11:27:00 AM

English (United Kingdom)

| Page 68: [584] Formatted | Yuan, Peng (GIK) | 12/23/2022 11:27:00 AM |

English (United Kingdom)

| Page 68: [585] Formatted | Yuan, Peng (GIK) | 12/23/2022 11:27:00 AM |

English (United Kingdom)

| Page 68: [586] Formatted | Yuan, Peng (GIK) | 12/23/2022 11:27:00 AM |

English (United Kingdom)

| Page 68: [587] Formatted | Yuan, Peng (GIK) | 12/23/2022 11:27:00 AM |

English (United Kingdom)

| Page 68: [588] Formatted | Yuan, Peng (GIK) | 12/23/2022 11:27:00 AM |

English (United Kingdom)

| Page 68: [589] Formatted | Yuan, Peng (GIK) | 12/23/2022 11:27:00 AM |

English (United Kingdom)

| Page 68: [590] Formatted | Yuan, Peng (GIK) | 12/23/2022 11:27:00 AM |

English (United Kingdom)

| Page 68: [591] Formatted | Yuan, Peng (GIK) | 12/23/2022 11:27:00 AM |

English (United Kingdom)

| Page 68: [592] Formatted | Yuan, Peng (GIK) | 12/23/2022 11:27:00 AM |

English (United Kingdom)

| Page 68: [593] Formatted | Yuan, Peng (GIK) | 12/23/2022 11:27:00 AM |

Font: Bold

| Page 68: [593] Formatted | Yuan, Peng (GIK) | 12/23/2022 11:27:00 AM |

Font: Bold

| Page 68: [594] Formatted | Yuan, Peng (GIK) | 12/23/2022 11:27:00 AM |

English (United Kingdom)

| Page 68: [595] Formatted | Yuan, Peng (GIK) | 12/23/2022 11:27:00 AM |

English (United Kingdom)

| Page 68: [596] Formatted | Yuan, Peng (GIK) | 12/23/2022 11:27:00 AM |

English (United Kingdom)

| Page 68: [597] Formatted | Yuan, Peng (GIK) | 12/23/2022 11:27:00 AM |

English (United Kingdom)

| Page 68: [598] Formatted | Yuan, Peng (GIK) | 12/23/2022 11:27:00 AM |

English (United Kingdom)

| Page 68: [599] Formatted | Yuan, Peng (GIK) | 12/23/2022 11:27:00 AM |

English (United Kingdom)

Page 68: [600] Formatted	Yuan, Peng (GIK)	12/23/2022 11:27:00 AM

English (United Kingdom)

Page 68: [601] Formatted	Yuan, Peng (GIK)	12/23/2022 11:27:00 AM

English (United Kingdom)

Page 68: [602] Formatted	Yuan, Peng (GIK)	12/23/2022 11:27:00 AM

English (United Kingdom)

Page 68: [603] Formatted	Yuan, Peng (GIK)	12/23/2022 11:27:00 AM

English (United Kingdom)

Page 68: [604] Formatted	Yuan, Peng (GIK)	12/23/2022 11:27:00 AM

English (United Kingdom)

Page 68: [605] Formatted	Yuan, Peng (GIK)	12/23/2022 11:27:00 AM

Font: Bold

Page 68: [605] Formatted	Yuan, Peng (GIK)	12/23/2022 11:27:00 AM

Font: Bold

Page 68: [606] Formatted	Yuan, Peng (GIK)	12/23/2022 11:27:00 AM

English (United Kingdom)

Page 68: [607] Formatted	Yuan, Peng (GIK)	12/23/2022 11:27:00 AM

English (United Kingdom)

Page 68: [608] Formatted	Yuan, Peng (GIK)	12/23/2022 11:27:00 AM

English (United Kingdom)

Page 68: [609] Formatted	Yuan, Peng (GIK)	12/23/2022 11:27:00 AM

English (United Kingdom)

Page 68: [610] Formatted	Yuan, Peng (GIK)	12/23/2022 11:27:00 AM

English (United Kingdom)

Page 68: [611] Formatted	Yuan, Peng (GIK)	12/23/2022 11:27:00 AM

English (United Kingdom)

Page 68: [612] Formatted	Yuan, Peng (GIK)	12/23/2022 11:27:00 AM

English (United Kingdom)

Page 68: [613] Formatted	Yuan, Peng (GIK)	12/23/2022 11:27:00 AM

English (United Kingdom)

Page 68: [614] Formatted	Yuan, Peng (GIK)	12/23/2022 11:27:00 AM

English (United Kingdom)

Page 68: [615] Formatted	Yuan, Peng (GIK)	12/23/2022 11:27:00 AM

English (United Kingdom)

Page 68: [616] Formatted	Yuan, Peng (GIK)	12/23/2022 11:27:00 AM

English (United Kingdom)

Page 68: [617] Formatted	Yuan, Peng (GIK)	12/23/2022 11:27:00 AM

Font: Bold

Page 68: [617] Formatted	Yuan, Peng (GIK)	12/23/2022 11:27:00 AM

Font: Bold

Page 68: [618] Formatted	Yuan, Peng (GIK)	12/23/2022 11:27:00 AM

English (United Kingdom)

Page 68: [619] Formatted	Yuan, Peng (GIK)	12/23/2022 11:27:00 AM

English (United Kingdom)

Page 68: [620] Formatted	Yuan, Peng (GIK)	12/23/2022 11:27:00 AM

English (United Kingdom)

Page 68: [621] Formatted	Yuan, Peng (GIK)	12/23/2022 11:27:00 AM

English (United Kingdom)

Page 68: [622] Formatted	Yuan, Peng (GIK)	12/23/2022 11:27:00 AM

English (United Kingdom)

Page 68: [623] Formatted	Yuan, Peng (GIK)	12/23/2022 11:27:00 AM

English (United Kingdom)

Page 68: [624] Formatted	Yuan, Peng (GIK)	12/23/2022 11:27:00 AM

English (United Kingdom)

Page 68: [625] Formatted	Yuan, Peng (GIK)	12/23/2022 11:27:00 AM

English (United Kingdom)

Page 68: [626] Formatted	Yuan, Peng (GIK)	12/23/2022 11:27:00 AM

English (United Kingdom)

Page 68: [627] Formatted	Yuan, Peng (GIK)	12/23/2022 11:27:00 AM

English (United Kingdom)

Page 68: [628] Formatted	Yuan, Peng (GIK)	12/23/2022 11:27:00 AM

English (United Kingdom)

Page 68: [629] Formatted	Yuan, Peng (GIK)	12/23/2022 11:27:00 AM

Font: Bold

Page 68: [629] Formatted	Yuan, Peng (GIK)	12/23/2022 11:27:00 AM

Font: Bold

Page 68: [630] Formatted	Yuan, Peng (GIK)	12/23/2022 11:27:00 AM

English (United Kingdom)

Page 68: [631] Formatted	Yuan, Peng (GIK)	12/23/2022 11:27:00 AM

English (United Kingdom)

Page 68: [632] Formatted	Yuan, Peng (GIK)	12/23/2022 11:27:00 AM

English (United Kingdom)

Page 68: [633] Formatted	Yuan, Peng (GIK)	12/23/2022 11:27:00 AM

English (United Kingdom)

Page 68: [634] Formatted	Yuan, Peng (GIK)	12/23/2022 11:27:00 AM

English (United Kingdom)

Page 68: [635] Formatted	Yuan, Peng (GIK)	12/23/2022 11:27:00 AM

English (United Kingdom)

Page 68: [636] Formatted	Yuan, Peng (GIK)	12/23/2022 11:27:00 AM

English (United Kingdom)

Page 68: [637] Formatted	Yuan, Peng (GIK)	12/23/2022 11:27:00 AM

English (United Kingdom)

Page 68: [638] Formatted	Yuan, Peng (GIK)	12/23/2022 11:27:00 AM

English (United Kingdom)

Page 68: [639] Formatted	Yuan, Peng (GIK)	12/23/2022 11:27:00 AM

English (United Kingdom)

Page 68: [640] Formatted	Yuan, Peng (GIK)	12/23/2022 11:27:00 AM

English (United Kingdom)

Page 68: [641] Formatted	Yuan, Peng (GIK)	12/23/2022 11:27:00 AM

Font: Bold

Page 68: [641] Formatted	Yuan, Peng (GIK)	12/23/2022 11:27:00 AM

Font: Bold

Page 68: [642] Formatted	Yuan, Peng (GIK)	12/23/2022 11:27:00 AM

English (United Kingdom)

Page 68: [643] Formatted	Yuan, Peng (GIK)	12/23/2022 11:27:00 AM

English (United Kingdom)

Page 68: [644] Formatted	Yuan, Peng (GIK)	12/23/2022 11:27:00 AM

English (United Kingdom)

Page 68: [645] Formatted	Yuan, Peng (GIK)	12/23/2022 11:27:00 AM

English (United Kingdom)

Page 68: [646] Formatted	Yuan, Peng (GIK)	12/23/2022 11:27:00 AM

English (United Kingdom)

Page 68: [647] Formatted	Yuan, Peng (GIK)	12/23/2022 11:27:00 AM

English (United Kingdom)

Page 68: [648] Formatted	Yuan, Peng (GIK)	12/23/2022 11:27:00 AM

English (United Kingdom)

Page 68: [649] Formatted	Yuan, Peng (GIK)	12/23/2022 11:27:00 AM

English (United Kingdom)

Page 68: [650] Formatted	Yuan, Peng (GIK)	12/23/2022 11:27:00 AM

English (United Kingdom)

Page 68: [651] Formatted	Yuan, Peng (GIK)	12/23/2022 11:27:00 AM

English (United Kingdom)

Page 68: [652] Formatted	Yuan, Peng (GIK)	12/23/2022 11:27:00 AM

English (United Kingdom)

Page 68: [653] Formatted	Yuan, Peng (GIK)	12/23/2022 11:27:00 AM

Font: Bold

Page 68: [653] Formatted	Yuan, Peng (GIK)	12/23/2022 11:27:00 AM

Font: Bold

Page 68: [654] Formatted	Yuan, Peng (GIK)	12/23/2022 11:27:00 AM

English (United Kingdom)

Page 68: [655] Formatted	Yuan, Peng (GIK)	12/23/2022 11:27:00 AM

English (United Kingdom)

Page 68: [656] Formatted	Yuan, Peng (GIK)	12/23/2022 11:27:00 AM

English (United Kingdom)

Page 68: [657] Formatted	Yuan, Peng (GIK)	12/23/2022 11:27:00 AM

English (United Kingdom)

Page 68: [658] Formatted	Yuan, Peng (GIK)	12/23/2022 11:27:00 AM

English (United Kingdom)

Page 68: [659] Formatted	Yuan, Peng (GIK)	12/23/2022 11:27:00 AM

English (United Kingdom)

Page 68: [660] Formatted	Yuan, Peng (GIK)	12/23/2022 11:27:00 AM

English (United Kingdom)

Page 68: [661] Formatted	Yuan, Peng (GIK)	12/23/2022 11:27:00 AM

English (United Kingdom)

Page 68: [662] Formatted	Yuan, Peng (GIK)	12/23/2022 11:27:00 AM

English (United Kingdom)

Page 68: [663] Formatted	Yuan, Peng (GIK)	12/23/2022 11:27:00 AM

English (United Kingdom)

Page 68: [664] Formatted	Yuan, Peng (GIK)	12/23/2022 11:27:00 AM

English (United Kingdom)

Page 68: [665] Formatted	Yuan, Peng (GIK)	12/23/2022 11:27:00 AM

Font: Bold

Page 68: [665] Formatted	Yuan, Peng (GIK)	12/23/2022 11:27:00 AM

Font: Bold

Page 68: [666] Formatted	Yuan, Peng (GIK)	12/23/2022 11:27:00 AM

English (United Kingdom)

Page 68: [667] Formatted	Yuan, Peng (GIK)	12/23/2022 11:27:00 AM

English (United Kingdom)

Page 68: [668] Formatted	Yuan, Peng (GIK)	12/23/2022 11:27:00 AM

English (United Kingdom)

Page 68: [669] Formatted	Yuan, Peng (GIK)	12/23/2022 11:27:00 AM

English (United Kingdom)

Page 68: [670] Formatted	Yuan, Peng (GIK)	12/23/2022 11:27:00 AM

English (United Kingdom)

Page 68: [671] Formatted	Yuan, Peng (GIK)	12/23/2022 11:27:00 AM

English (United Kingdom)

Page 68: [672] Formatted	Yuan, Peng (GIK)	12/23/2022 11:27:00 AM

English (United Kingdom)

Page 68: [673] Formatted	Yuan, Peng (GIK)	12/23/2022 11:27:00 AM

English (United Kingdom)

Page 68: [674] Formatted	Yuan, Peng (GIK)	12/23/2022 11:27:00 AM

English (United Kingdom)

Page 68: [675] Formatted	Yuan, Peng (GIK)	12/23/2022 11:27:00 AM

English (United Kingdom)

Page 68: [676] Formatted	Yuan, Peng (GIK)	12/23/2022 11:27:00 AM

English (United Kingdom)

Page 68: [677] Formatted	Yuan, Peng (GIK)	12/23/2022 11:27:00 AM

Font: Bold

Page 68: [677] Formatted	Yuan, Peng (GIK)	12/23/2022 11:27:00 AM

Font: Bold

Page 68: [678] Formatted	Yuan, Peng (GIK)	12/23/2022 11:27:00 AM

English (United Kingdom)

Page 68: [679] Formatted	Yuan, Peng (GIK)	12/23/2022 11:27:00 AM

English (United Kingdom)

Page 68: [680] Formatted	Yuan, Peng (GIK)	12/23/2022 11:27:00 AM

English (United Kingdom)

Page 68: [681] Formatted	Yuan, Peng (GIK)	12/23/2022 11:27:00 AM

English (United Kingdom)

Page 68: [682] Formatted	Yuan, Peng (GIK)	12/23/2022 11:27:00 AM

English (United Kingdom)

Page 68: [683] Formatted	Yuan, Peng (GIK)	12/23/2022 11:27:00 AM

English (United Kingdom)

Page 68: [684] Formatted	Yuan, Peng (GIK)	12/23/2022 11:27:00 AM

English (United Kingdom)

Page 68: [685] Formatted	Yuan, Peng (GIK)	12/23/2022 11:27:00 AM

English (United Kingdom)

Page 68: [686] Formatted	Yuan, Peng (GIK)	12/23/2022 11:27:00 AM

English (United Kingdom)

Page 68: [687] Formatted	Yuan, Peng (GIK)	12/23/2022 11:27:00 AM

English (United Kingdom)

Page 68: [688] Formatted	Yuan, Peng (GIK)	12/23/2022 11:27:00 AM

English (United Kingdom)

Page 68: [689] Formatted	Yuan, Peng (GIK)	12/23/2022 11:27:00 AM

Font: Bold

Page 68: [689] Formatted	Yuan, Peng (GIK)	12/23/2022 11:27:00 AM

Font: Bold

Page 68: [690] Formatted	Yuan, Peng (GIK)	12/23/2022 11:27:00 AM

English (United Kingdom)

Page 68: [691] Formatted	Yuan, Peng (GIK)	12/23/2022 11:27:00 AM

English (United Kingdom)

Page 68: [692] Formatted	Yuan, Peng (GIK)	12/23/2022 11:27:00 AM

English (United Kingdom)

Page 68: [693] Formatted	Yuan, Peng (GIK)	12/23/2022 11:27:00 AM

English (United Kingdom)

Page 68: [694] Formatted	Yuan, Peng (GIK)	12/23/2022 11:27:00 AM

English (United Kingdom)

Page 68: [695] Formatted	Yuan, Peng (GIK)	12/23/2022 11:27:00 AM

English (United Kingdom)

Page 68: [696] Formatted	Yuan, Peng (GIK)	12/23/2022 11:27:00 AM

English (United Kingdom)

Page 68: [697] Formatted	Yuan, Peng (GIK)	12/23/2022 11:27:00 AM

English (United Kingdom)

Page 68: [698] Formatted	Yuan, Peng (GIK)	12/23/2022 11:27:00 AM

English (United Kingdom)

Page 68: [699] Formatted	Yuan, Peng (GIK)	12/23/2022 11:27:00 AM

English (United Kingdom)

Page 68: [700] Formatted	Yuan, Peng (GIK)	12/23/2022 11:27:00 AM

English (United Kingdom)

Page 68: [701] Formatted	Yuan, Peng (GIK)	12/23/2022 11:27:00 AM

Font: Bold

Page 68: [701] Formatted	Yuan, Peng (GIK)	12/23/2022 11:27:00 AM

Font: Bold

Page 68: [702] Formatted	Yuan, Peng (GIK)	12/23/2022 11:27:00 AM

English (United Kingdom)

Page 68: [703] Formatted	Yuan, Peng (GIK)	12/23/2022 11:27:00 AM

English (United Kingdom)

Page 68: [704] Formatted	Yuan, Peng (GIK)	12/23/2022 11:27:00 AM

English (United Kingdom)

Page 68: [705] Formatted	Yuan, Peng (GIK)	12/23/2022 11:27:00 AM

English (United Kingdom)

Page 68: [706] Formatted	Yuan, Peng (GIK)	12/23/2022 11:27:00 AM

English (United Kingdom)

Page 68: [707] Formatted	Yuan, Peng (GIK)	12/23/2022 11:27:00 AM

English (United Kingdom)

Page 68: [708] Formatted	Yuan, Peng (GIK)	12/23/2022 11:27:00 AM

English (United Kingdom)

Page 68: [709] Formatted	Yuan, Peng (GIK)	12/23/2022 11:27:00 AM

English (United Kingdom)

Page 68: [710] Formatted	Yuan, Peng (GIK)	12/23/2022 11:27:00 AM

English (United Kingdom)

Page 68: [711] Formatted	Yuan, Peng (GIK)	12/23/2022 11:27:00 AM

English (United Kingdom)

Page 68: [712] Formatted	Yuan, Peng (GIK)	12/23/2022 11:27:00 AM

English (United Kingdom)

Page 68: [713] Formatted	Yuan, Peng (GIK)	12/23/2022 11:27:00 AM

Font: Bold

Page 68: [713] Formatted	Yuan, Peng (GIK)	12/23/2022 11:27:00 AM

Font: Bold

Page 68: [714] Formatted	Yuan, Peng (GIK)	12/23/2022 11:27:00 AM

English (United Kingdom)

Page 68: [715] Formatted	Yuan, Peng (GIK)	12/23/2022 11:27:00 AM

English (United Kingdom)

Page 68: [716] Formatted	Yuan, Peng (GIK)	12/23/2022 11:27:00 AM

English (United Kingdom)

Page 68: [717] Formatted	Yuan, Peng (GIK)	12/23/2022 11:27:00 AM

English (United Kingdom)

Page 68: [718] Formatted	Yuan, Peng (GIK)	12/23/2022 11:27:00 AM

English (United Kingdom)

Page 68: [719] Formatted	Yuan, Peng (GIK)	12/23/2022 11:27:00 AM

English (United Kingdom)

Page 68: [720] Formatted	Yuan, Peng (GIK)	12/23/2022 11:27:00 AM

English (United Kingdom)

Page 68: [721] Formatted	Yuan, Peng (GIK)	12/23/2022 11:27:00 AM

English (United Kingdom)

Page 68: [722] Formatted	Yuan, Peng (GIK)	12/23/2022 11:27:00 AM

English (United Kingdom)

Page 68: [723] Formatted	Yuan, Peng (GIK)	12/23/2022 11:27:00 AM

English (United Kingdom)

Page 68: [724] Formatted	Yuan, Peng (GIK)	12/23/2022 11:27:00 AM

English (United Kingdom)

Page 68: [725] Formatted	Yuan, Peng (GIK)	12/23/2022 11:27:00 AM

Font: Bold

Page 68: [725] Formatted	Yuan, Peng (GIK)	12/23/2022 11:27:00 AM

Font: Bold

Page 68: [726] Formatted	Yuan, Peng (GIK)	12/23/2022 11:27:00 AM

English (United Kingdom)

Page 68: [727] Formatted	Yuan, Peng (GIK)	12/23/2022 11:27:00 AM

English (United Kingdom)

Page 68: [728] Formatted	Yuan, Peng (GIK)	12/23/2022 11:27:00 AM

English (United Kingdom)

Page 68: [729] Formatted	Yuan, Peng (GIK)	12/23/2022 11:27:00 AM

English (United Kingdom)

Page 68: [730] Formatted	Yuan, Peng (GIK)	12/23/2022 11:27:00 AM

English (United Kingdom)

Page 68: [731] Formatted	Yuan, Peng (GIK)	12/23/2022 11:27:00 AM

English (United Kingdom)

Page 68: [732] Formatted	Yuan, Peng (GIK)	12/23/2022 11:27:00 AM

English (United Kingdom)

Page 68: [733] Formatted	Yuan, Peng (GIK)	12/23/2022 11:27:00 AM

English (United Kingdom)

Page 68: [734] Formatted	Yuan, Peng (GIK)	12/23/2022 11:27:00 AM

English (United Kingdom)

Page 68: [735] Formatted	Yuan, Peng (GIK)	12/23/2022 11:27:00 AM

English (United Kingdom)

Page 68: [736] Formatted	Yuan, Peng (GIK)	12/23/2022 11:27:00 AM

English (United Kingdom)

Page 68: [737] Formatted	Yuan, Peng (GIK)	12/23/2022 11:27:00 AM

Font: Bold

Page 68: [737] Formatted	Yuan, Peng (GIK)	12/23/2022 11:27:00 AM

Font: Bold

Page 68: [738] Formatted	Yuan, Peng (GIK)	12/23/2022 11:27:00 AM

English (United Kingdom)

Page 68: [739] Formatted	Yuan, Peng (GIK)	12/23/2022 11:27:00 AM

English (United Kingdom)

Page 68: [740] Formatted	Yuan, Peng (GIK)	12/23/2022 11:27:00 AM

English (United Kingdom)

Page 68: [741] Formatted	Yuan, Peng (GIK)	12/23/2022 11:27:00 AM

English (United Kingdom)

Page 68: [742] Formatted	Yuan, Peng (GIK)	12/23/2022 11:27:00 AM

English (United Kingdom)

Page 68: [743] Formatted	Yuan, Peng (GIK)	12/23/2022 11:27:00 AM

English (United Kingdom)

Page 68: [744] Formatted	Yuan, Peng (GIK)	12/23/2022 11:27:00 AM

English (United Kingdom)

Page 68: [745] Formatted	Yuan, Peng (GIK)	12/23/2022 11:27:00 AM

English (United Kingdom)

Page 68: [746] Formatted	Yuan, Peng (GIK)	12/23/2022 11:27:00 AM

English (United Kingdom)

Page 68: [747] Formatted	Yuan, Peng (GIK)	12/23/2022 11:27:00 AM

English (United Kingdom)

Page 68: [748] Formatted	Yuan, Peng (GIK)	12/23/2022 11:27:00 AM

English (United Kingdom)

Page 68: [749] Formatted	Yuan, Peng (GIK)	12/23/2022 11:27:00 AM

Font: Bold

Page 68: [749] Formatted	Yuan, Peng (GIK)	12/23/2022 11:27:00 AM

Font: Bold

Page 68: [750] Formatted	Yuan, Peng (GIK)	12/23/2022 11:27:00 AM

English (United Kingdom)

Page 68: [751] Formatted	Yuan, Peng (GIK)	12/23/2022 11:27:00 AM

English (United Kingdom)

Page 68: [752] Formatted	Yuan, Peng (GIK)	12/23/2022 11:27:00 AM

English (United Kingdom)

Page 68: [753] Formatted	Yuan, Peng (GIK)	12/23/2022 11:27:00 AM

English (United Kingdom)

Page 68: [754] Formatted	Yuan, Peng (GIK)	12/23/2022 11:27:00 AM

English (United Kingdom)

Page 68: [755] Formatted	Yuan, Peng (GIK)	12/23/2022 11:27:00 AM

English (United Kingdom)

Page 68: [756] Formatted	Yuan, Peng (GIK)	12/23/2022 11:27:00 AM

English (United Kingdom)

Page 68: [757] Formatted	Yuan, Peng (GIK)	12/23/2022 11:27:00 AM

English (United Kingdom)

Page 68: [758] Formatted	Yuan, Peng (GIK)	12/23/2022 11:27:00 AM

English (United Kingdom)

Page 68: [759] Formatted	Yuan, Peng (GIK)	12/23/2022 11:27:00 AM

English (United Kingdom)

Page 68: [760] Formatted	Yuan, Peng (GIK)	12/23/2022 11:27:00 AM

English (United Kingdom)

Page 68: [761] Formatted	Yuan, Peng (GIK)	12/23/2022 11:27:00 AM

Font: Bold

Page 68: [761] Formatted	Yuan, Peng (GIK)	12/23/2022 11:27:00 AM

Font: Bold

Page 68: [762] Formatted	Yuan, Peng (GIK)	12/23/2022 11:27:00 AM

English (United Kingdom)

Page 68: [763] Formatted	Yuan, Peng (GIK)	12/23/2022 11:27:00 AM

English (United Kingdom)

Page 68: [764] Formatted	Yuan, Peng (GIK)	12/23/2022 11:27:00 AM

English (United Kingdom)

Page 68: [765] Formatted	Yuan, Peng (GIK)	12/23/2022 11:27:00 AM

English (United Kingdom)

Page 68: [766] Formatted	Yuan, Peng (GIK)	12/23/2022 11:27:00 AM

English (United Kingdom)

Page 68: [767] Formatted	Yuan, Peng (GIK)	12/23/2022 11:27:00 AM

English (United Kingdom)

Page 68: [768] Formatted	Yuan, Peng (GIK)	12/23/2022 11:27:00 AM

English (United Kingdom)

Page 68: [769] Formatted	Yuan, Peng (GIK)	12/23/2022 11:27:00 AM

English (United Kingdom)

Page 68: [770] Formatted	Yuan, Peng (GIK)	12/23/2022 11:27:00 AM

English (United Kingdom)

Page 68: [771] Formatted	Yuan, Peng (GIK)	12/23/2022 11:27:00 AM

English (United Kingdom)

Page 68: [772] Formatted	Yuan, Peng (GIK)	12/23/2022 11:27:00 AM

English (United Kingdom)

Page 68: [773] Formatted	Yuan, Peng (GIK)	12/23/2022 11:27:00 AM

Font: Bold

Page 68: [773] Formatted	Yuan, Peng (GIK)	12/23/2022 11:27:00 AM

Font: Bold

Page 68: [774] Formatted	Yuan, Peng (GIK)	12/23/2022 11:27:00 AM

English (United Kingdom)

Page 68: [775] Formatted	Yuan, Peng (GIK)	12/23/2022 11:27:00 AM

English (United Kingdom)

Page 68: [776] Formatted	Yuan, Peng (GIK)	12/23/2022 11:27:00 AM

English (United Kingdom)

Page 68: [777] Formatted	Yuan, Peng (GIK)	12/23/2022 11:27:00 AM

English (United Kingdom)

Page 68: [778] Formatted	Yuan, Peng (GIK)	12/23/2022 11:27:00 AM

English (United Kingdom)

Page 68: [779] Formatted	Yuan, Peng (GIK)	12/23/2022 11:27:00 AM

English (United Kingdom)

Page 68: [780] Formatted	Yuan, Peng (GIK)	12/23/2022 11:27:00 AM

English (United Kingdom)

Page 68: [781] Formatted	Yuan, Peng (GIK)	12/23/2022 11:27:00 AM

English (United Kingdom)

Page 68: [782] Formatted	Yuan, Peng (GIK)	12/23/2022 11:27:00 AM

English (United Kingdom)

Page 68: [783] Formatted	Yuan, Peng (GIK)	12/23/2022 11:27:00 AM

English (United Kingdom)

Page 68: [784] Formatted	Yuan, Peng (GIK)	12/23/2022 11:27:00 AM

English (United Kingdom)

Page 68: [785] Formatted	Yuan, Peng (GIK)	12/23/2022 11:27:00 AM

Font: Bold

Page 68: [785] Formatted	Yuan, Peng (GIK)	12/23/2022 11:27:00 AM

Font: Bold

Page 68: [786] Formatted	Yuan, Peng (GIK)	12/23/2022 11:27:00 AM

English (United Kingdom)

Page 68: [787] Formatted	Yuan, Peng (GIK)	12/23/2022 11:27:00 AM

English (United Kingdom)

Page 68: [788] Formatted	Yuan, Peng (GIK)	12/23/2022 11:27:00 AM

English (United Kingdom)

Page 68: [789] Formatted	Yuan, Peng (GIK)	12/23/2022 11:27:00 AM

English (United Kingdom)

Page 68: [790] Formatted	Yuan, Peng (GIK)	12/23/2022 11:27:00 AM

English (United Kingdom)

Page 68: [791] Formatted	Yuan, Peng (GIK)	12/23/2022 11:27:00 AM

English (United Kingdom)

Page 68: [792] Formatted	Yuan, Peng (GIK)	12/23/2022 11:27:00 AM

English (United Kingdom)

Page 68: [793] Formatted	Yuan, Peng (GIK)	12/23/2022 11:27:00 AM

English (United Kingdom)

Page 68: [794] Formatted	Yuan, Peng (GIK)	12/23/2022 11:27:00 AM

English (United Kingdom)

Page 68: [795] Formatted	Yuan, Peng (GIK)	12/23/2022 11:27:00 AM

English (United Kingdom)

Page 68: [796] Formatted	Yuan, Peng (GIK)	12/23/2022 11:27:00 AM

English (United Kingdom)

Page 68: [797] Formatted	Yuan, Peng (GIK)	12/23/2022 11:27:00 AM

Font: Bold

Page 68: [797] Formatted	Yuan, Peng (GIK)	12/23/2022 11:27:00 AM

Font: Bold

Page 68: [798] Formatted	Yuan, Peng (GIK)	12/23/2022 11:27:00 AM

English (United Kingdom)

Page 68: [799] Formatted	Yuan, Peng (GIK)	12/23/2022 11:27:00 AM

English (United Kingdom)

Page 68: [800] Formatted	Yuan, Peng (GIK)	12/23/2022 11:27:00 AM

English (United Kingdom)

Page 68: [801] Formatted	Yuan, Peng (GIK)	12/23/2022 11:27:00 AM

English (United Kingdom)

Page 68: [802] Formatted	Yuan, Peng (GIK)	12/23/2022 11:27:00 AM

English (United Kingdom)

Page 68: [803] Formatted	Yuan, Peng (GIK)	12/23/2022 11:27:00 AM

English (United Kingdom)

Page 68: [804] Formatted	Yuan, Peng (GIK)	12/23/2022 11:27:00 AM

English (United Kingdom)

Page 68: [805] Formatted	Yuan, Peng (GIK)	12/23/2022 11:27:00 AM

English (United Kingdom)

Page 68: [806] Formatted	Yuan, Peng (GIK)	12/23/2022 11:27:00 AM

English (United Kingdom)

Page 68: [807] Formatted	Yuan, Peng (GIK)	12/23/2022 11:27:00 AM

English (United Kingdom)

Page 68: [808] Formatted	Yuan, Peng (GIK)	12/23/2022 11:27:00 AM

English (United Kingdom)

Page 68: [809] Formatted	Yuan, Peng (GIK)	12/23/2022 11:27:00 AM

Font: Bold

Page 68: [809] Formatted	Yuan, Peng (GIK)	12/23/2022 11:27:00 AM

Font: Bold

Page 68: [810] Formatted	Yuan, Peng (GIK)	12/23/2022 11:27:00 AM

English (United Kingdom)

Page 68: [811] Formatted	Yuan, Peng (GIK)	12/23/2022 11:27:00 AM

English (United Kingdom)

Page 68: [812] Formatted	Yuan, Peng (GIK)	12/23/2022 11:27:00 AM

English (United Kingdom)

Page 68: [813] Formatted	Yuan, Peng (GIK)	12/23/2022 11:27:00 AM

English (United Kingdom)

Page 68: [814] Formatted	Yuan, Peng (GIK)	12/23/2022 11:27:00 AM

English (United Kingdom)

Page 68: [815] Formatted   **Yuan, Peng (GIK)**   **12/23/2022 11:27:00 AM**

English (United Kingdom)

Page 68: [816] Formatted   **Yuan, Peng (GIK)**   **12/23/2022 11:27:00 AM**

English (United Kingdom)

Page 68: [817] Formatted   **Yuan, Peng (GIK)**   **12/23/2022 11:27:00 AM**

English (United Kingdom)

Page 68: [818] Formatted   **Yuan, Peng (GIK)**   **12/23/2022 11:27:00 AM**

English (United Kingdom)

Page 68: [819] Formatted   **Yuan, Peng (GIK)**   **12/23/2022 11:27:00 AM**

English (United Kingdom)

Page 68: [820] Formatted   **Yuan, Peng (GIK)**   **12/23/2022 11:27:00 AM**

English (United Kingdom)

Page 68: [821] Formatted   **Yuan, Peng (GIK)**   **12/22/2022 5:10:00 PM**

Centered, Space After: 6 pt, Line spacing: single

Page 68: [822] Formatted   **Yuan, Peng (GIK)**   **12/23/2022 11:27:00 AM**

English (United Kingdom)

Page 68: [823] Formatted   **Yuan, Peng (GIK)**   **12/23/2022 11:27:00 AM**

English (United Kingdom)

Page 68: [824] Formatted   **Yuan, Peng (GIK)**   **12/23/2022 11:27:00 AM**

English (United Kingdom)

Page 68: [825] Formatted   **Yuan, Peng (GIK)**   **12/23/2022 11:27:00 AM**

English (United Kingdom)

Page 68: [826] Formatted   **Yuan, Peng (GIK)**   **12/23/2022 11:27:00 AM**

English (United Kingdom)

Page 68: [827] Formatted   **Yuan, Peng (GIK)**   **12/23/2022 11:27:00 AM**

English (United Kingdom)

Page 68: [828] Formatted   **Yuan, Peng (GIK)**   **12/23/2022 11:27:00 AM**

English (United Kingdom)

Page 68: [829] Formatted   **Yuan, Peng (GIK)**   **12/23/2022 11:27:00 AM**

English (United Kingdom)

Page 68: [830] Formatted   **Yuan, Peng (GIK)**   **12/23/2022 11:27:00 AM**

English (United Kingdom)